GENETIC SCREENING FOR EFFECTORS OF Neu/ErbB2 SIGNALING

GENETIC IDENTIFICATION OF PHOSPHOTYROSINE SPECIFIC *DROSOPHILA* EFFECTORS OF Neu/Erb-B2 SIGNALING

by

W. MARK SETTLE, B.Sc. (Honours)

A Thesis
Submitted to the School of Graduate Studies
in Partial Fulfillment of the Requirements
for the Degree
Master of Science

McMaster University

MASTER OF SCIENCE (2002)
(Biology)

McMaster University
Hamilton, Ontario

TITLE: Genetic Identification of Phosphotyrosine Specific *Drosophila* Effectors of Neu/Erb-B2 Signaling

AUTHOR: W. Mark Settle, B.SC. (Honours), University of Western Ontario

SUPERVISOR: J. Roger Jacobs, Ph.D., Associate Professor, McMaster University

NUMBER OF PAGES: xii, 158

ABSTRACT

The *Drosophila* Epidermal Growth Factor Receptor (DEgfr) is the only fly orthologue of the vertebrate Neu/ErbB2 receptor tyrosine kinase (RTK) family. In *Drosophila,* DEgfr signaling is required in the developing wing discs, and for the determination and differentiation of wing veins. Expression of constitutively active rat Neu/ErbB2 transgenes, each having a single phosphotyrosine (pTyr) residue in the adaptor domain, generates cellular responses in *Drosophila* consistent with the activation of signaling cascades employed by intrinsic DEgfr.

We have performed extensive genetic screening to identify adaptor and second messenger pathways that are activated by individually reconstituted pTyr, by determining which signaling gene mutants alter *neu* wing phenotypes. In addition, we have screened for genetic deletions on the second and third chromosome that enhance or suppress the wing phenotypes generated by the *neu* add-back alleles. This approach has enabled us to identify several signaling proteins that differentially affect the Neu signaling pathway via association with specific pTyr residues. We have also identified 41 genomic regions in *Drosophila,* which modify signals from either individual or multiple *neu* add-back alleles.

As Neu signaling appears to function in a manner similar to the DEgfr, we sought to determine whether these receptors were capable of heterodimerizing. In

order to examine this we co-expressed a kinase inactive version of the *neu*^{YD} allele with activated *DEgfr*. Co-expression of these receptors suggested that the DEgfr was unable to dimerize with, and transphosphorylate, the YD pTyr on Neu, as no potent anti-apoptotic phenotype was detected. Additionally, co-expression of activated *neu* and the kinase inactive version of *neu*^{YD} resulted in a decrease in glial cell numbers, in relation to mis-expression of the activated *neu* allele alone. These findings suggest that Neu does not interact with the DEgfr, but rather functions via homodimerization of it's receptor subunits.

ACKNOWLEDGEMENTS

I would like to thank my supervisor, Dr. Roger Jacobs, for continued support and guidance during this project. I have grown to appreciate the amount of time and effort required for genetic research and, as a result, have become more independent and confident in my research abilities. For these opportunities to grow, both academically and personally, I am forever thankful.

To the members of the Jacobs lab, you have made my time at McMaster all the more memorable. To Adrienne Stevens, Mythili Nadella, Roni Gordon and Yvonne Sinniah, thanks for your help in easing into a new lab environment. To Amanda Hawley, Jamie Snider, Ying-Shu Huang and Kelly Teal I am indebted for your support, laughter and friendship.

I would especially like to thank Allison MacMullin who has provided moral support, technical advice, guidance and friendship that are beyond the call of duty. For these gifts I am grateful.

To my family and friends, you have been a great support to me over the past few years, and for that I thank you all. And finally, to Cheryl, who has grown to love and appreciate the world of fruit fly genetics. You have been a continual support to me during this degree, and for your encouragement and love I am blessed. Thank you for being there through my successes and hardships, for helping me achieve my goals and for making the journey all that more fun!

TABLE OF CONTENTS

LIST OF ILLUSTRATIONS

LIST OF ABBREVIATIONS

CNS	Central Nervous System
CSP	Canton S – P-element free
DAB	3, 3'-Diaminobenzidine tetrahydrochloride
DEgfr	*Drosophila* EGFR
DNA	Deoxyribonucleic acid
ECL	Enhanced Chemiluminescence
ECM	Extracellular matrix
EGFR	Epidermal Growth Factor Receptor
GAL4	Galactosidase transgene with 4 binding sites
HRP	Horseradish peroxidase
KD	Kinase dead
kDa	Kilodalton
LTR	Long terminal repeat
MG	Midline Glia
MMTV	Mouse mammary tumor virus
NMJ	Neuromuscular junction
PBD	Phosphotyrosine binding domain
PBS	Phosphate buffered saline
PBT	PBS with Triton
PI3K	Phosphatidyl inositol 3 kinase
PNS	Peripheral nervous system
pTyr	Phosphotyrosine
PVDF	Polyvinylidene Fluoride
RIPA	Radioimmunoprecipitation
RTK	Receptor tyrosine kinase
SDS	Sodium dodecyl sulphate
Sev	Sevenless
SH2	Scr Homology 2
SH3	Src Homology 3
UAS	Upstream activating sequence

CONTRIBUTIONS

Micheal Gordon, Stanford University, performed microinjection of the UAS-*neu* alleles, maintained the transgenic stocks and contributed to a large portion of the data in figure six (see legend for details). Jamie Snider, University of Toronto, kindly helped in generating the construct for the kinase inactive version of the neu^{YD} allele.

CHAPTER 1 INTRODUCTION

The growth and development of even simple organisms, requires the coordinated effort of thousands of initially equivalent cells, to form complex tissues containing many distinct cell types. From initial mesodermal, ectodermal and endodermal layers, a number of organs develop, a nervous system is established and numerous appendages and body segments are formed. In order for this to occur, individual cells must be able to recognize environmental cues, integrate multiple signals and then produce an appropriate developmental response (Huang and Rubin, 2000). Cells contain intrinsic signaling molecules, which are able to fill the requirements for each step of the developmental process. When transmembrane receptors recognize extracellular cues, intracellular proteins relay and amplify the signals, and effector molecules convert the signals to specific developmental outputs (Schlessinger, 2000). The molecular events responsible for regulating these signaling processes appear to be generally conserved and used repeatedly in different contexts throughout all developmental stages (Huang and Rubin, 2000).

Structural changes in these transmembrane receptors, which lead to increased kinase activity, result in an oncogenic potential. In some cases, major structural changes lead to receptor activation, while in other instances a single

amino acid substitution is sufficient to induce ligand-independent constitutive activity (Wides et al., 1990). The mechanisms by which structural changes lead to deregulation of the receptor's kinase activity provides a key to understanding the normal mechanism of signal transduction by these receptors.

1.1 CELL SIGNALING BY RECEPTOR TYROSINE KINASES

All metazoans have numerous genes that encode for proteins that function as membrane spanning cell surface receptors (reviewed by Schlessinger, 2000). These receptors can be classified based upon the ligands they recognize, their primary structures or the biological responses they induce. The activity of these cell surface receptors is regulated by a number of ligands that are able to bind to the extracellular domain of the receptors. These ligands include small organic molecules, lipids, carbohydrates, peptides and proteins (Schlessinger, 2000). One large family of cell surface receptors is endowed with intrinsic protein tyrosine kinase activity. These receptor tyrosine kinases (RTKs) catalyze the transfer of the γ phosphate of Adenosine Triphosphate (ATP) to hydroxyl groups of tyrosines on target proteins (Hunter, 1998). RTK's play an essential role in almost all fundamental cellular processes including cell cycle, cell migration, cell metabolism, cell survival, proliferation and differentiation (Schlessinger, 2000).

All RTKs contain an extracellular ligand-binding domain (often glycosylated) which is connected to the cytoplasmic domain by a single transmembrane helix. The cytoplasmic domain contains a conserved protein

tyrosine kinase (PTK) core, as well as additional regulatory sequences, which may be autophosphorylated and phosphorylated by heterologous protein kinases (Hunter, 1998). With the exception of the insulin receptor (IR) family of RTKs, all known RTKs exist as monomers in the cell membrane. Ligand binding induces dimerization of these receptors resulting in autophosphorylation of distinct tyrosine residues located within their cytoplasmic domains (Simon, 2000). These phosphorylated tyrosine residues (pTyr) serve as additional binding sites for cytoplasmic or plasma membrane associated proteins, which transduce a growth or differentiating signal to the nucleus (Figure 1). These signaling proteins interact with pTyr via Src homology 2 (SH2) or protein tyrosine binding (PTB) domains, enabling direct interaction with the activated receptor in a phosphotyrosine-dependent manner (Pawson and Nash, 2000). SH2 domains are protein modules of ~100 amino acids that recognize phosphotyrosine residue-containing peptides in the context of 3-6 carboxy-terminal amino acids (Pawson and Nash, 2000). The second messenger proteins may be enzymes, including kinases, phosphatases or phospholipases, which further propagate intracellular signaling cascades. Other adaptor proteins act as intermediates, by linking enzymes to the activated receptor, or activate them via association with the membrane (Schlessinger, 2000). For example, adaptor proteins such as Grb-2 or Shc associate with activated RTKs through their SH2 domains, and further recruit the guanine nucleotide exchange factor Son of Sevenless (Sos) through its SH3

Figure 1. Activation of Receptor Tyrosine Kinases (RTKs). Transmembrane RTKs exist as monomeric units, which dimerize in response to extracellular ligand cues. Once the ligand (marine blue) has bound specific binding sites and dimerization has occurred, the activated receptors transphosphorylate specific tyrosine residues (P) in the cytosolic domain. These phosphotyrosines serve as binding sites for the SH2 domains of additional adaptor proteins (purple) and second messengers. These adaptors are most often membrane linked and usually activate additional messenger proteins (not shown) to propagate a signal to the nucleus. Additionally, not all adaptors or second messengers are phosphorylated upon activation. Receptor binding ultimately initiates a signaling cascade that involves many intracellular proteins (green), which eventually function in activating specific nuclear transcription target genes.

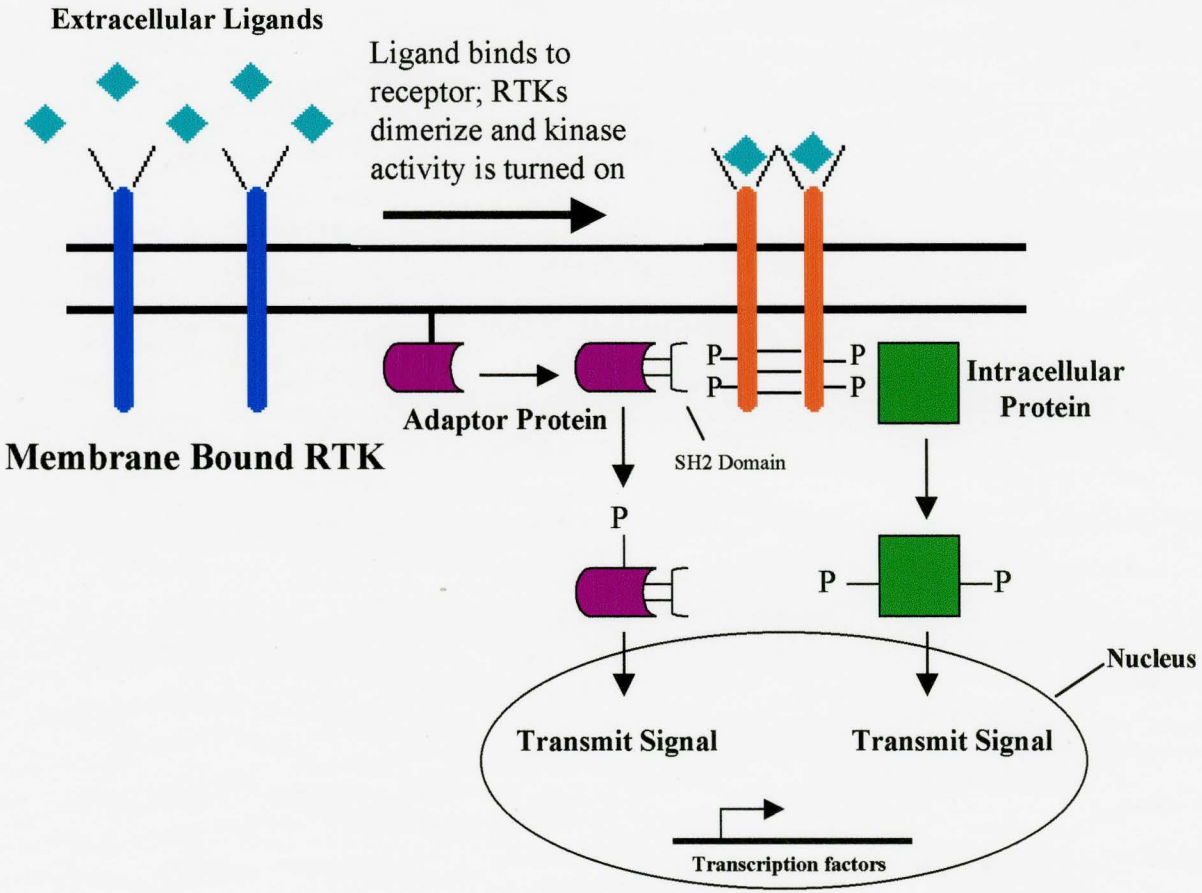
Extracellular Ligands
Ligand binds to receptor; RTKs dimerize and kinase activity is turned on
Membrane Bound RTK
Adaptor Protein
SH2 Domain
P
P
P
P
Intracellular Protein
P
P
P
Nucleus
Transmit Signal
Transmit Signal
Transcription factors

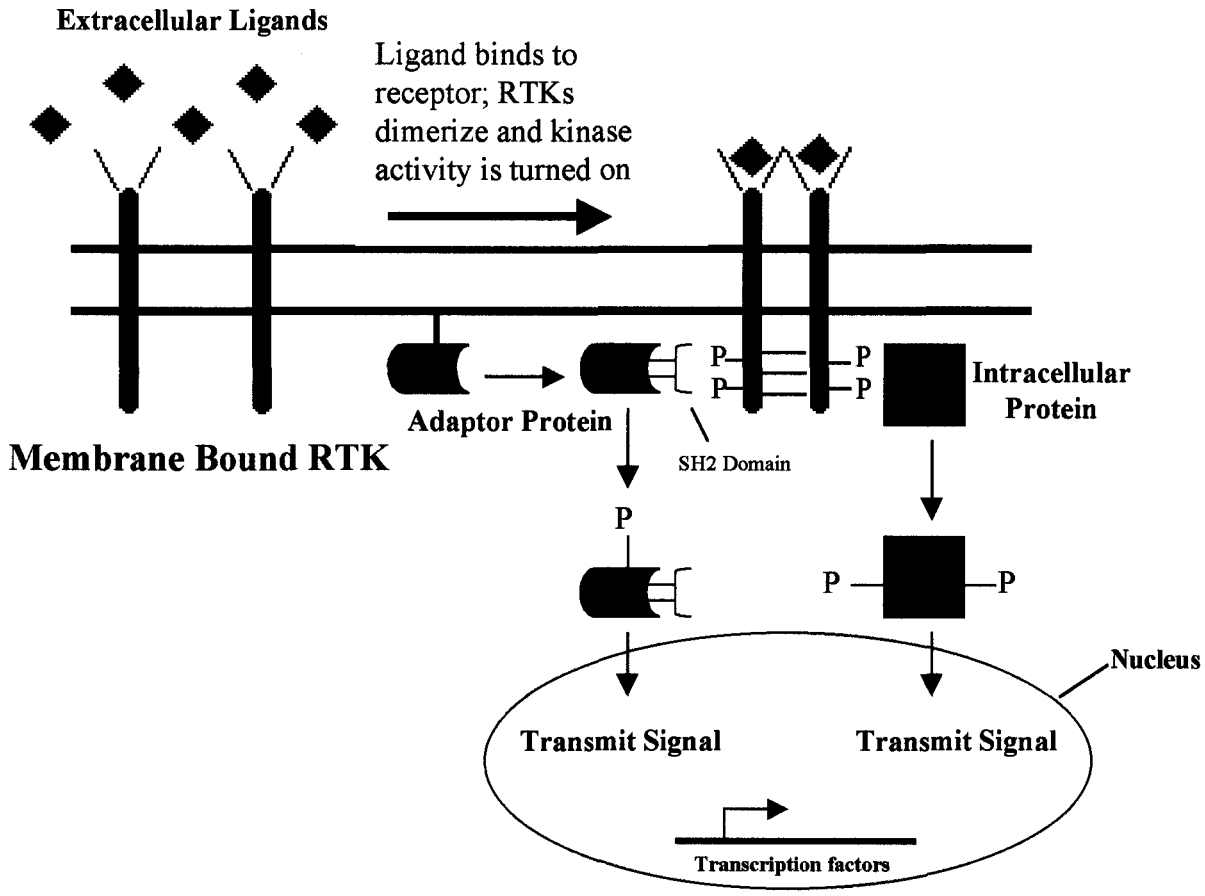
Extracellular Ligands
Ligand binds to receptor; RTKs dimerize and kinase activity is turned on
P
P
P
P
Intracellular Protein
Adaptor Protein
SH2 Domain
Membrane Bound RTK
P
P
P
Nucleus
Transmit Signal
Transmit Signal
Transcription factors

domain. This process leads to the activation of downstream Ras effectors such as Raf and PI-3K (Olivier et al., 1993).

Models for RTK signaling specificity

One of the poorly understood aspects of RTK signals, is the basis for their specificity. RTK activation induces a signal transduction pathway commonly referred to as the "RTK signaling cassette" (Ghiglione et al., 1999). This cassette includes the second messengers and adaptors that, upon association with the activated receptor, regulate the level of Ras-GTP in the cell. Accordingly, an increase in the level of Ras-GTP activates the Raf, MEK and MAPK serine/threonine kinase cascade (Ghiglione et al., 1999). The conservation of this signaling cassette among many RTKs undermines the importance of determining the molecular mechanisms, which elicit specific responses upon RTK activation. Additionally, RTK signaling can trigger either activation or repression of gene expression, adding another degree of complexity to the signaling output (Roch et al., 2002).

There are two basic models for how unique developmental responses might be generated in response to the activation of different RTKs. Qualitatively, specificity is thought to reside in the cell's developmental history, which includes the array of transcription factors that are present in the nucleus that can be regulated by MAPK activation. In contrast, RTK specificity may be due to intrinsic differences in the intracellular signaling pathway and the sub-cellular

localization of the activated receptor complexes. By this means, a quantitative difference in the strength or duration of the signal, as well as cross-talk between activated receptors, provides RTK specificity (Simon, 2000; Li and Perrimon, 1997).

1.2 PHOSPHOTYROSINE SPECIFICITY IN RTK SIGNALING

The activation of a single type of RTK leads to the activation of multiple intracellular signal transduction pathways. A simplistic model would suggest that each pathway would have a distinct function; however, this generalization has been called into question by numerous studies examining RTK mutants. One such study, of the platelet-derived growth factor (PDGF) RTK in cell culture, led to the conclusion that the downstream pathways are in fact redundant in terms of what genes they activate (Fambrough et al., 1999). Fambrough (1999) demonstrated that the simultaneous mutation of five SH2 binding sites, which greatly reduces the biological responsiveness of PDGFRβ function in cultured cells, had only minimal quantitative effects on early gene induction in response to ligand binding as measured by microarray hybridization. These data suggest that none of the sites tested (which bound PI-3K, Ras-GAP, SHP-2, and PLCγ) were essential for gene activation. Since PDGFRβ is known to be phosphorylated on 11 sites, it was suggested that those signaling sites which were not mutated in this study may play non-redundant roles in transcription. If this view were entirely

correct, then it would be assumed that RTKs function solely to activate generic transcription factors, whose activities would determine the response to signaling (Madhani, 2001).

Numerous studies oppose this view and provide clear evidence that individual RTK pTyr do in fact provide discrete signaling pathways, which elicit specific cellular responses. Earlier work done on the PDGF receptor implicated PLCγ and PI-3K as discrete downstream mediators of the PDGF receptor's mitogenic signal (Valius and Kazlauskas, 1993). Since the PDGFR initiates multiple, redundant mitogenic pathways, studying the effect of removing one of the binding proteins, when all the others can still associate, would be of little value. Valius and Kazlauskas (1993) circumvented this problem by creating a PDGFR mutant unable to bind PLCγ, RasGAP, PI-3K and a 64 kd protein and found that this mutant could not mediate PDGF-dependent DNA synthesis. A series of mutants were then created which individually restored the binding site for each of these receptor associated proteins (herein termed "add-back" allele). These were then tested for their ability to rescue the signaling capacity of the receptor. It was found that binding of either PLCγ to Y1021 or PI-3K to Y40/51 completely restored the ability of the PDGFR to initiate DNA synthesis (Valius and Kazlauskas, 1993). This was one of the first studies performed which identified the importance of testing individual RTK pTyr for their ability to rescue signaling from a mutant receptor. This approach identifies not only those

messenger proteins required to rescue mutant RTK signaling, but also the distinct pTyr site upon which these proteins bind.

Functional analysis of EGFR pTyr *in vivo*

Numerous studies of the PDGF and Epidermal Growth Factor (EGF) receptors have identified the sites of tyrosine phosphorylation on these RTKs and the proteins that associate with these sites. However, analyses in cell culture assays of the function of these sites have not always provided a clear answer of their contributions to the signaling output (Fambrough et al., 1999). To substantiate such findings, it is important to address these issues in an *in vivo* setting. Model systems such as *Drosophila* and *Caenorhabditis elegans* provide useful tools for such assays. Engineered animals offer an appropriate test since, in principle, ligands and receptors are expressed at physiological levels and in the correct temporal pattern and tissue context (Madhani, 2001).

Functional analysis of the EGFR has been performed by studies examining the signaling capability of individual pTyr residues. Pioneering research by Lesa and Sternberg (1997) was the first such study, which employed individual "add-back" alleles of the *C. elegans* EGFR homolgue LET-23. LET-23 has multiple functions during development and has eight potential SH2 binding sites. By analyzing transgenic nematodes for three distinct LET-23 functions (viability, vulval differentiation and fertility), they were able to show that six of eight potential sites functioned *in vivo*. Three sites were involved only in viability and

vulval differentiation, one site promoted wild-type fertility, one site mediated all three LET-23 functions and the other site mediated tissue-specific negative regulation (Lesa and Sternberg, 1997).

These studies demonstrate that putative SH2 binding sites are not equivalent *in vivo* and can mediate either positive or negative tissue specific regulation. Results from such experiments suggest that RTK tissue specificity *in vivo* is regulated by at least two independent mechanisms. Tissue-specific effectors and tissue-specific negative regulators act synergistically to propagate RTK signaling pathways in some cell types, while repressing it in others (Simon, 2002).

1.3 VERTEBRATE FAMILY OF EGF RECEPTORS

In contrast to *C. elegans* and *Drosophila*, wherein only a single EGF receptor exists, the vertebrate Epidermal Growth Factor Receptor (EGFR) family of RTKs consists of ErbB-1/EGFR, ErbB-2/Neu, ErbB-3 and ErbB-4. Activation of the EGFR family, by EGF and neuregulin ligands, is thought to play a critical role in both embryogenesis and oncogenesis. The biological activities of these receptors are achieved through various ligand-receptor and receptor-receptor (homodimeric and heterodimeric) interactions (Chan et al., 2002).

Gene targeting studies have demonstrated specific roles for each of the EGFR family members during normal mammalian development. For example,

erbB-2 and *erbB-4* knockout mice die at midgestation due to deficient cardiac function and display abnormal development of the peripheral nervous system (PNS) (Chan et al., 2002; Lin et al., 2000). ErbB-3 mutant mice have milder heart defects, allowing them to survive several days later through embryogenesis. However, sensory and motor neurons in these animals show signs of degeneration due to a lack of Schwann cell development (Lin et al., 2000).

Two aspects of EGFR signaling have been of particular interest, as they do not follow the accepted linear model of signaling cascades. Firstly, ErbB-2 binds no known ligand and secondly, ErbB-3 is devoid of catalytic activity (Chan et al., 2002). It is important to note that while activated ErbB receptors may partake in any combination of homodimerization or heterodimerization complexes, there is generally a greater preference for these complexes to include ErbB-2 due to its potent intrinsic kinase activity (Chan et al., 2002). Interestingly, the most potent mitogenic signal originates from heterodimerization of ErbB-2 and ErbB-3 (Yarden and Sliwkowski, 2000). Additionally, more potent signaling results from heterodimerization complexes, as opposed to homodimerization of ErbB receptors. This effect is likely due to proteosomal and lysosomal degredation of ErbB-1 and ErbB-2 homodimers through the action of c-Cbl, a ubiquitin ligase. Heterodimers are targeted to cellular recycling and therefore their signaling is longer and more potent (Yarden and Sliwkowski, 2000).

ErbB-2/Neu is overexpressed in about 30% of human breast cancers and is also frequently altered in lung and kidney carcinomas (Hynes and Stern, 1994). While activation of this gene correlates with poor patient prognosis, the precise mechanism by which ErbB-2 activation leads to oncogenic transformation or metastasis of epithelial cells is unknown. Four of five individual pTyr of activated Neu appear to contribute individually to cell transformation of cultured fibroblasts (Dankort et al., 1997); however, no single pTyr residue is able to substitute for signaling from a wild-type RTK. In the case of Neu, single pTyrs, which couple to the Ras pathway through Grb-2 (Y1144) or Shc (Y1227), can act to transform cultured fibroblasts (Dankort et al., 1997; Dankort et al., 2001). However, examination of these signaling pathways *in vivo* reveals that signaling through Grb-2 alone in mammary epithelia, results in a higher rate of metastasis than signaling through Shc alone (Dankort et al., 2001).

1.4 IDENTIFICATION OF PHOSPHOTYROSINE OUTPUTS

The identification of pTyr signaling outputs is largely established by experiments examining peptide inhibition, labeling of phosphotyrosines and protein co-immunoprecipitation *in vitro* (reviewed by Pawson and Nash, 2000; Schlessinger, 2000). A great deal of research has also addressed the role of SH2 and SH3 domains in pTyr receptor binding specificity. The potential flexibility of SH2 domains is noted by the ability of single amino acid substitutions to alter

binding specificity (Pawson and Nash, 2000). Songyang et al. (1995) demonstrated this by altering a Src SH2 domain to a Grb-2 like SH2 domain by altering a Threonine to a Tryptophan. This mutant Src SH2 domain mimicked Grb-2 at the structural level and functioned in *C. elegans* development as if it were a Grb-2 SH2 domain. This flexibility may have an evolutionary advantage, allowing for a rapid change of SH2 domain binding specificity, an thus allowing the formation of new signaling connections as metazoan organisms evolved (Pawson and Nash, 2000). *In vitro* experiments that identify pTyr outputs, or protein sequences required for receptor binding, can be validated by functional assessment *in vivo*. These assays further reveal the functional distinction of individual pTyr outputs.

1.5 *DROSOPHILA* IS A POWERFULL TOOL FOR SCREENING VERTEBRATE TRANSGENES

The potency of ErbB-2 signaling, its overwhelming predominance in human breast cancers and the many questions remaining with respect to it's dimeric partners and activating ligands have prompted us to further investigate this RTK in a model organism more amenable to genetic dissection. Genetic analysis is an efficient means for identifying signal pathways *in vivo*. The function and structure of many SH2 and PTB proteins in signaling is conserved in model organisms such as *C. elegans* and *Drosophila*. For example, the human GRB2 and *Drosophila* Drk proteins have been found to rescue *sem-5* function in

C. elegans. Furthermore, SEM-5 has been shown to associate with the human EGF receptor, and shares an identical architecture of its SH2 and SH3 domains with GRB2 (Stern et al., 1993). Additionally, the PTB and SH2 binding properties of *Drosophila* Shc (dShc) and mammalian Shc show highly conserved function (Lai et al., 1995).

Numerous studies have taken advantage of well-characterized signal transduction pathways in *Drosophila* to screen for proteins that are able to interact with vertebrate transgenes. These structure-function relationship studies of large multi-domain proteins, require simple model systems amenable to various genetic and *in vivo* biochemical analyses (Jackson et al., 2002). Bhandari and Shashidhara (2001) utilized this genetic approach to examine, *in vivo*, interactions between human Adenomatous Polyposis Coli (APC), β-catenin and other components of the Wnt signaling pathway. Mutations in human *Apc*, a tumor suppressor gene, predisposes individuals to both familial and sporadic colorectal cancer. Cell lines with mutations in the *Apc* gene show enhanced levels of β-catenin, which suggest that APC has a role in negatively regulating the cellular levels of β-catenin (Bhandari and Shashidhara, 2001). β-catenin, a transducer of Wnt signaling, is a potential oncogene, the enhanced activation of which is the cause of numerous cancers such as colon, ovarian, prostate, uterine and medulloblastoma. Using hAPC induced eye phenotypes as an assay in a screen for genetic modifiers of APC function, Bhandari and Shashidhara (2001) showed

that transgenic flies carrying full length human APC negatively regulated the function of Armadillo, the *Drosophila* homologue of β-catenin. This is turn resulted in further inhibition of Wingless (Wnt/Wg) signaling and gave rise to eye phenotypes similar to those associated with loss of Wg function. Further screening of these inducible eye phenotypes identified two new loci in *Drosophila* which may modulate Wnt signaling. Additionally, their work demonstrates that at least one of the currently used anti-cancer drugs specifically inhibits the Wnt signaling pathway when fed to flies.

Such studies have been duplicated many times, using a variety of inducible phenotypes to screen for loci in *Drosophila* which modulate signaling from human transgenes. Among others, this technique has successfully identified members of different signaling pathways involved in suppressing neurodegeneration induced by human Tau (Jackson et al., 2002) as well as suppressors of the photoreceptor degeneration and lethality associated with the human Huntingtin transgene (Kazantsev et al., 2002; Rubinsztein, 2002). Directly expressing human proteins in flies is fast gaining wide acceptance. Such a gain-of-function genetic approach allows researchers to study, not only the function of human proteins in relation to a specific disease, but also to study the diseases themselves (Jackson et al., 2002). Transgenic flies expressing human proteins can be used to identify additional components of genetic pathways as well as disease

inhibitors, as revealed by enhancer-suppressor screens (Bhandari and Shashidhara, 2001).

1.6 STRUCTURE AND SIGNALING CONSERVATION BETWEEN Neu AND THE DEgfr

The *Drosophila* epidermal growth factor receptor homologue (DEgfr) displays sequence similarity to both the epidermal growth factor receptor (ErbB-1) and the ErbB-2/Neu vertebrate proteins (Figure 2). Sequence comparison of Neu and the DEgfr reveals the highest degree of structural homology (79%) within the kinase domain of these two receptors. Although the docking domains share the least conserved structural similarity (31%), three of the identified phosphotyrosine residues in both Neu and the DEgfr show conserved (YA and YD) or identical (YC) peptide binding motifs flanking the known phosphorylation sites. DEgfr shares an overall 56% amino acid similarity with Neu. Given the relative structural conservation that these receptors share, and the observation that the DEgfr is able to increase phosphotyrosine levels in COS cells (Wides et al., 1990), suggests that these receptors share similar binding capabilities and that transgenic Neu may associate with those adaptor proteins involved in endogenous DEgfr signaling. Additionally, a single substitution in the transmembrane domain of the DEgfr, at a position comparable to the oncogenic Neu protein, results in activation of the DEgfr in a manner similar to Neu (Wides et al., 1990). The ability to mimic this effect suggests that such changes to enhance kinase activity

Figure 2. Comparison of the primary structure of Neu and the DEgfr. Sequence analysis of Neu and the DEgfr reveals a high degree of conservation between the kinase domain of these receptors. While the least conserved region is the docking domain, further analysis reveals that several identified pTyr sites in Neu show a high degree of sequence similarity with identified pTyr sites in the DEgfr. Only one identical peptide sequence (PEYL) can be seen flanking a pTyr site in both receptors, however two other pTyr sites are highly conserved, suggesting the possibility of conserved roles and function. This figure is kindly adapted from J. Roger Jacobs.

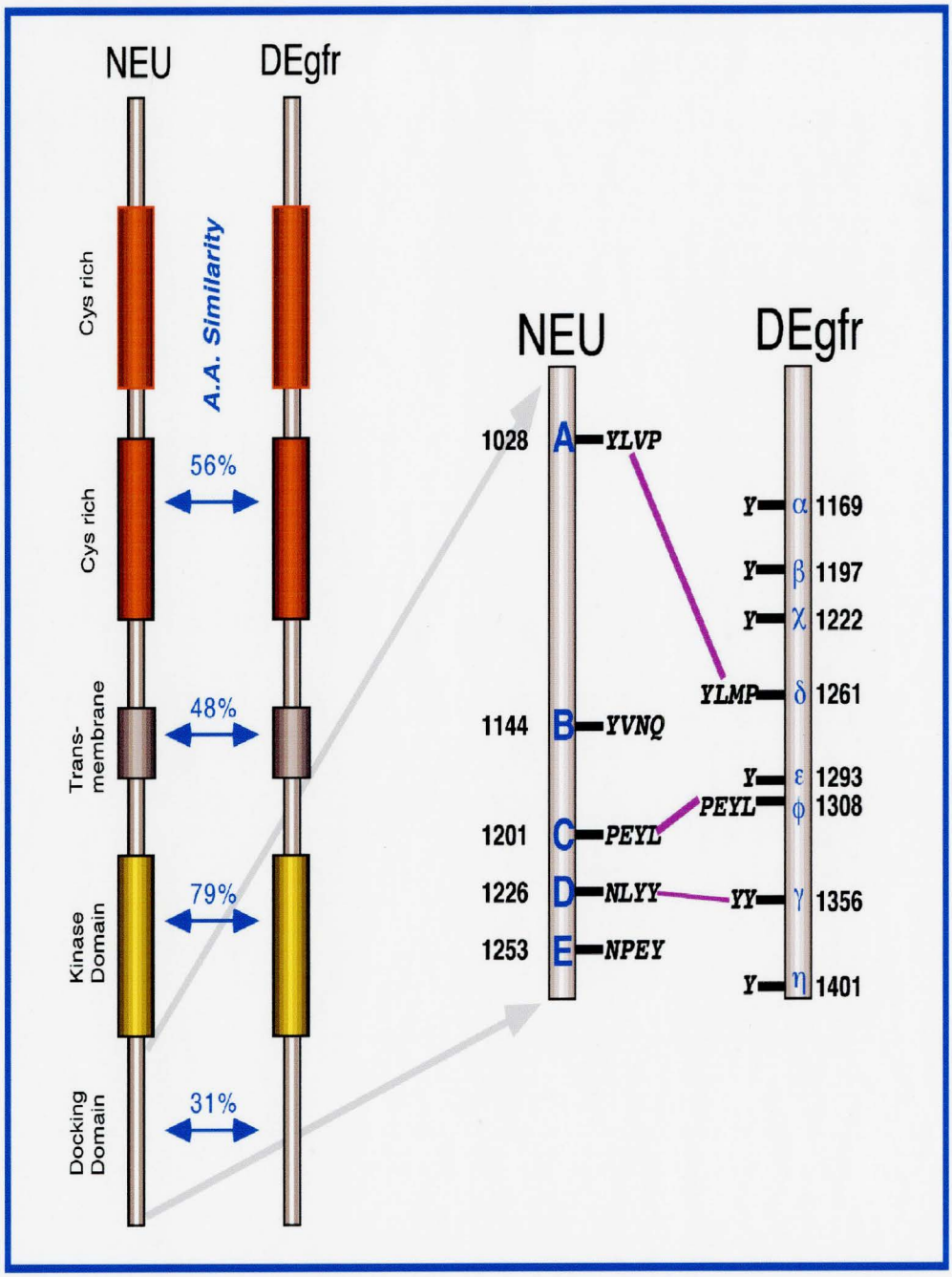
NEU
DEgfr
A.A. Similarity
Cys rich
Cys rich
Trans-membrane
Kinase Domain
Docking Domain
56%
48%
79%
31%
NEU
DEgfr
1028
A
YLVP
1144
B
YVNQ
1201
C
PEYL
1226
D
NLYY
1253
E
NPEY
YLMP
PEYL
YY
Y
α
1169
Y
β
1197
Y
χ
1222
δ
1261
Y
ε
1293
φ
1308
γ
1356
Y
η
1401

is general to this family, provided that the altered residue maintains the three-dimensional structure of the receptor (Wides et al., 1990). Given these similarities we have examined the complementary potential of known adaptor binding sites in Neu to interact with *Drosophila* signaling proteins.

Multiple Roles for the DEgfr During *Drosophila* Development

The sole *Drosophila* EGF receptor tyrosine kinase fulfills multiple roles during development, as indicated by the many names given to mutant alleles of the locus (*Egfr, faint little ball, torpedo* and *Ellipse*) (Reviewed by Schweitzer and Shilo,1997). Among its many roles, DEgfr signaling is required to specify ventral ectoderm after gastrulation, to provide polarity information in the ovary, to induce wing vein cell fate during wing development, to suppress apoptosis of the midline glial (MG) cell lineage and to provide waves of cell proliferation and differentiation during eye development (Raz et al., 1991). Specifically, DEgfr signaling in the midline functions by phosphorylating and inhibiting *head involution defective (hid)*, thereby suppressing apoptosis in those MG cells which will serve to maintain the cyto-architecture of the CNS. DEgfr signaling is activated by three ligands (Spitz, Gurken and Vein) and inhibited by one (Argos). Argos competes with activating ligands of the DEgfr and prevents receptor dimerization. Expression of *argos* is activated by DEgfr signals, and functions to restrict the time frame of DEgfr signaling and to maintain graded DEgfr

activation. Accordingly, in *argos* mutant embryos, the DEgfr pathway is hyperactivated (Schweitzer and Shilo,1997).

1.7 TRANSGENIC Neu GENERATES PHENOTYPES SIMILAR TO ACTIVATION OF DEgfr

Given the structural conservation of RTKs and the conserved signaling "cassettes" utilized among metazoans, we investigated whether the adaptor binding sites of a vertebrate RTK could successfully signal through adaptor proteins in *Drosophila*. Using an organism, such as *Drosophila*, which is easily manipulated by genetic dissection of signal transduction pathways is favorable for analyzing Neu receptor function. Many genes involved in signal transduction reveal gene dosage dependent phenotypes (Rogge et al., 1991; Simon et al., 1991). Accordingly, genetic screens that detect dosage sensitive modifiers of phenotypes resulting from mis-expression of an activated RTK, like Neu, should reveal genes whose functioning is required to propagate Neu signaling. By investigating Neu signaling in the wing, a non-essential tissue which does not affect viability, we were able to more readily assess the potency of Neu pTyr signals, the contribution of each pTyr to output pathways and the adaptors which are required for signaling from these individual pTyr (Figure 3).

Simultaneous point mutations in all five of the known pTyr of Neu, creating a Neu Tyrosine Phosphorylation Deficient (Neu^{NYPD}) allele, demonstrated that most of the oncogenic activity of Neu occurs through signaling

Figure 3. Adaptor proteins and second messengers involved in signaling from vertebrate and *Drosophila* Neu Phosphotyrosines. Initial models for the regulatory components of Neu signaling were based upon analysis of the primary sequence of the receptor and putative consensus binding domains. Adaptor proteins and second messengers were then identified, based upon the likelihood that they bind to or interact with these consensus domains on the Neu receptor (See Appendix, Figure 2). Our genetic data revealed that the vertebrate and *Drosophila* Neu output pathways show conserved signaling from Neu^{YD} and Neu^{YB}. While both vertebrate and *Drosophila* Shc function in Neu^{YD} signaling, further roles for Dshc are unknown as this protein lacks the Grb-2 binding site present in vertebrate Shc. Both receptors require Grb-2 in signaling from Neu^{YB}; however, much speculation remains over the function of the remaining Neu pTyr. Both model organisms activate a conserved signaling cassette that includes the guanine nucleotide exchange factor Sos and Ras/Raf pathways. In *Drosophila*, Neu^{YE} signaling does not respond to reduced Ras levels, but is suppressed by a reduction of Raf function. While very little is known about the signaling output of Neu^{YA}, this site appears to inhibit Neu RTK function in both model organisms. This figure is kindly adapted from J. Roger Jacobs.

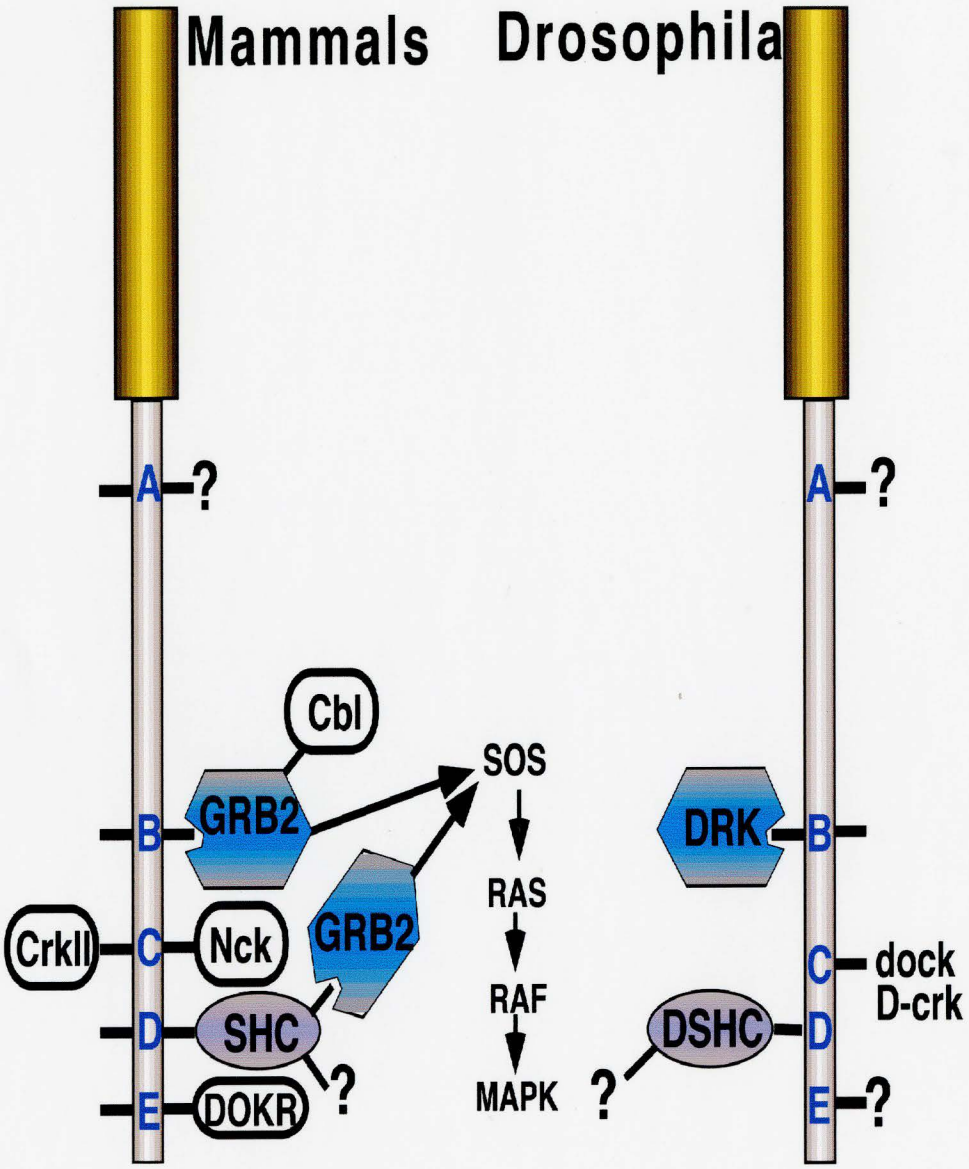
Mammals
Drosophila
A
?
Cbl
GRB2
B
SOS
RAS
RAF
MAPK
GRB2
CrkII
Nck
C
SHC
D
DOKR
E
?
DRK
B
C
dock
D-crk
DSHC
D
?
E
?
A
?

via pTyr. Reconstitution of single pTyr to Neu^{NYPD} demonstrated that transformation can be independently mediated via four of five Neu pTyr sites (Dankort et al., 1997; Dankort and Muller, 2000). We therefore, mis-expressed add-back *neu* alleles in the embryonic CNS midline and wing of *Drosophila,* two tissues known to require DEgfr signaling during pattern formation. Mis-expression of these *neu* alleles resulted in phenotypes consistent with increased activation of endogenous DEgfr signaling. We established phenotypes in the wing and midline that were suitable for analysis by dosage sensitive modifier genetics and have thus been able to identify several *Drosophila* adaptors and second messengers which function in signaling from individual Neu pTyr. Flies were examined which were heterozygous for individual *neu* add-back alleles and amorphic alleles of various adaptor proteins or second messengers. Gene function was assigned to individual Neu pTyr, by noting which alleles were able to suppress *neu* wing phenotypes, and thus Neu signaling. Mis-expression of *neu* "add-back" alleles provides a means of activating only a subset of downstream effectors, and thereby identifying genes that may have otherwise been missed due to potential functional redundancy. In addition to identifying components of the Neu signaling pathway, we expanded our study by screening for enhancers and suppressors of established *neu* wing phenotypes. Using second and third chromosome deficiency kits, we were able to identify a number of genomic regions and putative genes in *Drosophila* that enhanced or suppressed signaling

from the subset of *neu* alleles. Interestingly, we identified certain deficiency regions that affected signaling from only single Neu pTyr sites. This screening provides the starting point for a genetic approach to identifying novel genes involved in the regulation and signaling output of individual Neu pTyr.

Identifying new genes, which are involved in down-regulating the Neu signaling pathway in *Drosophila* could have profound effects in continuing vertebrate studies of Neu signaling components. Genetic screening in *Drosophila* provides a means for quickly and efficiently analyzing RTK signaling pathways *in vivo*. Ultimately, this research serves as a foundation for further studies aimed at isolating components of vertebrate Neu signaling pathways. The benefits of such studies could have profound effects in aiding the continual battle against the alarming predominance of Neu overexpression in many forms of human cancer.

CHAPTER 2 METHODS

2.1 *DROSOPHILA MELANOGASTER* FLY STOCKS

Drosophila melanogaster fly strains were obtained from the Bloomington Stock Centre, unless indicated otherwise. All fly lines were stored at room temperature (22-25°C) in polypropylene shell vials (Fisher Scientific, AS519) or 16 x 100 mm glass culture tubes (Fisher Scientific) supplemented with a sucrose-yeast agar food medium and capped with rayon rope (Fisher Scientific, APS205). The wild type CSP (Canton S P-element free) strain was used in all controls. Microinjection was performed on *yellow white⁻ (yw⁻)* embryos. Expression of *p[UAS-neu]* was regulated by *p[GAL4]* strains, simGAL4 (Xiao et al., 1996), GMRGAL4 (Hay et al., 1997), and C96 (Gustafson and Boulianne, 1996;Stewart et al., 2001).

2.2 MUTATIONS, DEFICIENCIES AND pUAST LINES

All mutants, deficiencies and pUAST lines used are reported in Table 2.1.

2.3 EMBRYO AND LARVAL COLLECTIONS

Embryo collection was performed by placing adult flies in 100 mL plastic beakers with holes punched in them for airflow. The beakers were capped with 60 X 15 mm plastic petri dishes, containing solidified apple juice agar and a dab of yeast paste to encourage egg laying. These "houses" were kept in the dark at

25°C, and changed twice daily to collect a mixture of embryonic developmental stages. Morning plates (09h00) were left for approximately eight hours before changing. In the evening (17h00), these plates were transferred to 18°C to slow development overnight and then transferred to 4°C the following morning to further halt development at approximately stage 17. Evening collections (17h00) were transferred to 18°C the following morning (09h00) and then transferred to 4°C that evening (17h00). Both sets of plate cycles were left at 4°C until the time of fixation (no later than 72 hours post-oviposition). This method allowed a mixture of mid stage to late stage embryos to be collected. Embryos were staged according to Campos-Ortega and Hartenstein (1985).

Third instar larvae were collected directly from yeast food vials. As these larvae are undergoing the "wandering stage" of development, those found to be crawling up the sides of the vial were deemed to be at the appropriate 3rd instar larval stage.

2.4 FIXATION PROTOCOL

Plates stored at 4°C were placed at room temperature for one hour prior to fixation to allow for mictotubule repolymerization. The embryos were then dechorionated by soaking them in a 50% bleach solution for five minutes and collected by rinsing them into a nitex sieve chamber with distilled water. The embryos were air dried on the sieve and then dunked into a scintillation vial

containing 5 mL of heptane, 4.5 mL of 1X PBS and 0.5 mL of 37% formaldehyde. The scintillation vial containing the embryos was placed on a rotator and the embryos were fixed this way for 30 minutes.

After fixation, the bottom layer (PBS + fixative) was removed and the embryos were devitellinized by vigorously spraying them with methanol and then shaking them quickly for approximately 20 seconds. The devitellinized embryos sank to the bottom of the vial and were transferred to a clean glass test tube using a pasteur pipet. The embryos were repeatedly washed with methanol, and transferred to a new glass tube after every third wash. Washes were complete after three changes of glassware. Embryos could then be stored at 4°C in methanol for future use (within a three week period).

2.5 IMMUNOCYTOCHEMISTRY PROTOCOL

Embryos ready for antibody labeling were hydrated by multiple PBT (1X PBS and 0.5 % Triton-X detergent) washes. Following a minimum of five PBT washes, the embryos were placed on a rotator for 20 minutes in PBT. After rotating, embryos were allowed to settle and the PBT was removed to approximately 40µl (ensuring embryos remained submerged). Embryos were then blocked to remove non-specific binding with a 1:20 dilution of normal goat serum (Jackson Immunoresearch Laboratories, Inc.) in PBT for 40 minutes at room temperature on an orbital shaker. The primary antibody was then added at the appropriate dilution and the embryos were placed on an orbital shaker at 4°C

for overnight incubation. The following day, the embryos were washed 5 times with PBT and then placed on a rotator for four hours at room temperature or overnight at 4°C to remove excess primary antibody. Following this extensive washing period, the embryos were re-blocked and then incubated on an orbital shaker for two hours at room temperature in the appropriate dilution of horseradish peroxidase (HRP) labeled or biotinylated secondary antibody. Embryos in HRP labeled secondary were washed 5 times with PBT and then rotated overnight at 4°C in PBT. Embryos in biotinylated secondary were rinsed for 2 hours on a rotator at room temperature in PBT. Following this wash, the PBT was removed and 100 µl of 2% A+B Vectastain Reagents (VectaStain) were added. These reagents were allowed to incubate with the embryos for 1 hour. The embryos were then rinsed 5 times with PBT in preparation for the peroxidase reaction.

To begin the HRP colourimetric reaction, the embryos were incubated in a 0.33 mg/ml solution of DAB in PBT for two minutes and then developed by adding 3 µl of 0.03% hydrogen peroxide. Once the desired color was observed, the reaction was stopped by diluting with PBT. The embryos were then dehydrated with successive ethanol gradients and stored in methyl salicylate.

2.6 X-GAL STAINING FOR β-GALACTOSIDASE DETECTION

X-gal staining was performed to screen fly lines for the stable incorporation of the AA142 glial enhancer trap. The presence of supernumary glia also indicated that individual *neu* alleles were incorporated.

Embryos were collected and dechorionated as described in section 2.3. Once dechorionated, embryos were rinsed into a nitex-lined multi-welled unit. The unit was blotted dry and then immersed in a 100 x 15 mm square polystyrene petri dish containing heptane. After this equilibriation, pure heptane was exchanged for heptane saturated with fixative (2.5% gluteraldehyde in 1X PBS, pH 7.4). The embryos were fixed for twenty minutes on an orbital shaker. The fixative was then removed and the embryos were washed twice with fresh heptane. PBT was applied forcibly to the embryos in the well to remove residual heptane and prevent clumping. The embryos were then washed in 4X changes of PBT every 15 minutes for one hour on a shaker. During this hour the X-gal solution (10mM PO_4 buffer [pH 7.2], 150mM NaCl, 1mM $MgCl_2$, 3.1 mM K4[Fe(CN)6]3H_2O, 3.1 mM K3[Fe(CN)6]3H_2O, 0.3% Triton) was warmed at room temperature. After the hour wash, the unit was placed in 10mL of room temperature X-gal reaction solution for five minutes, during which time another 10mL of the X-gal solution was warmed to 65°C (until solution turned cloudy). 250µl of 8% X-gal in dimethylsulfoxide was added to the heated solution. The heated X-gal solution and the unit were placed in the square petri dish and left at

room temperature overnight on an orbital shaker until the desired staining was observed.

2.7 TRANSGENES

The injection of pUAST activated rat *erbB2 (neuNT)*, *neuNYPD* (phosphorylation deficient; or tyrosine to phenylalanine transition at 1028, 1144, 1201, 1226, 1227 and 1253) and add back mutants restoring tyrosine to YA(Y1028), YB(Y1144), YC(Y1201), YD(Y1226/7) and YE(Y1253) was performed by Michael D. Gordon following procedures from 2.8. Jamie Snider kindly generated a kinase inactive form of *neuYD* by ligating a neu^{K757M} 5' NcoI fragment with a *neuYD* 3' NcoI fragment. Transgenes were shuttled from pcDNA3 vector as a Not1 fragment into pUAST with T4 ligase overnight at 14°C. The next day, the pUAST-$neu^{K757M/YD}$ ligation product was transformed into DH5alpha competent cells (Gibco). Transformants were screened by restriction digest and sequencing prior to injection.

2.8 PREPARATION OF DNA CONSTRUCTS FOR MICROINJECTION

DNA constructs were prepared for microinjection so that a total of 30 μg of DNA was present in a 5:1 ratio of the pUAST and helper vector pπ25.1. Individual DNA extractions were performed using endofree plasmid maxi kits (Qiagen, cat#. 12362). Once these constructs were combined, the volume was brought up to 100 μl with distilled water and then precipitated by adding 10 μl of

3M sodium acetate to the mixture. Following precipitation, 250 µl of 100% cold ethanol was added to the mixture, which was then placed at -80°C for 15 minutes. The constructs were then spun at 13 000 rpm for 15 minutes at 4°C. The pellet was washed with 100 µl 70% ethanol and spun again for an additional 5 minutes. After air drying for approximately 10 minutes the pellet was re-suspended in 50 µl injection buffer (10mM Tris-Hcl [pH 7.5], 0.1mM EDTA, 100mM NaCl, 30µM spermine, 70µM spermidine).

2.9 DNA MICROINJECTION

Microinjection of pUAST constructs was performed on *yw*⁻ embryos. The embryos were collected in fly houses as described in section 2.3; however, grape juice agar was used in place of apple juice agar, as it's higher sugar concentration increased egg laying. Fly houses were set-up and maintained at 25°C while plates were changed every thirty minutes so that early stage embryos could be collected and injected prior to pole cell formation. Embryos were dechorionated in a 50% bleach solution for 5 minutes and collected in a nitex sieve chamber. After air-drying, approximately 40-50 embryos were lined up on a strip of double sided adhesive tape (without exceeding 20 minutes), which was attached to a standard glass slide. Once complete, the embryos were placed in a desiccator on a bed on Anhydrous Calcium Sulfate (Drierite™) (W.A. Hammond Company, product #23001) for ten minutes. During this time additional embryos could be mounted

on another slide. Once desiccated, the embryos were covered in a thick layer of halocarbon oil. Injection was performed using a Leica inverted microscope. Needles were pulled from 100mm x 1mm borosil glass capillary tubing (FHC, cat.# 30-30-0) and broken by gently touching two ends of the needles to each other. Approximately 2-3 µl of the desired DNA construct was loaded into the glass needle using a Hamilton 26 gauge needle (Fisher Scientific, cat.# 14-813-1). Injection of the DNA construct was performed in the posterior of the embryo until a small bubble was barely visible within the embryo. Injected embryos were stored in a petri dish on a wet paper towel to provide necessary moisture. The embryos were incubated at 18°C for 48 hours, at which point surviving larvae were transferred to yeast food vials and kept at room temperature until they eclosed. Individual flies were crossed to appropriate *yw*⁻ adults and raised at room temperature, followed by close screening of the F_1 progeny. Flies exhibiting an eye pigmentation were isolated and crossed again to *yw*⁻ adults, after which, stocks were purified for their eye marker. Purified stocks were crossed to various marked balancers in order to map the location of the P-element insertion.

2.10 β-GALACTOSIDASE DETECTION IN WING IMAGINAL DISKS

Third instar larvae were collected and washed in cold 1X PBS for several minutes. Wing imaginal discs were dissected by grasping the larva at the posterior end, and pulling on the anterior mouthparts with fine point forceps.

Wing discs were gently teased away from the salivary glands, fat bodies and anterior parts of the gut, which were often attached as one large mass. The remaining wing discs (with the mouth hooks attached for easier handling) were fixed for 1 hour at room temperature or overnight at 4°C in 1% gluteraldehyde in PBS. Following fixation, the discs were washed twice for 10 minutes in PBS. During this time the X-gal staining solution was pre-warmed for 10 minutes at 37°C. The discs were then transferred to 500 µl of pre-warmed X-gal solution, to which 1/30 of 8% X-Gal in dimethylsulfoxide was added. Wing discs were left for several hours to overnight at room temperature on an orbital shaker. Once the desired staining was complete the discs were rinsed once with PBS and then re-suspended in 80% glycerol in PBS. The tissue was left in this solution for several hours and then transferred onto a slide in a drop of glycerol before mounting under a cover slip. Nail polish was used to permanently seal the coverslip for long-term storage.

2.11 WESTERN BLOT ANALYSIS

Proper translation of pUAST *neu*$^{K757M, YD}$ was verified using a heat shock promoter Gal4 driver and Western blot. Approximately 50 third instar larvae were collected and placed in 60 x 15 mm plastic petri dishes containing solidified apple juice agar. The plates were sealed with parafilm and heat shocked for 1 hour at 37°C. Following heat shock the larvae were given a 45 minute recovery period prior to homogenization. The larvae were collected and then homogenized

in cold RIPA lysis buffer (150 mM NaCl, 1.0% NP-40, 0.5% deoxycholate, 0.1% SDS, 50 mM Tris-HCl [pH 8.0], protease inhibitor cocktail tablets 1/10 ml (Roche, cat.# 1836170)). (1g tissue per 2 ml of RIPA). Once homogenized, the tissues were incubated on ice for 10 minutes and then centrifuged for five minutes at 3500 rpm to remove excess fly parts. The supernatant was collected, the concentration was determined and the samples were stored at -80°C.

Crude protein samples were defrosted and approximately 60 μg of protein (~12 μl) was mixed with 5 μl of 4X sample buffer (2% SDS, 10% glycerol, 100 mM DTT, 60 mM Tris [pH 8.0], 0.01% Bromophenol Blue) and boiled for five minutes. Protein samples were then loaded on a 12.5% Tris-HCl gel (Bio-Rad, cat. #161-1102) and run at 200V for 40 minutes. After the gel was run, the protein was transferred to a PVDF membrane that had been activated by presoaking in methanol. Prior to assembly of the Mini Protean II (Bio-Rad), the sponges, 3MM whatman filter papers and PVDF membrane were soaked in transfer buffer for five minutes. The western "sandwich" was then assembled and the protein was transferred for one hour at 100V at 4°C. After transfer, the PVDF membrane was washed 2X for five minutes each in post blot buffer (20 mM Tris-HCl, pH 7.2-7.4 , 150 mM NaCl, 01% (v/v) Tween 20) and then blocked for 60 minutes at room temperature on a shaker in a 5% skim milk powder in post blot buffer solution. After blocking, the membrane was incubated overnight at 4°C in

a 1:5000 dilution of pre-absorbed anti-ErbB2 1° antibody serum (Oncogene Science).

The following day, excess primary antibody was removed by washing 3X for ten minutes each in post blot buffer containing NP-40 (1:2000). Following the washes, the blot was incubated in a 1:10000 dilution of horseradish peroxidase labeled secondary antibody for one hour at room temperature. Excess secondary antibody was then removed by 2X ten minute washes in post blot buffer with NP-40, followed by 2X ten minute washes in 10mM Tris. The blot was then prepared for autoradiographic developing using Kodak X-ray film.

Equal volumes of reagent A and reagent B were mixed from the ECL Western blot detection kit (Amersham Pharmacia). Five ml of this solution was spread evenly over the blot and incubated for 3 minutes. Excess liquid was then removed and the blot was sealed in saran wrap. The sealed blot was then exposed to Kodak X-OMAT AR (XAR) film in the dark for various amounts of time and then developed to determine optimal exposure time.

2.12 LARGE SCALE WING SCREENING

Selected flies were mated in 16 x 100mm glass culture tubes (Fisher Scientific) containing sucrose-yeast agar food and several drops of dry active yeast to stimulate egg laying. At least 2-3 replicates of each cross were set-up to ensure that any noted interaction could be duplicated. All crosses were maintained at room temperature (22-25°C) until the majority of the F_1 flies had

eclosed. Wings were examined and scored as either "no interaction", "enhancement" or "suppression", depending upon the severity of the wing phenotype, the amount of ectopic vein tissue and the number of wing deltas present. A scale was designed according to these standards to rank the severity of the wing phenotypes from 1-9, with five indicating "no interaction", one indicating "extreme suppression" and nine indicating "severe enhancement" (See Appendix: Figure 1). To assign a numerical value to noted interactions, we scored the pooled affect of at least 40 wings from that genotype. A value was assigned if at least 75% - 95% of the examined wings had that score.

2.13 MOUNTING AND LIGHT LEVEL MICROSCOPY

Embryos were sorted in glass depression slides and prepared for light level microscopy by mounting selected individuals in methyl salicylate in Permount (Fisher) on frosted glass slides (Corning) using 18 mm^2 cover slips. These slides were allowed to dry for a minimum of 24 hours prior to examination under a Zeiss Axiophot microscope. Nerve cords were examined and photographed at 630x magnification. Wing preparation varied slightly from embryo. Cold anesthetized flies were submerged in 70% ethanol and dehydrated following successive ethanol gradients (80%, 90%, 95%, 100%). Flies were transferred to glass wells and selected wings were dissected with forceps and stored in methyl salicylate prior to mounting. Wings were prepared for microscopy by mounting in methyl salicylate in Permount (Fisher) on frosted glass slides (Corning) using

22 mm^2 coverslips. These slides were then stored or photographed at 300X magnification using a Nikon Coolpix 990 digital camera attached to a Nikon SMZ 1500 compound microscope. Wing photographs were stored directly to disk as 1-2 MB images on a Mac OS 9.2 computer. Colour slide film (Kodak Ektachrome 64T) was used to photograph embryos and developed commercially. Processed film was scanned using a slide scanner (Minolta) and all figures were prepared using Adobe Photoshop® 4.0.

Table 2.1 Mutants, pUAST lines and Deficiencies used for Genetic Screening.

Section 1: Mutants					
Gene (Allele)	**Cytological Location**	**Genetics**	**Proposed Function**	**Reported Mutant Phenotype**	**Reference**
Pole hole (phl^{C110}) *Source: M.P. Martin*	3A1150	X-ray mutagen, hypomorph	protein kinase involved in signal transduction downstream of *Ras*; required for normal rate of cell proliferation.	rough eye due to loss of R7 during ommitidial formation; mild wing vein phenotype.	Perrimon et al., 1985; White and Jarman, 2000
Ras oncogene at 85D ($ras85D^{05703}$) *Source: D. Montell*	85D21	P-element activity mutagen, hypomorph	Ras small monomeric GTPase involved in perineurial glial growth; growth, survival and differentiation in the eye.	defects in ovarian development and cuticle formation; rough eye phenotype.	Rorth, 1996, Schnorr and Berg, 1996
Son of Sevenless ($sos^{34Ea-6}Adh^{n4}$)	34D4	EMS mutagen, amorph	Ras guanyl-nucleotide exchange factor involved in Ras protein signal transduction.	some ommatidia lack receptor cells leading to mild rough eye phenotype.	Rogge et al., 1991
Corkscrew (csw^{LE120}) *Source: L. Perkins*	2D1	EMS mutagen, amorph	protein tyrosine phosphatase involved in multiple receptor signaling pathways and R7 cell fate determination.	maternal effect lethality; loss of muscle precursor cells.	Perkins et al., 1996
SHC-adaptor protein ($dshc^{111-40}$) *Source: S. Luschnig*	67B4	EMS mutagen, recessive	adaptor protein involved in multiple receptor signaling pathways	semi-lethal; germ band retraction defects; female sterility.	Luschnig et al., 2000
Downstream of Receptor Kinase (drk^{10626})	50B7	P-element activity mutagen, recessive	SH3/SH2 adaptor protein involved in Ras protein signal transduction.	embryos with patterning defects in head and tail regions.	Simon et al., 1993; Spradling et al., 1999

Gene (Allele)	Cytological Location	Genetics	Proposed Function	Reported Mutant Phenotype	Reference
Daughter of Sevenless (Dos $^{2.42}$) *Source: M. Simon*	62E7	EMS mutagen, recessive	SH2/SH3 adaptor protein involved in signal transduction.	cells in the eye can proliferate, but do not differentiate as photoreceptors - same as lack of *csw* function.	Herbst et al., 1996
Dreadlocks (dock^{P1}) *Source: Y. Rao*	21D3	P-element activity mutagen, amorph	SH2/SH3 adaptor protein involved with axon guidance.	lamina and neurons are disorganized; defects in receptor cell innervation.	Garrity et al., 1996
Disabled (dab$^{[MS4\text{-}R1]}$) *Source: E. Giniger*	73C1	X-ray mutagen, amorph	adaptor protein involved in axon guidance downstream of RTK signaling.	aberrant photoreceptor development	Hill et al., 1995
Dachshund (dac^{1})	36A1	amorph	RNA polymerase II transcription factor involved with eye development.	reduced, roughened or absent eyes and shortened legs.	Mardon et al., 1994
Scribbled (scrib^{1})	97B9	EMS mutagen, loss of function	establishment and maintenance of cellular polarity; apical localization of the DEgfr.	overgrowth of brain tissue and overgrown imaginal discs.	Bilder and Perrimon, 2000
Akt (Akt^{1}) *Source: A. Munovkian*	89B6	loss of function	protein serine/threonine kinase involved in anti-apoptotic signaling.	loss of embryonic cuticle	Staveley et al., 1998
Integrin-Linked Kinase (ILK 78Ca)	78C2	ethyl nitrosourea mutagen, amorph	protein serine/threonine kinase involved in integrin mediated signaling and focal adhesion	defects in somatic muscle attachment and wing blisters	Zervas et al., 2001

Gene (Allele)	Cytological Location	Genetics	Proposed Function	Reported Mutant Phenotype	Reference
Epidermal Growth Factor Receptor ($Egfr^{flb\text{-}2E07}$) *Source: Nusslein-Volhard*	57F5	EMS mutagen, hypomorph	protein tyrosine kinase involved in eye and wing morphogenesis, embryonic polarity and CNS patterning.	lack of midline glial cells; faint little ball phenotype.	Raz et al., 1991
Hedgehog (hh^{21})	94E1	EMS mutagen, loss of function	*Patched* and *Smooth* receptor ligand involved in segmentation.	loss of embryonic segmentation.	Ingham and Hidalgo, 1993; Forbes et al., 1993
Baboon ($babo^{32}$)	44F12	Delta2-3 mutagen, loss of function.	protein serine/threonine kinase; TGF beta receptor.	brain hemispheres and wing discs reduced in size.	Brummel et al., 1999
Patched (ptc^{9})	44E	EMS mutagen, loss of function	integral plasma membrane protein receptor involved in mitotic cycle control.	cell fate alterations; duplication of all segment boundaries; wing vein defects.	Riggleman et al., 1990
Smoothened (smo^{3})	21B7	EMS mutagen, amorph	G-protein coupled transmembrane receptor involved in blastoderm segmentation and mitotic cycle control	reorganized A/P wing patterning as well as segment polarity defects.	Chen and Struhl, 1996
Small wing (sl^{2})	14B15	X-ray mutagen, loss of function	Phospholipase C-gamma (PLC-gamma) enzyme involved in eye and wing morphogenesis.	reduction in wing length and a mildly rough eye; ectopic wing veins present.	Thackeray et al., 1998
Phyllopod ($phyl^{XS\text{-}2245}$)	51A7	X-ray mutagen, recessive	required for the formation of sensory organ precursor cells and cell fate specification in the eye; interacts with Ras85D.	defects in photoreceptor development and bristle patterning.	Chang et al., 1995

Section 2: pUAST lines		
pUAST Line	**Genetics**	**Reference**
RasV12 *Source: F. Karim*	constitutively active *Drosophila Ras* transgene that contains a glycine-to-valine mutation at residue 12.	Therrien et al., 1996
RasV12C40 *Source: F. Karim*	activated *Ras* mutant with an alteration of tyrosine to cysteine at position 40 in the effector domain. It is unable to bind *Raf* or other *Ras* responsive reporters (MAPK); however, it is a selective activator of PI3-kinase.	Rodriguez-Viciana et al., 1997
RasV12S35 *Source: F. Karim*	activiated *Ras* mutant with an alteration of threonine to serine at position 35 in the effector domain. It is able to bind to and activate the *Raf* signaling pathway only.	White et al., 1996
RasV12G37 *Source: F. Karim*	activated *Ras* mutant with an alteration of glutamic acid to glycine at position 37 in the effector domain. It is able to bind to and activate *Ral guanine nucleotide exchange factor (GEF)* which connects *Ras* to the GTPase *Ral*. It cannot activate *Raf*.	White et al., 1996
RasN17 *Source: D. Montell*	expresses a dominant-negative form of the *Ras* protein that contains a serine-to-asparagine mutation at residue 17 - inhibits EGF induced activation of *Ral* and inhibits Ras GEF's.	Rayter et al., 1992
DER^{A887T} (12-4) Source: *N. Baker*	constitutively active DEgfr that contains an alanine to threonine mutation at residue number 887.	Lesokhin et al., 1999
DN DEgfr *Source: M. Freeman*	Dominant Negative *Drosophila* Egfr receptor.	Freeman, 1996

pUAST Line	Genetics	Reference
DRaf	*Drosophila* Raf – activates the MAPK signaling cascade.	Kumar and Moses, 2001
Dp110 (CAAX) *Source: S. Leevers*	membrane targeted Dp110 which activates the PI3K pathway via the p85 SH2 adaptor subunit of p110.	Leevers, S. J. et al., 1996
Dp110 (II) *Source: S. Leevers*	wild-type Dp110 which activates the PI3K pathway via the p85 SH2 adaptor subunit of p110.	Leevers, S. J. et al., 1996
FAK Δ56 (Focal adhesion Kinase) *Source: T. Hunter*	protein tyrosine kinase which interacts with a number of down-stream signaling proteins, including the adaptor protein Grb2 and the p85-subunit of phosphatidylinositol 3 kinase (PI3 kinase). Involved with integrin signaling.	Fujimoto, J. et al., 1999
gHid14 (Head Involution Defective)	inducer of apoptosis - downregulation of the Ras/MAPK pathway induces cell death by upregulating *hid* expression	Abbott, M. K. and Lengyel, J. A., 1991

Section 3: Deficiencies		
Chromosome	**Genetics**	**Reference (Kits Available from Bloomington Stock Center)**
Second Chromosome (Deficiency Kit)	deficiency kit uncovers 72% of the second chromosome using 85 different mutant lines.	see Appendix for full list of deficiencies screened, their breakpoints and contributors. Shipped July 28, 1999
Third Chromosome (Deficiency Kit)	deficiency kit uncovers 75% of the third chromosome using 87 different mutant lines.	see Appendix for full list of deficiencies screened, their breakpoints and contributors. Shipped July 15, 2001

CHAPTER 3 RESULTS

3.1 ACTIVATION OF *neu* TRANSGENES.

To examine the phenotypes associated with mis-expression of *neu* transgenes, tissues were selected that are known to require signaling from the *Drosophila* Epidermal Growth Factor receptor (*DEgfr*), the sole *Drosophila* orthologue to vertebrate ErbB receptors. Additionally, modifiers of *neu* signaling were more easily assessed when visible adult structures not required for viability were affected. Thus we targeted expression of *neu* transgenes to the wing, a tissue known to respond to DEgfr signaling, using the GAL4 activation system (Brand et al., 1994). *P[GAL4]C96* is strongly expressed in the wing disc dorsal-ventral boundary and had no effect on viability (Stewart et al., 2001; Figure 4). *C96* was thus used for screening all adaptor mutants and deficiency lines against each *neu* transgene. Mis-expression of *neu* with many GAL4 drivers proved to be lethal before or during pupation (data not shown); however, these effects were not seen with *Sim-Gal4* or *C96*, GAL4 drivers whose expression is restricted to post-mitotic cells, or cells not required for viability.

Figure 4. The Wing Margin *C96GAL4* Driver is Strongly Expressed in Larval Wing Imaginal Discs. Third instar larvae wing imaginal discs were fixed and stained for *β-galactosidase,* to detect *C96* GAL4 expression patterns in UAS-*tau lacZ/+; C96/+* wing discs. Punctate expression can be detected throughout the imaginal disc (arrows); however, the majority of *C96* expression is restricted to the dorsal ventral boundary of the wing disc (arrowhead).

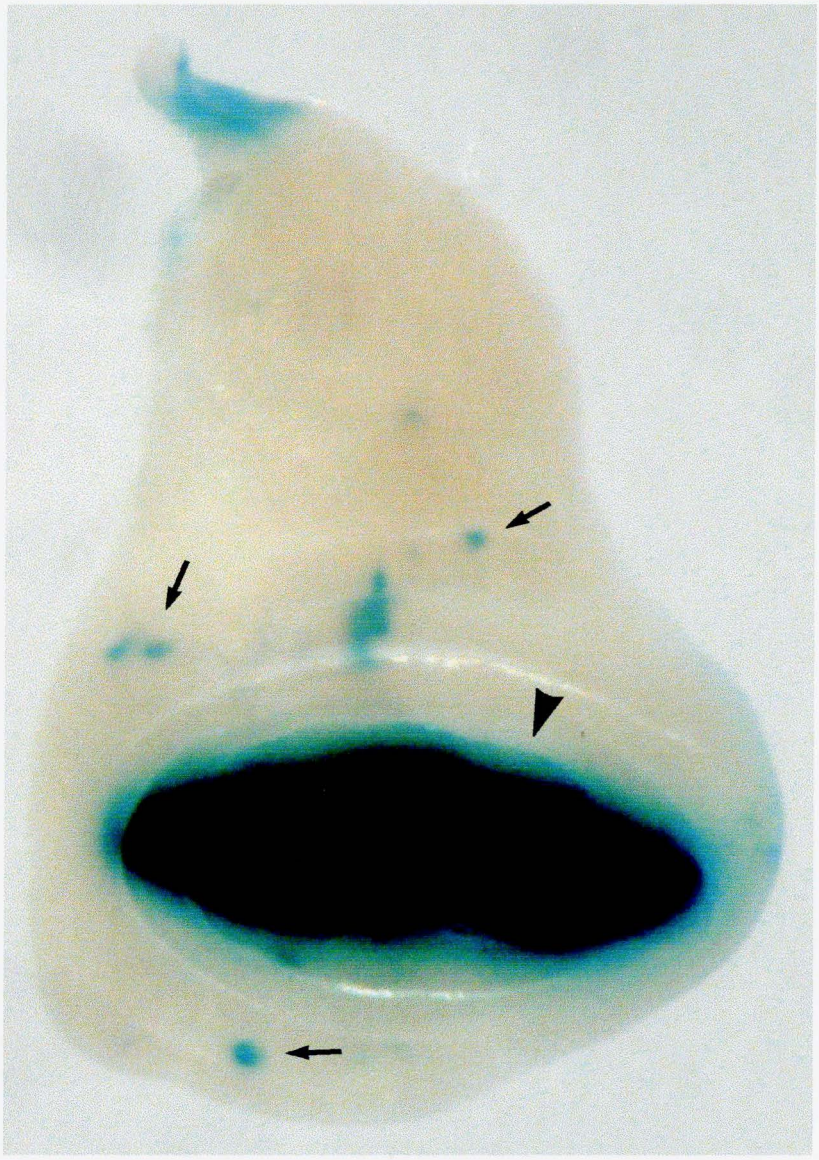

3.2 MIS-EXPRESSION OF NEU MUTANTS PRODUCES DISTINCT WING VEIN AND CNS PHENOTYPES.

Neu Signaling in the Wing Margin

To explore the functional conservation of receptor signaling between vertebrate and invertebrate models, we generated *Drosophila* transgenic for multiple "add-back" alleles of *neu*. Each Neu add-back allele has all of the known phosphorylation sites in the docking domain, except for one, converted to Phenylalanine (YA, pTyr 1024; YB, pTyr 1144; YC, pTyr 1201; YD, pTyr 1226/1227; YE, pTyr 1253). These mutants retain only the single indicated phosphorylation site. The *neu* transgenes also carry an activating mutation which maintains constitutively active Neu signaling via increased homodimerisation of mutant receptors (Bargmann and Weinberg, 1988; Weiner et al., 1989).

To examine Neu signaling in the wing, the *C96* GAL4 enhancer trap was selected, in which expression is restricted to cells at the dorsal to ventral boundary of the wing (Gustafson and Boulianne, 1996; Stewart et al., 2001). Each *neu* transgene, except for YA (Fig. 5I), generated a mutant wing phenotype. Neu^{YA} lacks transforming potential in mammalian cells and likely has an inhibitory role in Neu signals (Dankort et al., 1997). Neu mis-expression in the wing resulted in ectopic veins, a loss of wing margin and wing delta formation (Fig. 5E,G, B-J). The severity of the wing phenotype is closely correlated with the specific add back allele. The greatest degree of wing margin loss is seen with neu^{YD} (Fig. 5H);

Figure 5. Mis-expression of Neu Add-Back Mutants Produces Distinct Wing Vein Defects. Neu add-back mutants were mis-expressed at the wing margin with *p[GAL4]C96*. Active neu^{NT} (E) produced a severe wing phenotype which included ectopic vein formation, large wing deltas and margin loss. The *neu* add-back alleles resulted in a differential severity of margin and notch phenotypes (B,D,F,G-I, *neu* transgene indicated at bottom left). Expression of neu^{YA} (I) did not alter wing morphology relative to a control *C96* wing (A). Arrowheads mark wing deltas and arrows refer to margin loss in all panels, and also in an enlargement of a neu^{YC} wing (J, left) and a neu^{YB} wing (J, right). Similar expression of activated DEgfr at the wing margin resulted in notch formation on the posterior margin of the wing (C).

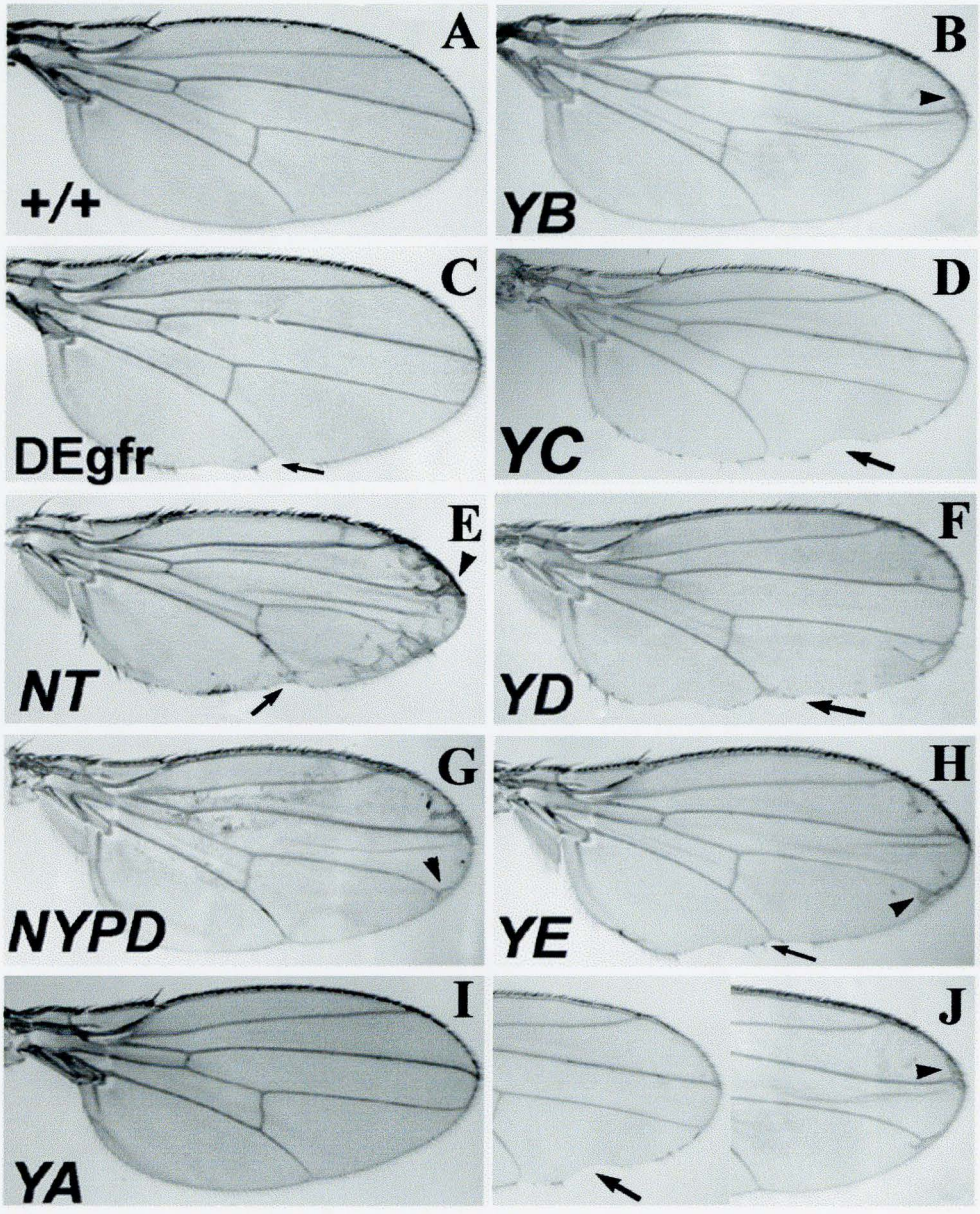
A
+/+
B
YB
C
DEgfr
D
YC
E
NT
F
YD
G
NYPD
H
YE
I
YA
J

however, the largest wing deltas and greatest overall loss of wing morphology is noted with the active *neu* allele (neu^{NT}) (Fig. 5E). A kinase active *neu* allele, lacking all known phosphorylation sites (neu^{NYPD}), was still able to generate a mild wing phenotype (Fig. 5G); however, it did generate a phenotype more severe than that which may have been predicted by expression in the midline glial (MG) cell lineage (Fig. 6G). The resulting wing phenotype is not entirely unexpected though, as neu^{NYPD} is able to retain weak transforming potential in mouse mammary tissue (Dankort et al., 2001). Expression of activated DEgfr in the wing margin generated notches along the posterior half of the wing (Fig. 5C). The similar notches resulting from *neu* mis-expression are likely to be a functional outcome of Neu signaling, because wing veins are specified by DEgfr signals (Sturtevant et al., 1993; Sturtevant and Bier, 1995).

Neu signaling in the Midline of the CNS

DEgfr dosage dependent signaling has previously been established in several *Drosophila* tissues, including the eye, wing and MG. Neu mis-expression in the MG was examined because the output is well characterised as suppression of apoptosis. The relative levels of signaling are also easily quantified by examining MG cell number (Lanoue and Jacobs, 1999; Jacobs, 2000). This was scored by expression of the AA142 enhancer trap, which directs expression of nuclear targeted β-galactosidase (Klambt et al., 1991).

The MG cell lineage begins as a precursor pool of 10-12 cells per embryonic segment (Dong and Jacobs, 1997). This number is reduced to 3 MG per embryonic segment by stage 16 of embryogenesis, as a result of differential apoptosis (Fig. 6A). Elevated DEgfr signaling in the midline of the CNS increased MG cell number to approximately 5 (Fig. 6C). When we expressed the active *neu* mutant in the midline of the CNS this number was increased to about 7 MG cells per embryonic segment (Fig. 6E). Consistently, the most dramatic suppression of apoptosis with the MG assay, corresponding to expression of the neu^{NT} allele, parallels with the most severe wing phenotype, also resulting from neu^{NT} mis-expression. The increase in MG cell number was likely due to suppression of apoptosis effected by signaling from pTyr in the docking domain of the receptors. In particular, Neu^{NYPD}, which lacks all known pTyr had no significant effect on MG cell number (Fig. 6G).

Each add-back allele of *neu* was similarly tested in the MG apoptosis assay, yielding distinct results. Neu^{YA} had no significant effect on MG number (Fig. 6B), consistent with an inhibitory role in RTK signaling in mammalian cells (Dankort et al., 1997). The remaining alleles increased MG number between 13% to 100%, with neu^{YD} producing the most effective suppression of apoptosis, with a potency close to Neu^{NT} (Fig. 6D). Midline expression of the remaining add-back alleles, YB, YC and YE (Fig. 6D, F and I respectively) resulted in 4 to 5 MG per segment.

Figure 6. Mis-expression of Neu Suppresses Apoptosis in the Midline Glia. The nuclei of the MG were visualized in sagittal view by antibody detection of β-galactosidase, expressed in the MG by the AA142 enhancer trap (A). Activated RTKs were expressed in the midline using *simGAL4* (see methods). Expression of an activated *Drosophila Egfr* in the midline resulted in a 66% increase in the MG cell number (C). Activated *neu* more than doubled MG numbers (E), while similar expression of *neu* lacking all of the known pTyr residues had no effect on MG number (G). Mis-expression of each of the add-back *neu* alleles in the midline, YA (B), YB(D), YC(F), YD(H) and YE(I) suppressed apoptosis to differing degrees, elevating the number of surviving MG between 13 and 100%. All saggital views are dorsal on top, anterior to the left. MG counts, standard deviation and the number of segments assessed are indicated in the lower right of each panel. This figure was generated by J. Roger Jacobs. Panels A-H are from work performed by Michael Gordon.

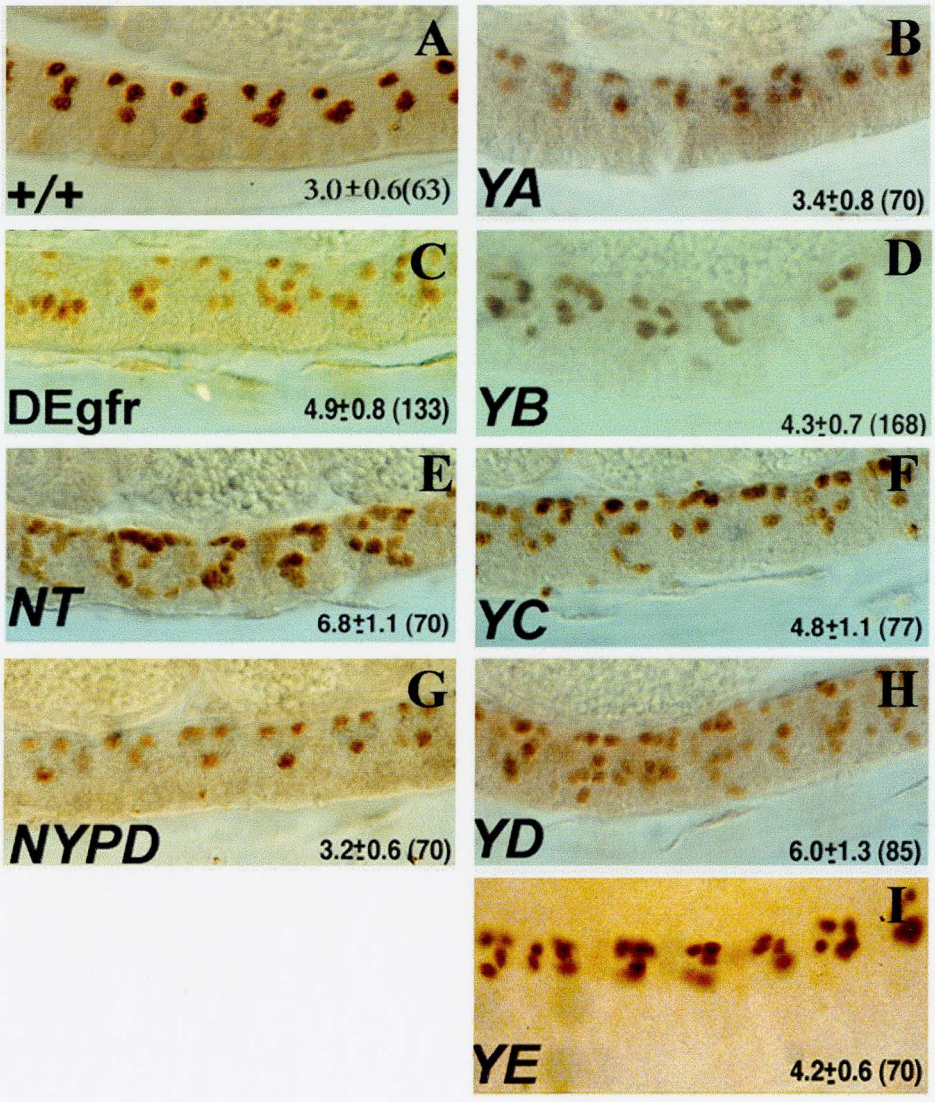
A
+/+
3.0±0.6(63)
B
YA
3.4±0.8 (70)
C
DEgfr
4.9±0.8 (133)
D
YB
4.3±0.7 (168)
E
NT
6.8±1.1 (70)
F
YC
4.8±1.1 (77)
G
NYPD
3.2±0.6 (70)
H
YD
6.0±1.3 (85)
I
YE
4.2±0.6 (70)

3.3 IDENTIFICATION OF ADAPTERS REQUIRED FOR NEU SIGNALING IN *DROSOPHILA*

To identify second messengers (*ras, raf, dab, sos and PLCγ*) and adaptors (*shc, Grb-2, Nck and shp-2*) thought to participate in signaling from Neu, wings were examined from *UAS-neu/+; C96/+* flies also heterozygous for amorphic alleles of a number of putative interacting genes. Interactions were noted by examining the resultant phenotypes in the wings of the F_1 progeny. Specific adaptors and second messengers were designated as being required for signaling by individual Neu pTyr, by noting which add back alleles displayed a suppression or enhancement of the *neu* wing phenotype. The results of this screen are summarized in Table 3.1, wherein no modification of the *neu* phenotype is scored as 5 and complete suppression is scored as 1. Suppression could not be scored from the wild-type morphology after neu^{YA} expression (Table 3.1). At least two replicates of each cross were performed so that a minimum of 40 wings could be examined for putative interactions. The enhancement or suppression of the *neu* wing phenotypes were numerically scored according to the severity of the wing morphology, including the number of wing deltas, the number of ectopic veins and the overall degree of wing margin loss (see Methods 2.12; Appendix, Fig. 1).

Wings examined from flies heterozygous for $DShc^{111\text{-}40}$, which encodes a SH2 binding adaptor protein, reveal a complete suppression of signaling from Neu^{YD}, but no effect upon any other pTyr site on Neu (Table 3.1; Fig. 7J). A

Table 3.1. Summary of Second Messenger Modifiers of *neu* Wing Phenotypes. A number of amorphic adaptors and second messenger modifiers were screened against individual *neu* add back alleles to determine potential candidates involved in signaling from specific Neu pTyr. The results are summarized and scored numerically, with no interaction indicated as five, and complete suppression of the wing phenotype as one.

Second messenger modifiers of *neu* wing phenotypes

	SHC	Grb-2	Sos	Ras	raf	Gab-1	Dab	shp-2	Nck	PLCg
	Dshc	*drk*	*sos*	*ras*	*phl*	*dos*	*dab*	*csw*	*dock*	*sl*
NYPD	5	4	1	1	3	5	2	1	5	5
YA	5	5	5	5	5	5	5	5	5	5
YB	5	3	2	1	4	1	2	1	5	5
YC	4	3	4	3	3	3	3	3	5	5
YD	1	2	2	1	4	4	4	2	5	5
YE	5	5	4	5	3	4	3	5	5	5

Figure 7. A reduction in *Dshc* function suppresses signaling from Neu^{YD}. *Dshc* encodes an SH2 adaptor binding protein which binds directly to activated pTyr residues. Mis-expression of *neu* add back alleles reveals a complete suppression of Neu^{YD} signaling in the wing in *Drosophila* haplosufficient for *Dshc* (J). The remaining *neu* alleles are unaffected by a reduction in *Dshc* function (B, D, F, H and L).

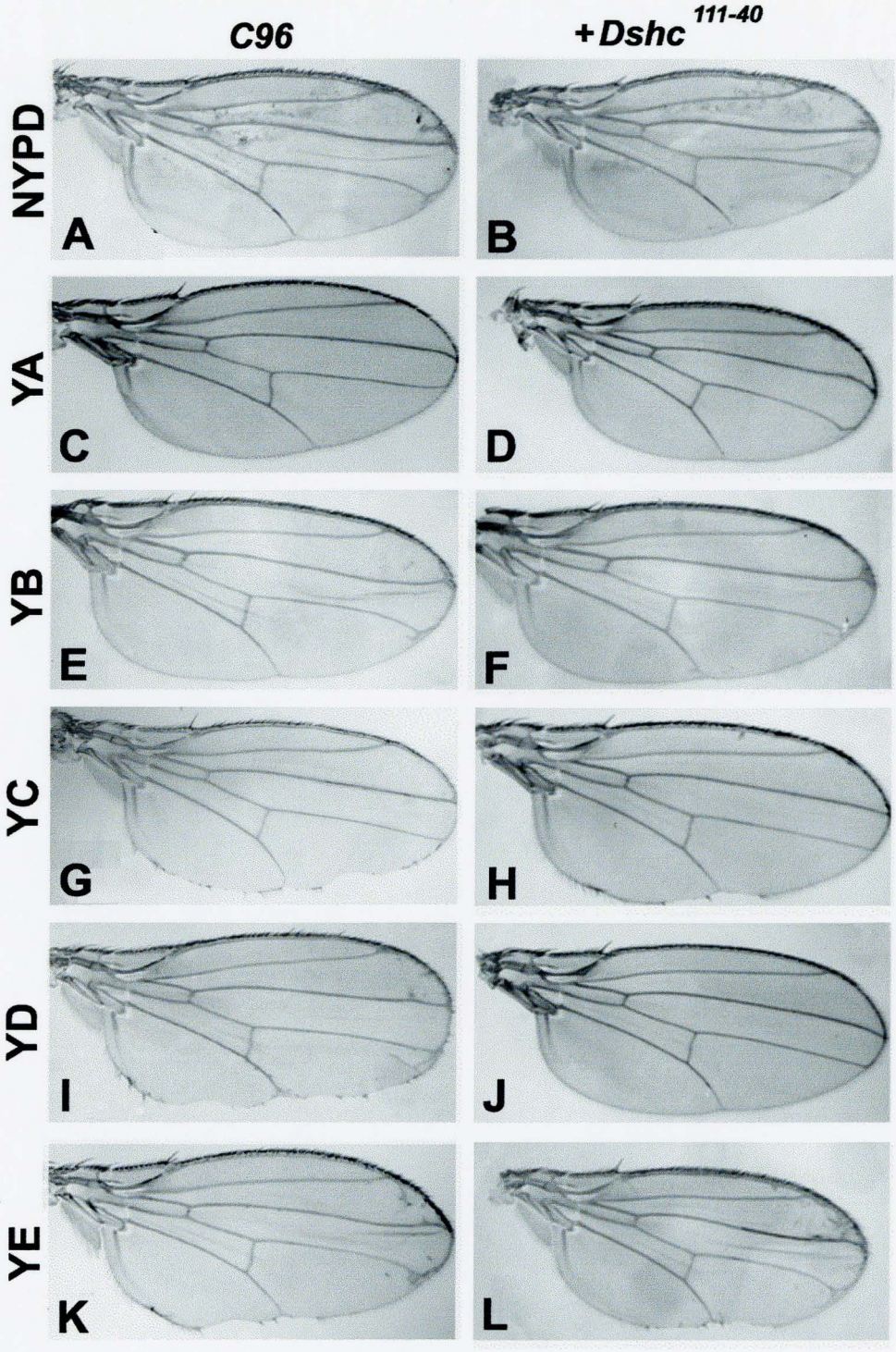
C96
+Dshc 111-40
NYPD
YA
YB
YC
YD
YE
A
B
C
D
E
F
G
H
I
J
K
L

reduction in Grb-2 (*drk*) adaptor function suppressed signaling from Neu^{YB}, Neu^{YC} and Neu^{YD} but had a negligible effect on Neu^{YE} (Table 3.1; Fig 8F, H, J and L, respectively). As Neu^{YD} is known to signal via association with SHC, and Dshc lacks the mammalian Grb-2 binding site, a suppressed *neu^{YD}* phenotype was not expected in a *drk^{10626}* mutant background. A reduction in Gab-1 (*dos$^{2.42}$*), Dab (*dab$^{[M54-R1]}$*), or Shp-2 (*csw^{LE120}*) adaptor function suppressed signaling most potently from Neu^{YB}. These mutations did; however, weakly suppress signaling from other *neu* pTyr, but had negligible effects on suppressing Neu^{YE} (Table 3.1).

A reduction in *sos* function, which encodes a guanine nucleotide exchange factor that activates Ras, suppressed all *neu* induced wing phenotypes (Table 3.1, Fig. 9B, D, F, H, J and L); however, signaling was most potently suppressed from *neu^{YD}*, *neu^{YB}* and *neu^{NYPD}* alleles. It was therefore suggestive that Neu^{YE} and Neu^{YC} may activate both *ras*-dependent and *ras*-independent pathways. As seen with reduced *sos* function, all *neu* induced wing phenotypes were suppressed by a reduction in *ras* function, except for Neu^{YE} (Table 3.1; Fig 10, middle column). Phenotypes generated from *neu$^{NYPD, YB}$* and *^{YD}* were completely suppressed by reduced *ras* function; however, the *neu^{YC}* phenotype was only partially suppressed (Table3.1; Fig. 10K). In contrast, a reduction in *raf (phl)* function attenuated Neu$^{YB, YC}$ and ^{YD} signals. Reduced *raf* function did however appreciably suppress Neu^{YE} signaling (Table 3.1; Fig 10R). The weaker suppression by *raf* relative to *ras* suggests that either *raf* function is less dosage sensitive, or that the output

Figure 8. A reduction in Grb-2 *(drk)* function partially suppresses signaling from Neu^{YD}. d*rk* encodes an adaptor binding protein which binds directly to activated pTyr residues. Mis-expression of *neu* add back alleles reveals a partial suppression of Neu^{YD} signaling in the wing in the absense of fully functional Drk (J). Neu^{YA} and Neu^{YE} signaling are unaffected by reduced Drk (D and L, respectively), while the remaining *neu* alleles are mildly suppressed by a reduction in *drk* function (B, F, and H).

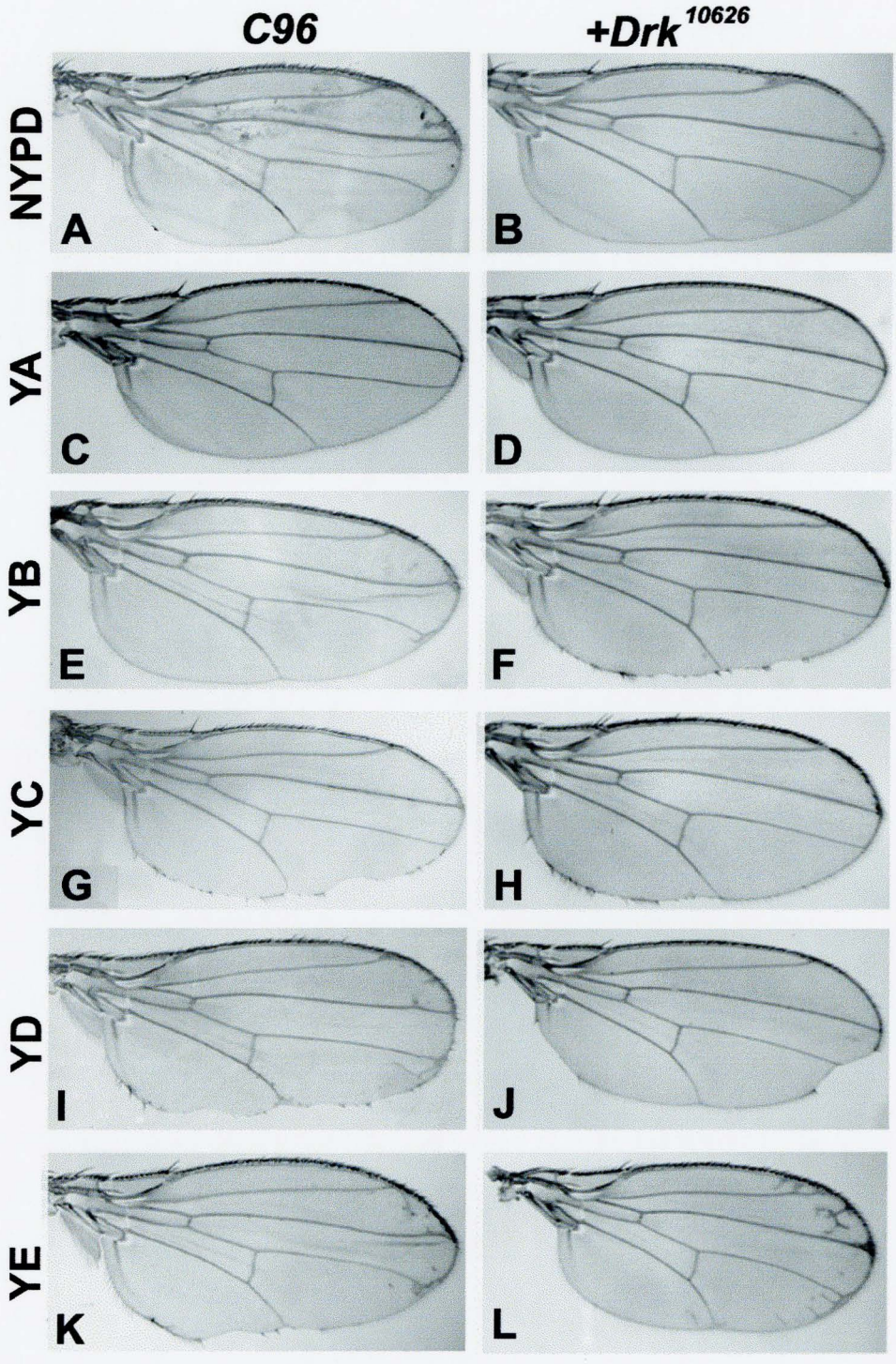
C96
+Drk 10626
NYPD
A
B
YA
C
D
YB
E
F
YC
G
H
YD
I
J
YE
K
L

Figure 9. A reduction in *sos* function suppresses signaling from all Neu pTyr. *sos* encodes a guanine nucleotide exchange factor protein which phosphorylates, and thereby activates Ras. Mis-expression of *neu* add back alleles reveals suppressed signaling from each Neu pTyr, except YA (D); however, signaling was most potently suppressed from Neu^{YD} (J), ^{YB} (F) and ^{NYPD} (B). Neu^{YC} and ^{YE} revealed only partially suppressed phenotypes, suggesting that these pTyr may activate both *ras*-dependent and *ras*-independent signaling pathways.

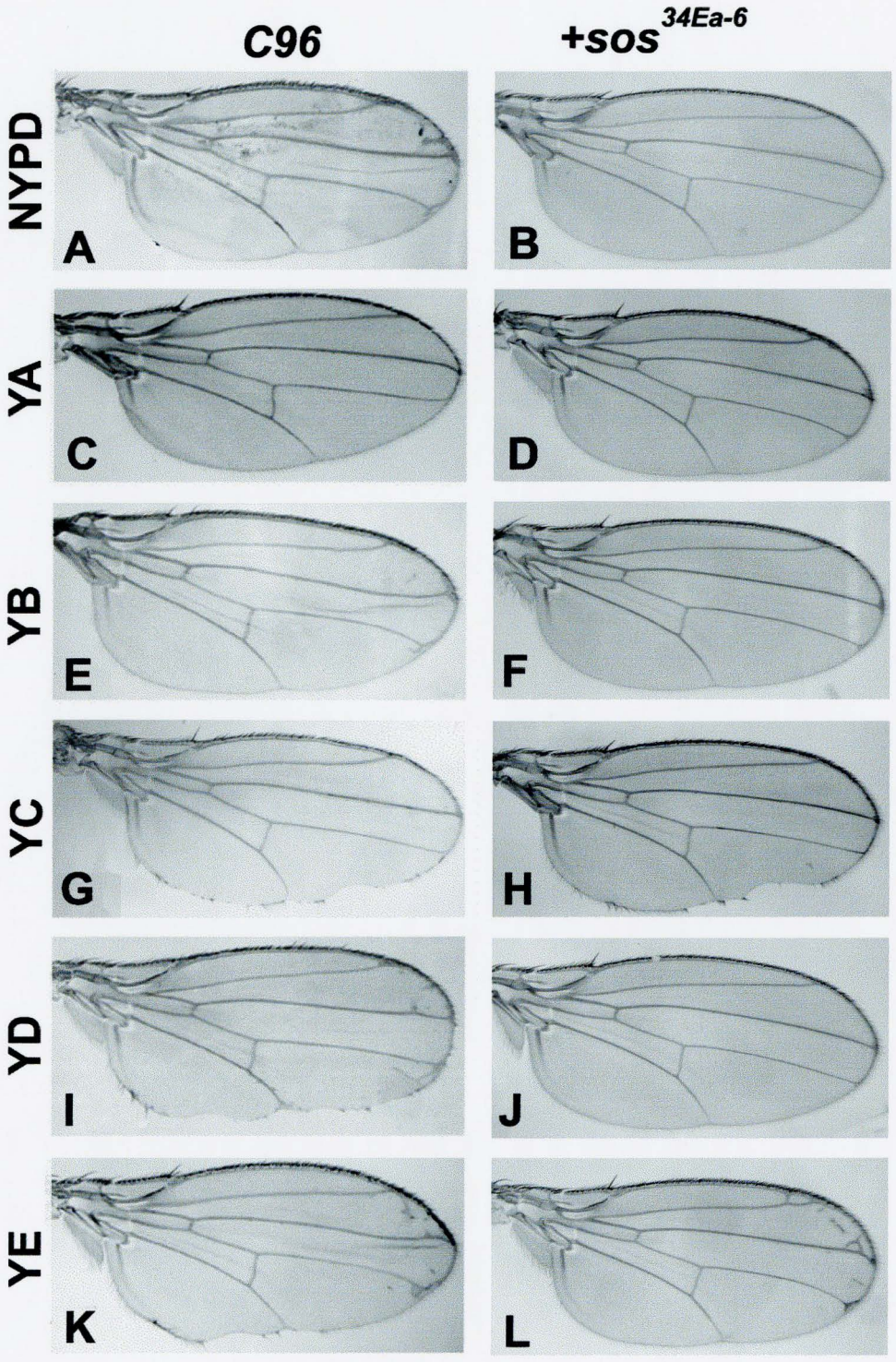
C96
+sos 34Ea-6
NYPD
YA
YB
YC
YD
YE
A
B
C
D
E
F
G
H
I
J
K
L

Figure 10. Neu^{YE} signaling in the wing is unaffected by reduced Ras levels, but does respond to a reduction in Raf. Mis-expression of *neu* add back alleles revealed that Neu^{YE} signaling was insensitive to a reduction in *ras* function (Q). Conversely, a reduction in *raf* suppressed the *neu^{YE}* phenotype (R), but had a milder suppressive effect on Neu^{YB,YC} and ^{YD} (I, L and O, respectively).

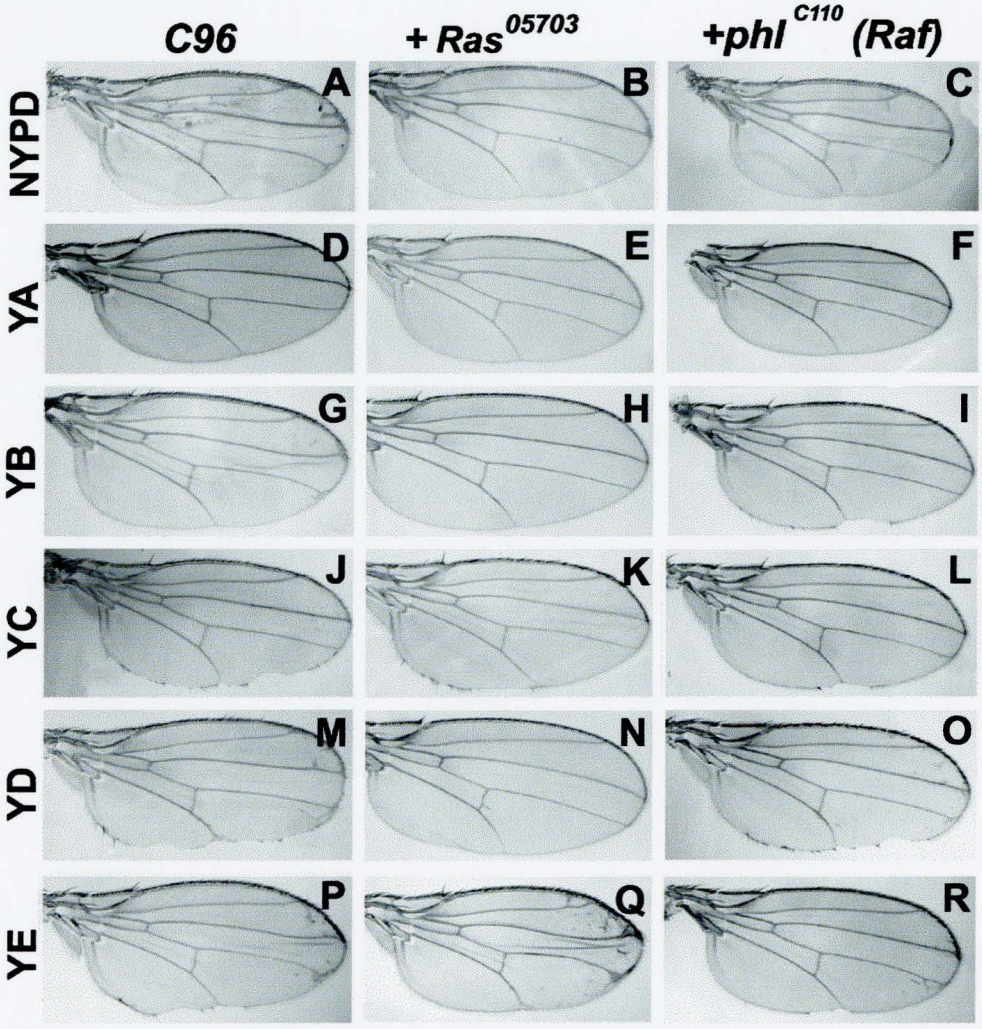
C96
+ Ras 05703
+phl C110 (Raf)
NYPD
YA
YB
YC
YD
YE
A
B
C
D
E
F
G
H
I
J
K
L
M
N
O
P
Q
R

signaling pathway of each Neu pTyr can also employ Raf independent pathways in generating wing phenotypes. These data suggest that while Neu^{YE} signaling does include Raf dependent function, it does not require Ras as a second messenger in its signaling pathway.

3.4 Ras LEVELS DO NOT AFFECT Neu^{YE} SIGNALING IN THE MIDLINE

A reduction in *ras* function was seen to have negligible effects in suppressing Neu^{YE} signaling in the wing. To determine if the signaling output pathway from Neu^{YE} was conserved in multiple *Drosophila* tissues, we sought to examine mutant *ras* signaling in the midline of the CNS. The MG assay was used to quantify signaling in *ras* mutant heterozygotes, by examing cell counts in these embryos. Analogous to Neu^{YE} signaling in the wing, a reduction in *ras* function did not significantly reduce Neu^{YE} function in the midline (Fig. 11). The active *neu* allele showed the most dramatic decline in the number of MG cells that survived apoptosis, with counts falling from approximately seven MG per segment to roughly three. $Neu^{YD, YC}$ and ^{YB} showed a successive decrease in MG numbers, respectively. No significant difference in the number of MG cells was noted with the neu^{NYPD} and neu^{YA} alleles (Fig. 11).

Figure 11. Neu^{YE} signaling in the midline is unaffected by reduced Ras levels. Similar to signaling in the wing, a reduction in *ras* levels in the midline did not suppress the *neu^{YE}* phenotype, as demonstrated by the number of MG cells surviving differential rounds of apoptosis. The most potent reduction in the number of surviving MG cells was noted with the active *neu* allele, followed by *neu$^{YD, YC, YB}$* and ^{YE}, respectively. Reducing *ras* levels in the presence of active *neu* decreased MG numbers from approximately 7 to roughly 3 cells per embryonic segment. In contrast, *neu^{YE}* showed a minimal reduction of approximately 4 MG per segment to roughly 3.8 MG per segment. Neu^{YA} and ^{NYPD} signaling were also unaffected by reduced *ras* levels. The mean number of MG cells per embryonic segment are plotted ± standard deviation, for each treatment. Asterisks above the coupled data series indicate those counts which are significantly different at a P>0.001 with 95% confidence intervals.

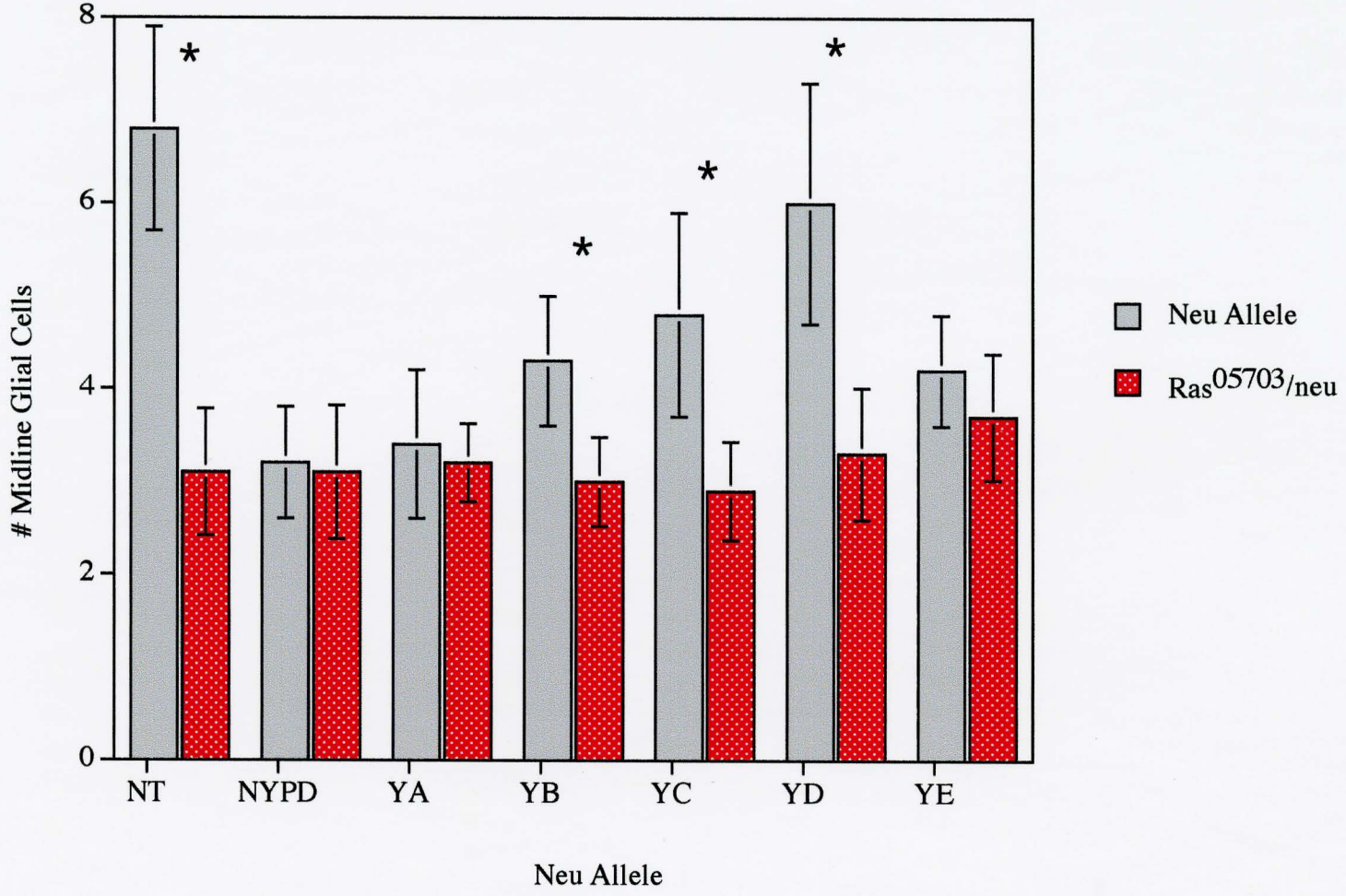
Midline Glial Cells
8
6
4
2
0
*
*
*
*
NT
NYPD
YA
YB
YC
YD
YE
Neu Allele
Neu Allele
Ras05703/neu

3.5 OVEREXPRESSION OF THE *ras/raf* PATHWAY DISRUPTS WING VEIN MORPHOLOGY

As reduced *ras* function was seen to suppress Neu signaling in the wing, we wanted to determine whether wing vein morphology was disrupted by overexpressing active *ras* mutants. When active *rasV12* was overexpressed along the wing margin, ectopic veins as well as margin loss were detected (Fig. 12B). Conversely, overexpression of dominant-negative *rasN17* had no effect on wing vein morphology (Fig. 12F). To determine precise pathways activated downstream of *ras* in wing vein specification, several active *ras* mutants were tested which selectively propagate specific signaling pathways. An active *rasV12C40* mutant, which selectively activates PI3-kinase, had no visible effects on wing vein formation (Fig. 12E). Similarly, overexpression of the *rasV12G37* mutant, which can bind Ral but not Raf, had no visible phenotype (Fig. 12D). Interestingly, activated RasV12S35, which selectively binds to and activates Raf, has no phenotype when mis-expressed in the wing (Fig. 12C), yet it's effects are lethal when mis-expressed in the *Drosophila* eye (data not shown). Overexpression of *raf* however, produced severe margin loss and vein deletion in the wing (Fig. 12G).

Overexpression of active Ras in the wing may be limited by the amount of available Raf protein; however, as you move further down the signaling cascade pathway, a greater proportion of the signal would be expected to reach it's nuclear

Figure 12. Overexpression of the *ras /raf* pathway in the wing margin, produces wing vein defects. When active *rasV12* is overexpressed in the wing margin, ectopic wing vein and margin loss are readily detected (B). Active *ras* mutants, which selectively activate the PI3-K pathway (E ; *rasV12C40*), Ral (D; *rasV12G37*) or Raf (C; *rasV12S35*) do not affect wing morphology in comparison to a *C96* wild-type wing (A). Additionally, a dominant-negative *rasN17* has no effect on wing growth (F); however, overexpression of *raf* in the wing produces severe margin loss (arrow), as well as a deletion of wing vein tissue (arrowhead) (G).

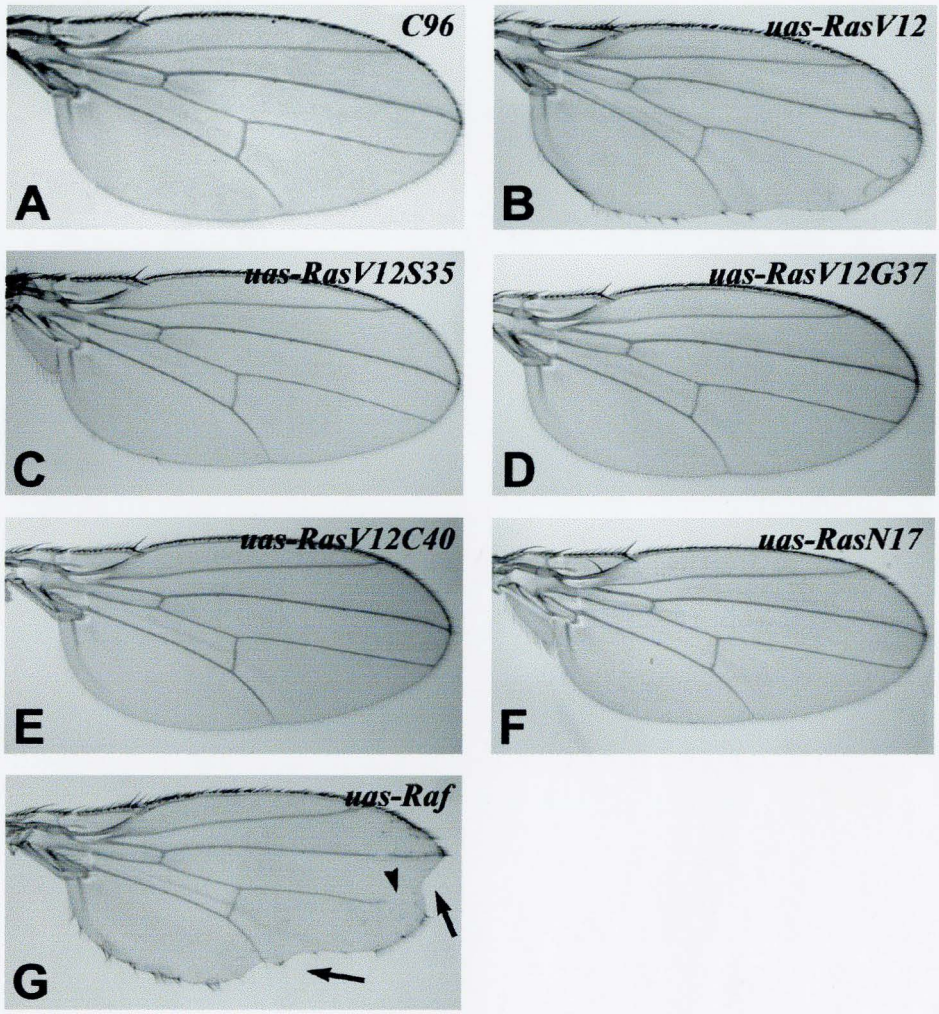
C96
A
uas-RasV12
B
uas-RasV12S35
C
uas-RasV12G37
D
uas-RasV12C40
E
uas-RasN17
F
uas-Raf
G

targets to elicit a cellular response. As Raf is known to phosphorylate and thus activate numerous transcription factors, the increased potency of the wing phenotype, in comparison to *ras,* is not entirely unexpected.

3.6 Neu DIMERIZATION IN THE MIDLINE OF THE CNS

In examining the developing wing and CNS, the GAL4 expression system drove *neu* expression over intrinsic DEgfr signaling. It was possible that Neu signaling may have required transactivation of DEgfr, or activation of Neu by DEgfr, if they were able to form heterodimers. This event is unlikely, as Neu^{NYPD} was seen to have no effect on MG cell number (Fig. 6G). To further address the issue of possible transactivation of Neu by DEgfr, we designed a kinase inactive allele of neu^{YD}. The $Neu^{K757M, YD}$ mutant carried a mutation of lysine to methionine at position 757 of the transmembrane domain rendering it kinase inactive. Transgenic fly lines were established and tested by Western Blot to ensure proper translation of the *neu* mutant (Fig. 13). Western blot analysis revealed the 185 kDa Neu protein. Midline expression of $neu^{K757M, YD}$ did not significantly affect MG cell number, suggesting that DEgfr is unable to activate Neu (Fig. 14B). In addition, co-expressing activated *DEgfr* and $neu^{K757M, YD}$ did not suppress MG cell numbers, relative to activated *DEgfr* alone (Fig. 14D). In contrast, when neu^{NT} and $neu^{K757M, YD}$ were co-expressed, nearly normal numbers

Figure 13. Protein Expression of *neu*^{K757M,YD} is Detected Using Western Blot Analysis. Third instar larvae were heat shocked for one hour to induce translation in *HSGAL4*/+; *p[uas neu*^{K757M,YD}*]*/+ strains. After a 30 minute recovery, larvae were homogenized in RIPA lysis buffer so that crude protein samples could be prepared. These were run on a Tris-HCL protein gel and then transferred to a PDVF membrane. The membrane was blocked and then incubated in the appropriate dilutions of primary and secondary antibody prior to detection using the ECL Western blot detection kit. Arrows indicate expression of a protein band, in each strain, which corresponds to the correct Neu size of 185 kDa. These bands correspond to the 185 kDa band seen from NDL2-5 mouse mammary tumor cell protein lysates. (Arrowhead). This cell line overexpresses the *neu* proto-oncogene under the control of the mouse mammary tumor virus (MMTV) long terminal repeat (LTR) (Siegel et al., 1999). Blank lanes to the left of each strain show the non-heat shocked samples for the respective line.

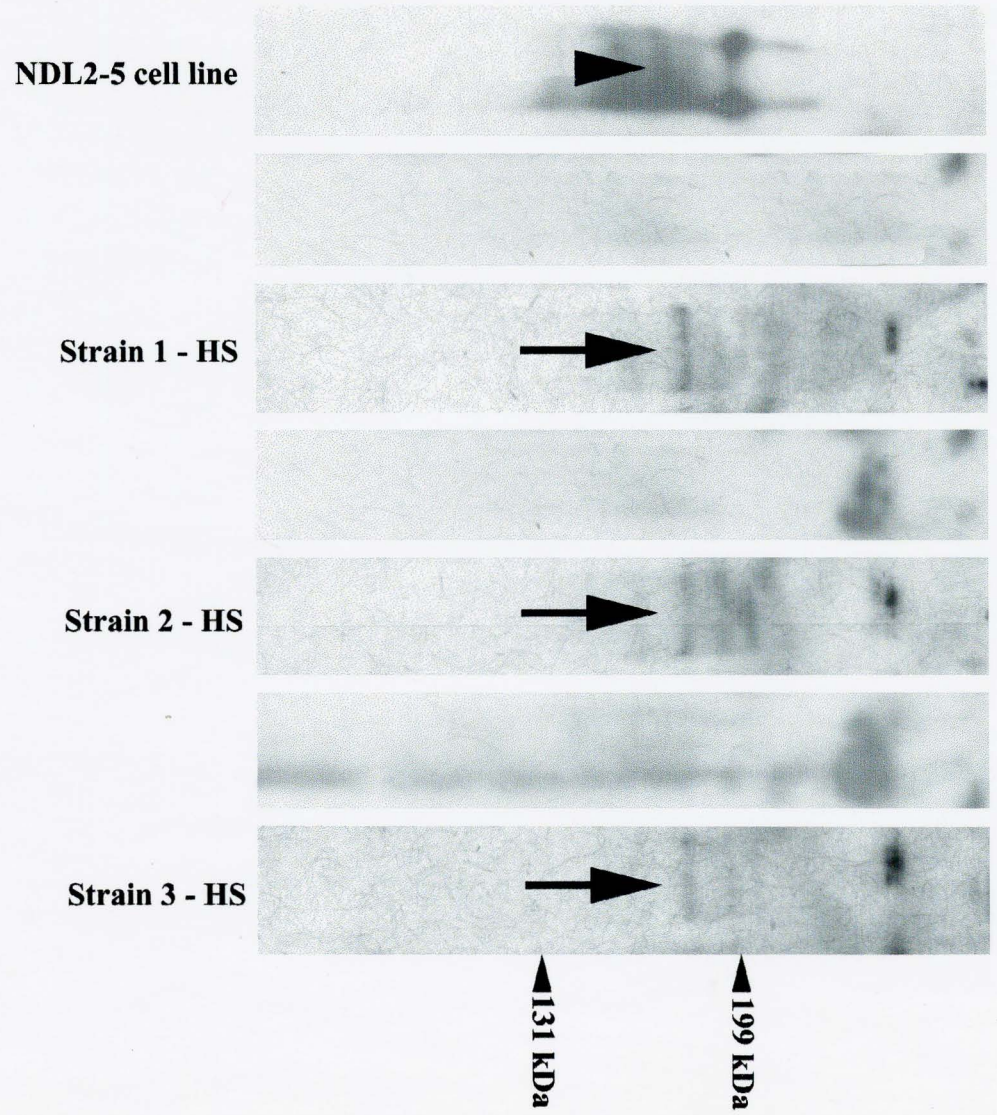
NDL2-5 cell line
Strain 1 - HS
Strain 2 - HS
Strain 3 - HS
131 kDa
199 kDa

Figure 14. Mis-expression of Neu$^{K757M, YD}$ provides evidence for homo-dimerization of Neu receptors in the midline of the CNS. Generation of a kinase inactive allele of *neu^{YD}* allowed for an investigation into whether Neu was able to form heterodimers with the DEgfr. Mis-expression of *neu$^{K757M, YD}$* in the midline did not affect MG numbers (B), relative to control embryos (A). Co-expression of *neu$^{K757M, YD}$* and an active *DEgfr* showed no decrease in MG numbers (D), in relation to overexpression of the DEgfr (C). However, when active *neu* was co-expressed with *neu$^{K757M, YD}$* in the midline, a dramatic reduction in the number of MG cells was noted (F), relative to active *neu* alone (E). This reduction suggests that Neu is able to homodimerize, but does not form dimers with the DEgfr, or play any role in transactivation of this receptor.

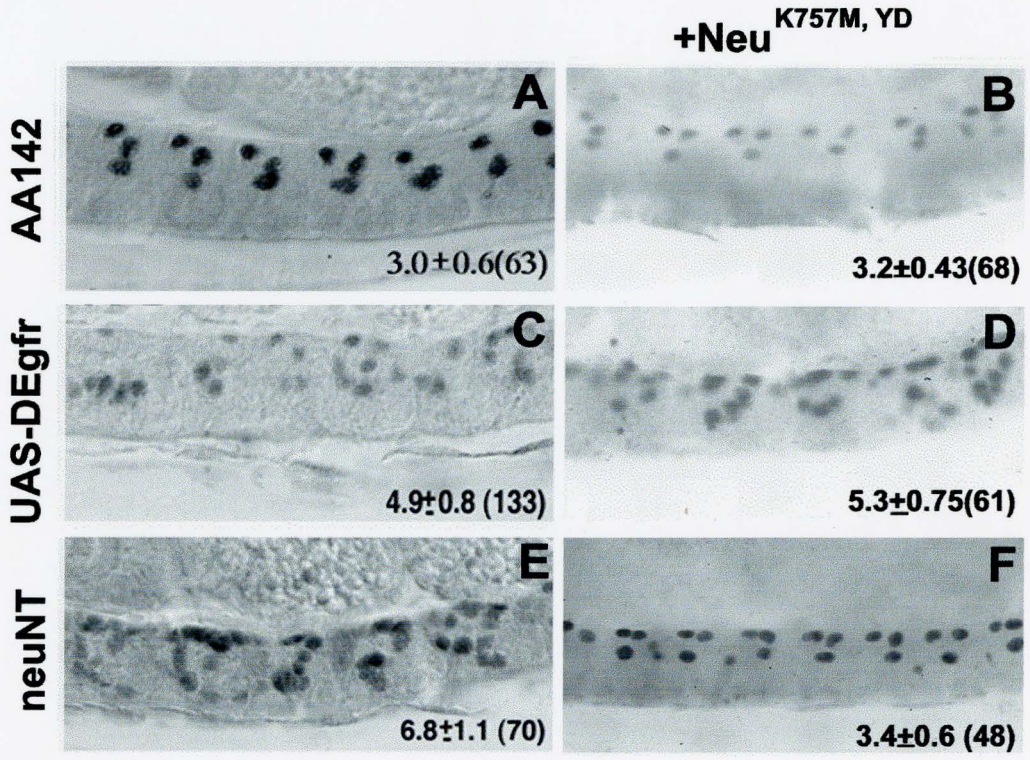
+Neu K757M, YD
AA142
UAS-DEgfr
neuNT
A
B
C
D
E
F
3.0±0.6(63)
3.2±0.43(68)
4.9±0.8 (133)
5.3±0.75(61)
6.8±1.1 (70)
3.4±0.6 (48)

of MG were observed, suggesting that Neu^{NT} was potently suppressed upon dimerization with $Neu^{K757M, YD}$ (Fig. 14F).

In contrast to expression in the midline of the CNS, $neu^{K757M,YD}$ appeared to suppress signaling from the DEgfr during wing development. While $neu^{K757M,YD}$ had no wing phenotype (Fig. 15B), it suppressed the notch phenotype which resulted when activated *DEgfr* was driven in the wing (Fig. 15D). However, co-expression of neu^{NT} and $neu^{K757M, YD}$ showed a reduction in the potency of the wing phenotype (Fig. 15F), which resulted when activated *neu* was mis-expressed alone (Fig. 15E). Observing wing and midline phenotypes suggests that, while Neu likely functions via homodimerization, it may also play some role in sequestering DEgfr signals.

3.7 DEFICIENCY SCREENING REVEALED PUTATIVE *neu* INTERACTING GENES

After having characterized the specific *neu* wing phenotypes, which result upon mis-expression of the *neu* add back alleles (Figure 5), we sought to identify putative genes that participate in modifying or suppressing signaling from Neu. Wings were examined from *UAS-neu/+; C96/+* flies also heterozygous for either a second or third chromosome deficiency. Large scale genetic screening of second and third chromosome deficiency stocks was performed to identify putative genes and genomic regions in *Drosophila,* required for signaling from specific Neu pTyr. An interaction was determined by noting those deficiencies

Figure 15. Neu suppresses the DEgfr in the wing. In contrast to mis-expression in the midline, Neu appears to suppress DEgfr signaling in the wing. Mis-expression of $neu^{K757M, YD}$ in the wing has no visible phenotype (B). However, when active *DEgfr* and $neu^{K757M, YD}$ are co-expressed, the notch phenotype, associated with overexpression of the DEgfr, (C) is abolished (D). Supporting evidence seen from mis-expression in the midline, Neu does appear to homodimerize in the wing. Active *neu* produces severe wing vein defects, including ectopic vein tissue, margin loss and wing deltas (E). When active *neu* is co-expressed with $neu^{K757M, YD}$ a dramatic reduction in the potency of the wing phenotype is detected (F). While Neu maintains the ability to homodimerize in the wing, it may play an additional role in sequestering signals from the DEgfr.

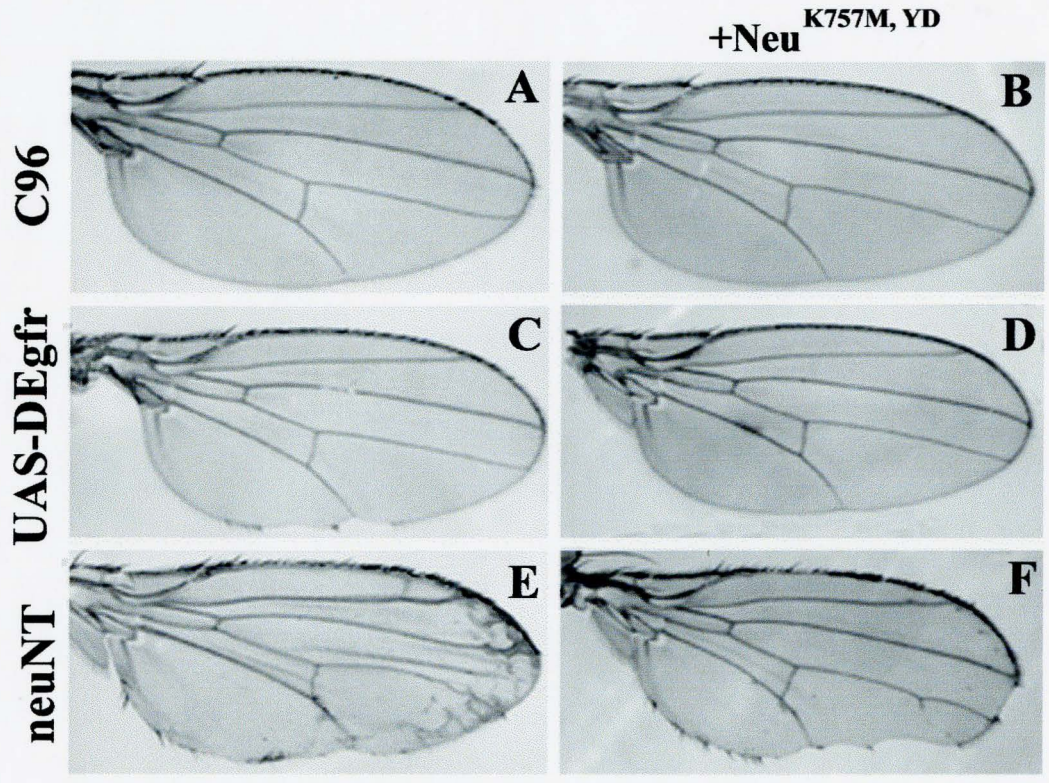
+Neu K757M, YD
C96
UAS-DEgfr
neuNT
A
B
C
D
E
F

that enhanced or suppressed the *neu* add-back wing phenotypes. As with the adaptor and second messenger screens, at least two replicates of each cross were performed so that a minimum of 40 wings could be observed for assigning a numerical value to the modified wing phenotype (See Appendix, Figure 1). Deficiency screening was performed on 172 stocks uncovering 72% and 75% of the second and third chromosome, respectively. A number of deficiencies enhanced or suppressed signaling from each *neu* allele, while others affected signaling from only a single Neu pTyr. In total, 16 second chromsome deficiencies were found to interact with Neu signaling. Third chromsome screening revealed 25 deficiencies that affected *neu* wing phenotypes (Table 3.2 and 3.3). Two second chromosome deficiencies [Df(2L)cl-h3 and Df(2L)H20] greatly suppressed signaling from Neu^{YD} alone (Table 3.2). In contrast, Df(2L)Prl and Df(3R)slo8 severely enhanced only the Neu^{YD} phenotype (Table 3.2 and 3.3). These results can also be seen when examining other Neu pTyr. For example, Df(2L)prd1.7 and Df(3L)E44 enhanced Neu^{YE} signaling alone, while deficiencies (2R)ES1, (2L)TW50 and (2R)017 greatly suppressed Neu^{YE} signals. Additionally, several deficiencies generally enhanced [Df(2R)CX1, Df(3R)ea and Df(3R)DI-BX12] or suppressed [Df(2L)Mdh and Df(3L)st-f13] most of the *neu* alleles (Table 3.2 and 3.3). Enhancement and suppression of the wing phenotypes were scored on a scale from one to nine, with five indicating no interaction, one being complete suppression of *neu* signaling, and nine as severe enhancement of the *neu* wing phenotype.

Table 3.2. Summary of Enhancers and Suppressors of Neu Signaling from a Second Chromosome Deficiency Screen. Eighty-two second chromosome deficiency lines were screened against each individual *neu* add-back allele to determine genomic regions involved in modifying signaling from specific Neu pTyr. The results are summarized and scored numerically, with an empty box indicating no interaction, complete suppression of the wing phenotype scored as one and severe enhancement of the wing phenotype as nine. For the range of wing phenotypes and logic used in assigning specific values to the resulting wings, refer to the Appendix, Figure 1; Methods 2.12.

Second Chromosome Deficiency Screen for Enhancers and Suppressors of Neu Signaling - 85 Deficiency lines tested - 72% of the Chromosome Uncovered									
Deficiency (Bloomington Stock Number)	**Breakpoints**	**Number of Genes within Deficiency**	**Putative Interacting Genes**	**NYPD**	**YA**	**YB**	**YC**	**YD**	**YE**
Df(2R)X58-12 (282)	058D01-02;059A	142	Dve, Gp150, wrapper, Cdk9				2		
Df(2R)X58-7,pr(1)cn(1) (283)	058A01-02;058E04-10	184	Tbp,PpN58A,PpD5				1	1	
Df(2R)CX1,b[1]pr[1] (442)	049C01-04;050C23-D02	220	E(Egfr)B56, Nrk, Drk, RacGAP		7	7	7	8	7
DF(2R)017 (543)	056F05;056F01/5	42	Toll-7, 18w						3
Df(2R)P34 (757)	055E02-04;056C01-11	136	CG7417					3	
Df(2L)cl-h3 (781)	025D02-04;026B02-05	191	CG14030, Kr-h1, myotubularin, tkv					1	
Df(2R)nap9 (1007)	042A01-02;042E06-F01, 041A-B;042BC	249	Bub1 (protein kinase), Scr42A (protein tyrosine kinase)					3	
Df(2L)Mdh, cn[1] (1045)	030D-30F;031F, 030D01-E01;032D01-032F03	127	CG13125 (protein phosphatase regulator), CG4588 (serine/threonine kinase)	1		1	4		4
Df(2R)knSA3 (1150)	051B05-11;051F05-13, 003C01-12;003C01-02;021F-022A08	311	auk, xen, knot			2	2	4	
Df(2R)or-BR6 (1682)	059D05-10;060B03-08, 040;060E04[L]40F;059E[R]	313	PHDP			2		2	2
Df(2L)Prl (3079)	032F01-03;033F01-02	151	Unknown					9	
Df(2R)ES1 (3157)	060E06-08;060F01-02	101	Distal-less, Kruppel, Tkr						3
Df(2L)H2O (3180)	036A08-09;036E01-02	189	dachshund, grapes					1	
Df(2L)TW50, cn[1] (3189)	036E04-F01;038A06-07	85	Ptp36E, CG7180					2	1
Df(2L)prd1.7 (3344)	033B02-03;034A01-02	176	kek1, Tor						8
Df(2R)Chi,g230 (4542)	060A03-07;060B04-07	170	gbb (glass bottom boat), chip					3	

Table 3.3. Summary of Enhancers and Suppressors of Neu Signaling from a Third Chromosome Deficiency Screen. Eighty-seven third chromosome deficiency lines were screened against each individual *neu* add-back allele to determine genomic regions involved in modifying signaling from specific Neu pTyr. The results are summarized and scored numerically, with an empty box indicating no interaction, complete suppression of the wing phenotype scored as one and severe enhancement of the wing phenotype as nine. For the range of wing phenotypes and logic used in assigning specific values to the resulting wings, refer to the Appendix, Figure 1; Methods 2.12.

Third Chromosome Deficiency Screen for Enhancers and Suppressors of Neu Signaling - 87 Deficiency lines tested - 75% of the Chromosome Uncovered									
Deficiency (Bloomington Stock Number)	**Breakpoints**	**Number of Genes within Deficiency**	**Putative Interacting Genes**	**NYPD**	**YA**	**YB**	**YC**	**YD**	**YE**
Df(3R)ea, kni[ri-1] p[p] (383)	088E07-13;089A01	195	CG6535(phosphatidylinositol 3-kinase), Gyc89A	7		7	7	7	7
Df(3R)D605 (823)	097E03;098A05	102	Serrate (Egfr ligand), Pelle, Bigmax				2		
Df(3L)AC1 (997)	067A02;067D07-13	204	Shc					2	
Df(3R)by62, red[1] (1893)	085D11-14;085F06	235	Protein Phosphatase D3, Ras85D, Fps85D, CG9746, CG8866,CG8286,CG16899				8		
Df(3R)p-XT103 (1962)	085A02;085C01-02	149	Relish, Hunchback, Map kinase kinase 4, CG7994				1		
Df(3R)Tpl10 (1990)	083C01-02;084B01-02, 083D04-05;084A04-05;098F01-02	272	zen, Scr, Dfd, pb, Ama, Taf250				2		
Df(3L)R-G7, rho[ve-1] (2400)	062B08-09;062F02-05	175	Dos, Misshapen, Roughened				1		
Df(3L)st-f13, Ki[1] (2993)	072C01-D01;073A03-04	210	thread (apoptosis inhibitor), argos	2		1	1	3	4
Df(3R)ry615 (3007)	087B11-13;087E08-11	295	single-minded				1	3	2
Df(3R)DI-BX12, ss[1] (3012)	091F01-02;092D03-06	198	center-divider, squeeze, Ire, Ire-1			7	7	9	7
Df(3L)h-122, h[i22] (3024)	066D10-11;066E01-02	112	Unknown				7		6
Df(3L)ZN47 (3096)	064C;065C	280	vvl, pcv, vein						3
Df(3R)e-R1, Ki[1] (3340)	093B06-07;093D02	124	bagpipe, tinman, E(Egfr)C22			1	2	2	4
Df(3R)slo8 (3468)	096A02-07;096D02-04	227	slingshot					8	
Df(3L)31A (3627)	078A;078E, 078D;079B	177	SAK					2	
Df(3L)HR119 (3649)	063C02;063F07	113	sprouty, arrowhead					3	
Df(3L)M21, kni[ri-1] p[p] (3650)	062F;063D, 062A;064C	141	Unknown					2	
Df(3L)C190 (4366)	069F03-04;070C03-04	152	capricious, tartan					2	
Df(3L)Pc-2q, ry[506] (4430)	078C05-06;078E03-079A01	132	Aef1				2		2
Df(3R)DG2 (4431)	089E01-F04;091B01-02	354	frayed, fluted, Dad, deterin						2
Df(3L)iro-2, Sb[sbd-2] (4507)	069B01-05;069D01-06	62	mirror						2
Df(3R)H-B79, e[*] (4962)	092B03;092F13	176	bwk, Ire, capicua			2	2	2	4
Df(3L)XS533 (5126)	076B04;077B	205	tricornered						2
Df(3R)e1025-14 (5694)	082F08-10;083A01-03	99	Ksr					2	4
Df(3L)E44 (5915)	069D02;069E03-05	41	Ptp69D						9

CHAPTER 4 DISCUSSION

The overexpression and involvement of the vertebrate family of Epidermal Growth Factor RTKs in numerous human cancers has been well documented (Siegel et al., 1999; Siegel et al., 1994; Bargmann and Weinberg, 1988). In this thesis we have aimed at illustrating the signaling pathways of discrete pTyr outputs of the Neu/ErbB2 RTK. Our goals were, not only to dissect the signaling pathway of this receptor, but also to identify putative *Drosophila* genes involved in the enhancement or suppression of this receptor's signaling capacity. In this regard, we have examined the signaling pathway of misexpressed transgenic Neu by screening individual Neu pTyr against amorphic alleles of a number of second messengers and adaptor proteins. This screen was performed by misexpressing *neu* add back alleles in the fly wing. This approach had numerous benefits, as the fly is readily susceptible to genetic manipulation and can be mated and amplified in a relatively short time span. Additionally, screening in the wing allowed us to examine cell signaling in a non-essential *Drosophila* tissue, such that lethality was not a factor. In this manner, we have demonstrated that each of the five identified pTyr of Neu are alternate activators of orthologous SH2/PTB signaling proteins, and can each contribute to signaling in *Drosophila* tissues.

In addition to deciphering the signaling components of this receptor, we sought to determine whether transgenic Neu was capable of dimerizing with the sole member of the *Drosophila* EGFR family. In addition to homodimerizing, the Neu receptor also serves as a binding partner for each of the remaining three members of the vertebrate EGFR family. While the overall greatest degree of structural similarity exists between the DEgfr and vertebrate ErbB1, Neu/ErbB2 also shows conserved similarity to the DEgfr, with up to 79% amino acid similarity between the kinase domains of these two receptors. We have addressed the issue of heterodimerization versus homodimerization of Neu receptors, by co-expressing activated alleles of both *neu* and the *DEgfr* in two *Drosophila* tissues. We used the wing and midline for co-expression of these alleles since putative interactions could be easily determined by analyzing the resulting wing phenotype, or by assessing MG cell numbers.

4.1 Neu SIGNALING AT THE WING MARGIN

We have illustrated that expression of activated mammalian Neu in transgenic *Drosophila* generates phenotypes comparable to overexpression of intrinsic DEgfr signaling. The rat *neu* oncogene is able to suppress apoptosis in the MG cell lineage and is capable of expanding the domains of wing veins. These are both previously characterized, dosage sensitive *DEgfr* hypermorphic phenotypes (Lanoue and Jacobs, 1999; Sturtevant and Bier, 1995). Most Neu pTyr were able to generate phenotypes when mis-expressed in the wing margin.

Consistent with the MG assay, the wing proved most sensitive to signaling from Neu^{YD}. Additionally, no wing phenotype was detected from mis-expression of the neu^{YA} allele, consistent with an inhibitory role in mammalian signaling pathways (Dankort et al., 1997; Dankort et al., 2001). The lack of apparent Neu^{YA} signaling may reflect inhibitory feedback of YA upon the NYPD signal. Therefore, isolating mutations that confer a wing phenotype to the neu^{YA} allele may identify genes required for the repression of RTK signaling.

Deficiency screening revealed one genomic region that might contain such a candidate gene. Heterozygotes of Df(2R)CX1 and neu^{YA} displayed an enhancement of the YA wing phenotype. Unfortunately, this large deficiency uncovers 220 genes that encode for several adaptor proteins, one enhancer of Egfr signaling as well as many genes with unknown function. Additionally, the remaining *neu* add back alleles showed equally enhanced wing phenotypes, suggesting that this may be a consequence of perturbed wing development, rather than a genetic interaction with neu^{YA}. Further investigation of this region, with smaller deficiencies, is required to more precisely pinpoint putative genes responsible for the observed enhancement. This will hopefully allow us to identify single or multiple genes implicated in inhibitory feedback.

In contrast to mis-expression in the midline, neu^{NYPD} generated a visible phenotype in the wing. Although it is lacking any characterized transforming pTyr, Neu^{NYPD} retains transformation potential in mammals (Dankort et al., 2001).

It is possible that Neu^{NYPD} acts as a dimeric partner for other ErbB receptors, and thus signals via association with them. This lends further support to the notion that Neu^{NYPD} may activate additional signaling pathways. Further studies and screening are required to identify these messengers.

While the signaling cassettes of many RTK pathways are generally conserved, some mammalian second messengers have no apparent ortholog in *Drosophila*, such as the p62 DOK family (Lock et al., 1999). In this sense, it was interesting that each of the identified Neu pTyr appeared to signal in *Drosophila*. Although the docking domain of this receptor shows the least degree of similarity to the endogenous DEgfr receptor (31%), Neu appears to mediate signaling in a manner comparable to the DEgfr. Therefore, we have suggested that the signaling pathways employed by these RTKs are conserved, and that orthologs can be functionally determined in *Drosophila*.

Such studies are highly useful in investigating the specific roles for various genes as well as in determining whether or not mammalian transgenes can complement gene function. For example, studies have previously demonstrated that both Human GRB2 and *Drosophila* Drk can compensate for *C. elegans* SEM-5 during vulval induction (Stern et al., 1993). Having noted that *neu* transgenes were able to complement *Drosophila* gene function, we next aimed at dissecting the pathway employed by the individual pTyr residues of this RTK.

4.2 DOSAGE SENSITIVE SCREENING FOR MODIFIERS OF Neu SIGNALING

The complexity and intricacy of signal transduction pathways can be dissected in screens that identify genetic enhancers or suppressors of a phenotype of a dominant allele. This thesis employed the wing in a productive screen, to identify second messengers of Neu. Similar studies have provided the first identification of numerous second messengers, such as *sos* and *ksr* (Rogge et al., 1991; Therrien et al., 1995). Such studies have had profound implications in mapping out components of signal transduction pathways, as well as providing information regarding the hierarchical functioning of these genes. As demonstrated by Bhandari and Shashidhara (2001), dominant phenotypes generated by a mammalian oncogene expressed in *Drosophila* can be used in a modifier screen to uncover novel genes involved in well characterized signal transduction pathways. In this thesis we have demonstrated that dosage sensitive modifier genetics in *Drosophila* can also be used to dissect signal transduction pathways activated by a mammalian oncogenic RTK.

Transgenic *neu* lines were crossed to a variety of amorphic alleles of second messenger and adaptor protein mutants. Adaptor or second messenger function was assigned to individual pTyr when a genetic interaction was detected between the mutated *Drosophila* gene and the mammalian transgene. Our

screening provided several interesting insights into Neu signaling and specific output pathways.

The adaptor protein Grb-2 participates in propagating mammalian YB signals. Binding of Grb-2 to YB is required for transformation of rat fibroblasts by Neu^{YB} (Dankort et al., 1997). Additionally, inhibiting Grb-2 function is effective in suppressing Neu^{YB} signals (Dankort et al., 2001). Our screening did not implicate YB as the sole binding site of *Drosophila* Grb-2 (*drk*). We found that mutations in *drk* suppressed signaling from multiple pTyr outputs, including YB. Interestingly, we found that mutations in *drk* suppressed neu^{YD} wing phenotypes. Mammalian Shc associates directly with Neu^{YD}, and further recruits Grb-2 through Y317 to signal to Ras (Rozakis-Adcock et al., 1993; Salcini et al., 1994; Lai et al., 1995). While Dshc likely associates with YD, it lacks the binding site required for Grb-2 binding. Although unexpected, these results suggest that additional signaling components may be involved downstream of Dshc in *Drosophila.* Among these, Grb-2 may be directly implicated via association with unidentified pTyr on DShc, or by recruitment from additional second messengers.

As our results for Grb-2 function were somewhat unclear, we sought to test genes whose functions were required either upstream or downstream of *drk.* Using *Drosophila* orthologs of Sos, Ras, Gab-1, Dab and Shp-2, we observed more specific suppression of neu^{YB} wing phenotypes. In *Drosophila,* Drk may be

activated by Shp-2 (*csw*), which itself may be recruited by Gab-1 (*dos*), which associates with both the Sev and DEgfr RTKs (Cleghon et al., 1998; Herbst et al., 1999; Johnson Hamlet and Perkins, 2001). Dab (*dab*) and Sos (*sos*) function downstream of Grb-2 to activate Ras signaling pathways. Our screening showed a strong suppression of neu^{YB} signals by mutations in *csw* and *dos* and milder suppression by mutations in *sos* and *dab*. These data suggest that certain Grb-2 functions are specific to YB activation and that these functions are similar to association with the Sev or DEgfr RTKs due to the conserved involvement of *csw*, *dos*, *sos* and *drk* signaling components.

Peptide binding studies have indicated that Shc could bind to and signal from pTyr YC and YE (Lai et al., 1995); however, Shc will repeatedly immunoprecipitate with Neu^{YD} in culture (Dankort et al., 1997; Dankort et al., 2001). Our screening has indicated that YD signals are completely suppressed in the absence of Dshc. Additionally, it appears that YD is the only pTyr that shows a genetic interaction with Dshc.

The adaptor proteins Nck and PLCγ interact directly with ErbB-2 (Peles et al., 1991; Dougall et al., 1996); however, we did not detect a genetic interaction with the *Drosophila* orthologs, *dock* and *sl*. Conversely, with the exception of YE, we found that Neu signaling is sensitive to reduced *ras* function. Dankort et al. (1997) showed that inhibiting Ras with Rap1A peptide decreased fibroblast transformation signals from all Neu pTyr, with YC being the least affected. In

contrast, we found Neu^{YC} to be sensitive to reduced *ras* function, and that Neu^{YE} was insensitive to *ras*. However, YE signals were suppressed by reduced Raf levels, suggesting that this pTyr may activate Ras independent routes to Raf activation.

Our results support some, but not all of the signaling pathways that were expected, based upon *in vitro* cell transformation experiments (Figure 16). This may have been due in part because the specific genes in question were not dosage sensitive. In order to resolve this issue, further screening with dominant negative alleles is required. Additionally, structural differences between *Drosophila* and mammalian adaptors may alter the affinity of *Drosophila* adaptor proteins to specific pTyr relative to their mammalian orthologues.

In order to further investigate Neu signaling pathways and identify novel genes implicated in specific pTyr outputs, expanded modifier screens are required. Further knowledge can also be gained by examining the conservation of Neu signaling pathways in additional *Drosophila* tissues. We found that, when mis-expressed in the midline, Neu^{YE} was insensitive to reduced *ras* function in terms of suppressing apoptosis of the MG. It is promising that signal output pathways from Neu^{YE} appear to be conserved in the wing and CNS; however, it is necessary to test additional second messengers and adaptors in order to reveal the specific differences in signaling between different cell types.

Figure 16. Summary Diagram of the *Drosophila* Second Messenger and Adaptor Proteins that Genetically Interact with Transgenic Neu. Our genetic data supports some of the interactions that were previously identified for several adaptor proteins in cell transformation experiments (Dankort et al., 1997; Dankort et al., 2001). In accordance with these studies, we found that Shc (red) associates exclusively with Neu^{YD} and completely suppresses YD signals in its absence. Additionally we found that YB and YD signals were suppressed in a Grb-2/Drk (green) mutant background. This was unexpected for YD, since DShc lacks the binding site for Grb-2, suggesting that additional signaling components may be involved downstream of DShc. We did find that YB and YD signals were most potently suppressed by a lack of *sos* function (blue), suggesting these pathways propagate signaling via the *ras/raf* pathway (yellow and pink, respectively). Furthermore, we found that *csw, dos* and *dab* strongly suppressed YB signals suggesting that certain Grb-2 functions are specific to YB activation. These functions are similar to association with the Sev or DEgfr RTKs due to the conserved involvement of *csw*, *dos*, *sos* and *drk* signaling components.

We found that Neu^{YE} was the only pTyr insensitive to reduced *ras* function, however YE signals did respond to reduced *raf* levels. This suggests that YE signaling may induce Ras-independent events leading to Raf activation. In addition, we found that orthologues for the adaptor proteins Nck and PLCγ (Dock and sl, respectively) did not interact genetically with transgenic Neu.

Moreover, no interaction was detected with *phyllopod,* which is required for the differentiation of the R1 and R6 rhabdomeres in the fly eye. This is achieved via conserved activation of the *ras* pathway.

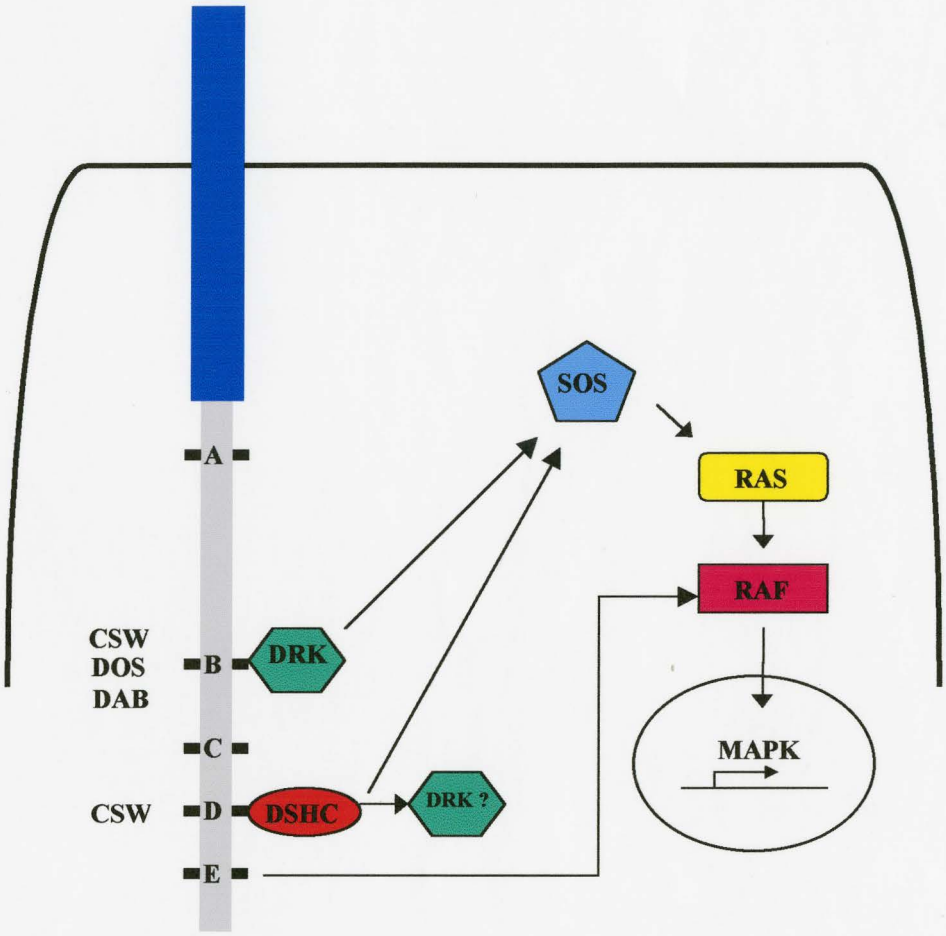

Dock ?
Sl ?
Phyllopod ?

We are currently screening the *Drosophila* midline with several of the adaptor and second messenger alleles, used during the wing assay. We hope to be able to verify the roles of specific adaptor proteins, such as DShc and Drk, which modified specific Neu pTyr in the wing.

The specificity of cell signaling is often tissue specific. For example, the DEgfr functions in the midline CNS to provide anti-apoptotic signals to the MG cell lineage. However, it's roles during wing development are to provide cell identity, as well as specify patterning and growth. The intracellular signaling cascades employed by active Neu may differ in a tissue specific manner. Using the MG assay we can determine if DShc and Drk are functionally redundant and if they share conserved signaling pathways in multiple *Drosophila* tissues.

4.3 GENETIC ENHANCERS AND SUPPRESSORS OF Neu SIGNALING

Many studies have used genetic screening to identify genomic regions that interact with viable alleles of signal transduction genes (Li et al., 2000; Bhandari and Shashidhara, 2001; Huang and Rubin, 2000; Firth et al., 2000). We employed similar genetic screening to identify genomic regions in *Drosophila* that were able to enhance or suppress signaling from transgenic Neu signals in the wing. Second and third chromosome deficiency screening revealed 41 regions that either enhanced or suppressed Neu signaling. These regions can be further subdivided by noting which deficiencies affected most of the *neu* add back alleles,

versus those deficiencies that altered signaling from only one or two identified Neu pTyr. Only one of the 172 deficiencies tested altered the *neu*^{YA} wing phenotype. As this site is implicated as an inhibitor of Neu function, this is a promising first step in identifying putative genes involved in RTK suppression. In addition, seven deficiencies affected four or more of the *neu* add back alleles and 25 of the deficiencies affected signals from only one of the identified Neu pTyr. The 25 deficiency regions, which affected only individual output pathways, were searched for putative genes responsible for the observed interaction. Candidates for these interactions included a number of protein tyrosine kinases, protein phosphatases and serine/threonine kinases. Additionally, a number of RNA polymerase transcription factors and adaptor genes were identified, such as *dachshund*, *mirror*, *Shc*, *Dos*, *ras*, and *MAPK*. The DEgfr ligands *argos*, *vein* and *serrate* were also uncovered. Many of these genomic regions also include a large number of uncharacterized genes as well as genes involved in wing proliferation and differentiation, such as *distal-less* and *capicua*. Of these 25 interactions, 6 showed suppression of the *neu*^{YE} phenotype and 2 demonstrated enhancement of YE signaling only. This is encouraging since YB and YD signaling outputs have been well characterized (Dankort et al., 1997; Dankort et al., 2001), yet much speculation remains over the signaling pathway employed by Neu^{YE}. In addition, 6 deficiencies modified Neu^{YC} signals exclusively. Our genetic data for YC suggests that signals from this pTyr are affected by reduced

ras levels, while other transformation studies have found YC to be relatively insensitive to *ras* function (Dankort et al., 1997). Accordingly, NeuYC may activate additional second messengers or adaptors in *Drosophila* that differ from those signaling components used in the vertebrate system. Further screening of these genomic regions may reveal novel genes implicated in a *Drosophila* model of transgenic Neu^{YC} signaling.

Expanded modifier screening will further explore the *Drosophila* genome for genes that are required in the output of Neu signals. Investigating the interacting genomic regions with smaller deficiencies will hopefully allow us to identify novel genes implicated in signaling from the identified Neu pTyr. Additionally, verifying these genetic interactions in the midline, using the MG assay, may reveal environment specific differences in signaling between different cell types. Deciphering these candidate *Drosophila* genes is the first step in identifying mammalian orthologues that function in the network of signaling pathways that are activated by oncogenic RTKs. In addition to mapping out signaling pathways, identifying functions for these signal transduction proteins should reveal their specific roles in the induction of human malignancies.

4.4 Neu SUPPRESSES APOPTOSIS OF THE MIDLINE GLIAL CELL LINEAGE

Mis-expression of *neu* add-back alleles in the midline demonstrated a suppression of apoptosis of the MG cell lineage. The potency of the anti-

apoptotic phenotype strongly correlated with the transforming potential of identified pTyr residues (Dankort et al., 1997). Neu^{YD} signaling generated the most potent suppression of apoptosis. As previously discussed, mammalian Shc binds YD and further recruits Grb-2 through Y317. The *Drosophila* Shc orthologue, Dshc, lacks this pTyr and most likely signals through a Grb-2 independent pathway (Lai et al., 1995). Shc may also signal independently of GRB2 and Ras by the adaptor protein Gab2. This in turn relays directly to the PI-3K/Akt pathway, to provide anti-apoptotic signals (Gu et al., 2000).

Neither neu^{YA} or neu^{NYPD} suppressed apoptosis of the MG when mis-expressed in the midline, although Neu^{NYPD} signals generated a detectable wing phenotype. The lack of an anti-apoptotic effect from neu^{NYPD} was somewhat unexpected as the neu^{NYPD} phenotype in the wing was suppressed in a *raf* mutant background, and anti-apoptotic signals in the MG function mainly through Raf (Kurada and White, 1998).

4.5 DIMERIZATION OF Neu RECEPTORS

In the human and rat model, Neu is capable of both homodimerization, as well as heterodimerization with other members of the EGFR family. Since the fly has only one EGFR family member, that shares a relatively moderate degree of structural similarity with Neu, we examined whether or not these receptors were capable of transactivating specific pTyr residues via heterodimerization. To

accomplish this we created a single point mutation in the transmembrane domain of the *neu*^{YD} add back allele to generate a kinase dead version of this mutant (*neu*^{K757M,YD}). We chose to maintain the YD pTyr residue as it generates a potent signal upon transactivation, which is readily detectable in both the wing and glial assay. Furthermore, as NYPD cannot signal through the DEgfr, any resulting phenotype would be specific to signaling from YD. We conceived that, if Neu heterodimerized with the DEgfr, the "kinase dead" capacity of Neu would sequester DEgfr signals; however, the DEgfr should opposingly transphosphorylate, and thereby activate, the YD pTyr remaining on the Neu receptor. As a result, we would expect a characteristic YD phenotype.

The *neu*^{K757M,YD} allele alone had no visible phenotype in the wing nor did it suppress apoptosis of the MG when mis-expressed in the midline. When *neu*^{K757M,YD} was co-expressed with activated *DEgfr*^{A887T} in the midline, resulting glial numbers were not increased to those numbers seen with YD signaling, but rather they were consistent with overexpression of endogenous DEgfr signaling. In contrast, co-expression of *neu*^{K757M,YD} and actived *neu*^{NT} resulted in a decrease of glial cell numbers, relative to the anti-apoptotic phenotype observed with *neu*^{NT} alone. These results suggest that Neu does not interact or dimerize with the DEgfr; however, homodimerization of Neu receptors is likely. These results are further supported by examining mis-expression of *neu*^{NYPD} in the midline. Neu^{NYPD} signals have no effect on suppressing apoptosis of the MG. If Neu were

capable of dimerization with the DEgfr we would have expected that this pTyr deficient Neu receptor would still be able to activate and elicit a response from the endogenous DEgfr. Alternately, our results support the notion that the Neu^{NYPD} receptors are homodimerizing, and thus no signal output is detected.

Studies of the transmembrane region of Neu receptors have revealed that a conserved, site-specific Val, Glu and Gly tripeptide (VEG domain) is responsible for transformation and signal transduction of the wild-type Neu receptor (Burke et al., 1997). Loss or mis-localization of this domain greatly reduces the tendency for these receptors to dimerize. Additionally, the transmembrane domains of ErbB receptors self-associate strongly in the absence of their extracellular domains (Mendrola et al., 2002). It has therefore been suggested that the transmembrane region is largely responsible for the stable association and dimerization of Neu receptors *in vivo*. Since the DEgfr lacks the conserved VEG domain and shares only 48% sequence similarity of the transmembrane domain with Neu, it is not surprising that co-expression of these receptors in the midline does not support evidence for heterodimerization capabilities.

Our wing assay data suggested that $Neu^{K757M,YD}$ suppressed active $DEgfr^{A887T}$ signals. Co-expression of these alleles resulted in a loss of the notch phenotype, seen with overexpression of the DEgfr on it's own. However, further supporting the notion of homodimerization, co-expression of $neu^{K757M,YD}$ and

neu^{NT} resulted in a mild wing phenotype, in comparison to the severe phenotype associated with *neu*^{NT} alone.

4.6 FUTURE RESEARCH

Future research with the *neu* add back alleles will involve continued screening of amorphic alleles of signal transduction genes and transcription factors, to identify additional genes implicated in Neu signaling. This could include *Drosophila* orthologues of the members of the Wnt pathway, Elk-1 transcription factors, members of the JAK/STAT pathway and Ets transcription factors. In addition, kinases involved in regulating apoptosis, such as cdk1 could be tested as well as *Drosophila* orthologues of vertebrate ECM proteins, such as Erbin, which are involved in the basolateral localization of the Neu receptor in the vertebrate system. Our hope is to eventually isolate and identify novel second messenger and adaptor genes required for signaling from the identified Neu pTyr. Continued screening will include the X chromosome deficiency kit (available from the Bloomington Stock Center) to explore the *Drosophila* genome for putative signal transduction genes on this chromosome. These include the tyrosine phosphatase *corkscrew* and the serine/threonine kinase *raf*.

By searching Flybase, we have tried to identify candidate genes that are most likely responsible for the noted enhancement or suppression of Neu signaling. Of most interest to us were those genomic regions that modified

individual Neu signals. From these results, we have since obtained deficiency stocks that uncover smaller regions of the large deficiencies, initially obtained from the Bloomington stock kits. By screening these smaller deficiencies we should be able to more precisely pinpoint the genomic region responsible for the noted interactions. Eventually, our hopes are that we will be able to isolate and identify single genes responsible for modifying individual Neu signals. Once we have established such a genetic interaction, we can then focus on further validating an interaction *in vitro*. Additionally, mutagenesis experiments could be used on identified novel genes, in the hopes of generating null alleles, which will further demonstrate the *in vivo* function of these putative signaling proteins.

REFERENCES

Abbott, M. K. and Lengyel, J. A. (1991) Embryonic head involution and rotation of male terminalia require the *Drosophila* locus *head involution defective*. *Genetics* **129**: 783-9.

Bargmann, C.I. and Weinberg, R.A. (1988) Oncogenic activation of the *neu*-encoded receptor protein by point mutation and deletion. *EMBO J.* 7: 2043-2052.

Bhandari, P. and Shashidhara, L.S. (2001) Studies on human colon cancer gene *APC* by targeted expression in *Drosophila*. *Oncogene* **20**: 6871-6880.

Bilder, D. and Perrimon, N. (2000) Localization of apical epithelial determinants by the basolateral PDZ protein Scribble. *Nature* **403**: 676-680.

Brand, A.H., Manoukian, A.S. and Perrimon, N. (1994) Ectopic expression in Drosophila. *Methods Cell Biol.* **44**: 635-654.

Brummel, T., Abdollah, S., Haerry, T.E., Shimell, M., Merriam, J., Raftery, L., Wrana, J.L. and O'Connor, M.B. (1999) The *Drosophila* activin receptor baboon signals through dSmad2 and controls cell proliferation but not patterning during larval development. *Genes Dev.* **13**: 98-111.

Burke, C.L., Lemmon, M.A., Coren, B.A., Engelman, D.M. and Stern, D.F. (1997) Dimerization of the p185^{neu} transmembrane domain is necessary but not sufficient for transformation. *Oncogene* **14**: 687-696.

Campos-Ortega, J.A. and Hartenstein, V. (1985) The embryonic development of *Drosophila melanogaster*. Springer-Verlag: Berlin.

Chan, R., Hardy, W., Laing, M., Hardy, S. and Muller, W.J. (2002) The catalytic activity of the ErbB-2 receptor tyrosine kinase is essential for embryonic development. *Mol and Cell Biol.* **22**: 1073-1078.

Chang, H.C., Solomon, N.M., Wassarman, D.A., Karim, F.D., Therrien, M., Rubin, G.M. and Wolff, T. (1995) *phyllopod* functions in the fate determination of a subset of photoreceptors in *Drosophila*. *Cell* **80**: 463-472.

Chen, Y. and Struhl, G. (1996) Dual roles for Patched in sequestering and transducing Hedgehog. *Cell* **87**: 553—563.

Cleghon, V., Feldmann, C., Ghiglione, C., Copeland, T.D., Perrimon, N., Hughes, D.A., and Morrison, D.K. (1998) Opposing actions of CSW and RasGAP modulate the strength of Torso RTK signaling in the *Drosophila* terminal pathway. *Mol. Cell* **2**: 719-727.

Dankort, D.L., Maslikowski, B., Warner, N., Kanno, N., Kim, H., Wang, Z., Moran, M.F., Oshima, R.G., Cardiff, R.D. and Muller, W.J. (2001) Grb2 and Shc adapter proteins play distinct roles in Neu (ErbB-2) induced mammary tumorigenesis: Implications for human breast cancer. *Mol. Cell Biol.* **21**: 1540-1551.

Dankort, D.L. and Muller, W.J. (2000) Signal transduction in mammary tumorigenesis: a transgenic perspective. *Oncogene* **19**: 1038-1044.

Dankort, D.L., Wang, Z., Blackmore, V., Moran, M. and Muller, W.J. (1997) Distinct tyrosine autophosphorylation sites negatively and positively modulate Neu-mediated transformation. *Mol. and Cell. Biol.* **17**: 5410-5425.

Dong, R. and Jacobs, J.R. (1997) Origin and differentiation of supernumary midline glia in *Drosophila* embryos deficient for apoptosis. *Dev. Biol.* **190**: 165-177.

Dougall, W.C., Qian, X., Miller, M.J. and Greene, M.I. (1996) Association of signaling proteins with a nonmitogenic heterodimeric complex composed of epidermal growth factor receptor and kinase-inactive p185c-neu. *DNA Cell Biol.* **15**: 31-40.

Fambrough, D., McClure, K., Kazlauskas, A. and Lander, E.S. (1999) Diverse signaling pathways activated by growth factor receptors induce broadly overlapping, rather than independent, sets of genes. *Cell* **97**: 727-741.

Firth, L., Manchester, J., Lorenzen, J.A., Baron, M. and Perkins, L.A. (2000) Identification of genomic regions that interact with a viable allele of the *Drosophila* protein tyrosine phosphatase *corkscrew*. *Genetics* **156**: 733-748.

Forbes, A.J., Nakano, Y., Taylor, A.M. and Ingham, P.W. (1993) Genetic analysis of *hedgehog* signalling in the *Drosophila* embryo. *Ingham, Brown, Martinez Arias,* **1993**: 115-124.

Freeman, M. (1996) Reiterative use of the EGF receptor triggers differentiation of all cell types in the *Drosophila* eye. *Cell* **87**: 651-660.

Fujimoto, J., Sawamoto, K., Okabe, M., Tagaki, Y., Tezuka, T., Yoshikawa, S., Ryo, H., Okano, H. and Yamamoto, T. (1999). Cloning and characterization of DFak56, a homolog of focal adhesion kinase, in *Drosophila melanogaster. J. Biol. Chem.* **274**: 29196-201.

Garrity, P.A., Rao, Y., Salecker, I., McGlade, L., Pawson, T. and Zipursky, S.L. (1996) *Drosophila* photoreceptor axon guidance and targeting requires the dreadlocks SH2/SH3 adapter protein. *Cell* **85**: 639-650.

Ghiglione, C., Perrimon, N. and Perkins, L. (1999) Quantitative variations in the level of MAPK activity control patterning of the embryonic termini in *Drosophila. Dev. Biol.* **205**: 181-193.

Gu, H., Maeda, H., Moon, J.J., Lord, J.D., Yoakim, M., Nelson, B.H. and Neel, B.G. (2000) New role for Shc in activation of the phosphatidylinositol 3-kinase/Akt pathway. *Mol. Cell Biol.* **20**: 7109-7120.

Gustafson, K. and Boulianne, G. L. (1996) Distinct expression patterns detected within individual tissues by the GAL4 enhancer trap technique. *Genome* **39**: 174-182.

Hay, B. A., Maile, R. and Rubin, G.M. (1997) P-element insertion-dependent gene activation in the *Drosophila* eye. *Proc Natl Acad Sci USA* **94**:5195-5200.

Herbst, R., Carroll, P., Allard, J., Schilling, J., Raabe, T. and Simon, M.A. (1996) Daughter of sevenless is a substrate of the phosphotyrosine phosphatase Corkscrew and functions during sevenless signaling. *Cell* **85**: 899-909.

Herbst, R., Zhang, X., Qin, J. and Simon, M.A. (1999) Recruitment of the protein tyrosine phosphatase CSW by DOS is an essential step during signaling by the sevenless receptor tyrosine kinase. *EMBO J.* **18**: 6950-6961.

Hill, K.K., Bedian, V., Juang, J.L. and Hoffmann, F.M. (1995) Genetic interactions between the *Drosophila* Abelson, Abl, tyrosine kinase and failed axon connections (Fax), a novel protein in axon bundles. *Genetics* **141**: 595-606.

Huang, A. and Rubin, G. (2000) A misexpression screen identifies genes that can modulate RAS1 pathway signaling in *Drosophila melanogaster*. *Genetics* **156**: 1219-1230.

Hunter, T. (1998) The Croonian lecture, 1997. The phosphorylation of proteins on tyrosine: its role in cell growth and disease. *Philos. Trans. R. Soc. Lond. B. Biol. Sci.* **353**: 583-605.

Hynes, N.E. and Stern, D.F. (1994) The biology of ErbB-2/Neu/HER-2 and its role in cancer. *Biochim. Biophys Acta.* **1198**: 165-184.

Ingham, P.W. and Hidalgo, A. (1993) Regulation of *wingless* transcription in the *Drosophila* embryo. *Development* **117**: 283-291.

Jackson, R.G., Wiedau-Pazos, M., Sang, T., Wagle, N., Brown, C., Massachi, S. and Geschwind, D. (2002) Human wild-type Tau interacts with *wingless* pathway components and produces neurofibrillary pathology in *Drosophila*. *Neuron* **34**: 509-519.

Jacobs, J.R. (2000) The midline glia of *Drosophila*: a molecular genetic model for the developmental functions of glia. *Prog. Neurobiol.* **62**: 475-508.

Jaulin-Bastard, F., Saito, H., Bivic, A., Ollendorff, V., Marchetto, S., Birnbaum, D. and Borgt, J. (2001) The ERBB2/HER2 receptor differentially interacts with ERBIN and PICK1 PSD-95/DLG/ZO-1 domain proteins. *J. Biol. Chem.* **276**: 15256-15263.

Johnson Hamlet, M.R. and Perkins, L.A. (2001) Analysis of corkscrew signaling in the Drosophila epidermal growth factor receptor pathway during myogenesis. *Genetics* **159**: 1073-1087.

Kavanaugh, W.M., Turck, C.W. and Williams, L.T. (1995) PTB domain binding to signaling proteins through a sequence motif containing phosphotyrosine. *Science* **268**: 1177-1179.

Kazantsev, A., Walker, H., Slepko, N., Bear, J., Preisinger, E., Steffan, J., Zhu, Y., Gertler, F., Housman, D., Marsh, J. and Thompson, L. (2002) A bivalent Huntingtin binding peptide suppresses polyglutamine aggregation and pathogenesis in *Drosophila*. *Genetics* **30:** 367-376.

Klambt, C., Jacobs, J.R. and Goodman, C.S. (1991) The midline of the *Drosophila* central nervous system: a model for the genetic analysis of cell fate, cell migration and growth cone guidance. *Cell* **64**: 801-815.

Kumar, J.P. and Moses, K. (2001) The EGF receptor and notch signaling pathways control the initiation of the morphogenetic furrow during *Drosophila* eye development. *Development* **128**: 2689-2697.

Kurada, P. and White, K. (1998) Ras promotes cell survival in *Drosophila* by downregulating hid expression. *Cell* **95**: 319-329.

Lai, K.M., Olivier, J.P., Gish, G.D., Henkemeyer, M., McGlade, J. and Pawson, T. (1995) A *Drosophila shc* gene product is implicated in signaling by the DER receptor tyrosine kinase. *Mol. Cell Biol* **15**: 4810-4818.

Lanoue, B.R., Gordon, M.D., Battye, R. and Jacobs, J.R. (2000) Genetic analysis of vein function in the *Drosophila* embryonic nervous system. *Dev. Genet.* **25**: 321-330.

Leevers, S. J., Weinkove, D., MacDougall, L.K., Hafen, E. and Waterfield, M.D. (1996) The *Drosophila* phosphoinositide 3-kinase Dp110 promotes cell growth. *EMBO J.* **15**: 6584-94.

Lesa, G.M. and Sternberg, P.W. (1997) Positive and negative tissue-specific signaling by a nematode epidermal growth factor receptor. *Mol. Biol. Cell* **8**: 779-793.

Lesokhin, A.M., Yu, S., Katz, J. and Baker, N. E. (1999) Several levels of EGF receptor signaling during photoreceptor specification in wild-type, *Ellipse*, and null mutant *Drosophila*. *Dev. Biol.* **205**: 129-144.

Li, W., Noll, E. and Perrimon, N. (2000) Identification of autosomal regions involved in *Drosophila* Raf function. *Genetics* **156**: 763-774.

Li, W. and Perrimon, N. (1997) Specificity of receptor tyrosine kinase signaling pathways: Lessons from *Drosophila*. *Genetic Engineering* **19**: 167-182.

Lin, W., Sanchez, H., Deerinck, T., Morris, J., Ellisman, M. and Lee, K. (2000) Aberrant development of motor axons and neuromuscular synapses in erbB2-deficient mice. *Proc Natl Acad Sci USA* **97**: 1299-1304.

Lock, P., Casagranda, F. and Dunn, A.R. (1999) Independent SH2-binding sites mediate interaction of Dok-related protein with RasGTPase-activating protein and Nck. *J. Biol. Chem.* **274**: 22775-22784.

Luschnig, S., Krauss, J., Bohmann, K., Desjeux, I. and Nusslein-Volhard, C. (2000) The *Drosophila* SHC adaptor protein is required for signaling by a subset of receptor tyrosine kinases. *Molec. Cell* **5**: 231-241.

Madhani, H.D. (2001) Accounting for specificity in receptor tyrosine kinase signaling. *Cell* **106**: 9-11.

Mardon, G., Solomon, N.M. and Rubin, G.M. (1994) dachshund encodes a nuclear protein required for normal eye and leg development in *Drosophila*. *Development* **120**: 3473-3486.

Mendrola, J.M., Berger, M.B., King, M.C. and Lemmon, M.A. (2002) The single transmembrane domains of ErbB receptors self-associate in cell membranes. *J. Biol. Chem.* **7**: 4704-4712.

Obermeier, A., Tinhofer, I., Grunicke, H.H. and Ullrich, A. (1996) Transforming potentials of epidermal growth factor and nerve growth factor receptors inversely correlate with their phospholipase C gamma affinity and signal activation. *EMBO J.* **15**: 73-82.

Olivier, J.P., Raabe, T., Henkemeyer, M., Dickson, B., Mbamalu, G., Margolis, B., Schlessinger, J., Hafen, E. and Pawson, T. (1993) A *Drosophila* SH2-SH3 adaptor protein implicated in coupling the sevenless tyrosine kinase to an activator of Ras guanine nucleotide exchange, Sos. *Cell* **73**: 179-191.

Pawson, T. and Nash, P. (2000) Protein-protein interactions define specificity in signal transduction. *Genes Dev.* **14**: 1027-47.

Peles, E., Levy, R.B., Or, E., Ullrich, A. and Yarden, Y. (1991) Oncogenic forms of the neu/HER2 tyrosine kinase are permanently coupled to phospholipase C gamma. *EMBO J.* **10**: 2077-2086.

Perkins, L., Johnson, M., Melnick, M.B. and Perrimon, N. (1996) The nonreceptor protein tyrosine phosphatase corkscrew functions in multiple receptor tyrosine kinase pathways in *Drosophila*. *Dev. Biol.* **180**: 63-81.

Perrimon, N., Engstrom, L. and Mahowald, A.P. (1985) A pupal lethal mutation with a paternally influenced maternal effect on embryonic development in *Drosophila melanogaster. Dev. Biol.* **110**: 480-491.

Rayter, S.I., Woodrow, M., Lucas, S.C., Cantrell, D.A. and Downward, J. (1992) p21ras mediates control of IL-2 gene promoter function in T cell activation. *EMBO* **11**: 4549-56.

Raz, E., Schejter, E. and Shilo, B. (1991) Interallelic complementation among DER/*flb* alleles: Implications for the mechanism of signal transduction by receptor-tyrosine kinases. *Genetics* **129**: 191-201.

Ricci, A., Lanfrancone, L., Chiari, R., Belardo, G., Pertica, C., Natali, P.G., Pelicci, P.G. and Segatto, O. (1995) Analysis of protein-protein interactions involved in the activation of the Shc/Grb-2 pathway of the ErbB-2 kinase. *Oncogene* **11**: 1519-1529.

Riggleman, B., Schedl, P. and Wieschaus, E. (1990) Spatial expression of the *Drosophila* segment polarity gene *armadillo* is post-transcriptionally regulated by *wingless. Cell* **63**: 549-560.

Roch, F., Jimenez, G. and Casanova, J. (2002) EGFR signaling inhibits Capicua-dependent repression during specification of *Drosophila* wing veins. *Development* **129**: 993-1002.

Rodriguez-Viciana, P., Warne, P.H., Khwaja, A., Marte, B.M., Pappin, D.J., Das, P., Waterfield, M.D., Ridley, A. and Downward , J. (1997) Role of phosphoinositide 3-OH kinase in cell transformation and control of the actin cytoskeleton by Ras. *Cell*, **89**: 457–467.

Rogge, R.D., Karlovich, C.A. and Banerjee, U. (1991) Genetic dissection of a neurodevelopmental pathway: Son of sevenless functions downstream of the sevenless and EGF receptor tyrosine kinases. *Cell* **64**: 39-48.

Rorth, P. (1996) A modular misexpression screen in *Drosophila* detecting tissue-specific phenotypes. *Proc. Natl. Acad. Sci. USA* **93**: 12418-12422

Rozakis-Adcock, M., Fernley, R., Wade, J., Pawson, T. and Bowtell, D. (1993) The SH2 and SH3 domains of mammalian Grb2 couple the EGF receptor to the Ras activator mSos1. *Nature* **363**: 83-85.

Rubinsztein, C.D. (2002) Lessons from animal models of Huntington's disease. *Trends in Genetics* **18**: 202-210.

Salcini, A.E., McGlade, J., Pelicci, G., Nicoletti, I., Pawson, T. and Pelicci, P.G. (1994) Formation of Shc-Grb2 complexes is necessary to induce neoplastic transformation by overexpression of Shc proteins. *Oncogene* **9**: 2827-2836.

Schlessinger, J. (2000) Cell signaling by receptor tyrosine kinases. *Cell* **103**: 211-225.

Schnorr, J.D. and Berg, C. A. (1996) Differential activity of Ras1 during patterning of the *Drosophila* dorsoventral axis. *Genetics* **144**: 1545-1557.

Schweitzer, R. and Shilo, B. (1997) A thousand and one roles for the *Drosophila* EGF receptor. *TIG* **13**: 191-196.

Siegel, P.M., Dankort, D.L., Hardy, W.R. and Muller, W.J. (1994) Novel activating mutations in the *neu* proto-oncogene involved in induction of mammary tumors. *Mol. Cell. Biol.* **14**: 7068-7077.

Siegel, P.M., Ryan, E., Cardiff, R.D. and Muller, W.J. (1999) Elevated expression of activated forms of Neu/ErbB-2 and ErbB-3 are involved in the induction of mammary tumors in transgenic mice: implications for human breast cancer. *EMBO* **18**: 2149-2164.

Simon, M. A. (2000) Receptor tyrosine kinases: Specific outcomes from general signals. *Cell* **103**: 13-15.

Simon, M. A., Bowtell, D.D., Dodson, G.S., Laverty, T.R. and Rubin, G.M. (1991) Ras1 and a putative guanine nucleotide exchange factor perform crucial steps in signaling by the sevenless protein tyrosine kinase. *Cell* **67**: 701-716.

Simon, M. A., Dodson, G.S. and Rubin, G.M. (1993) An SH3-SH2-SH3 protein is required for $p21^{Ras1}$ activation and binds to sevenless and Sos proteins in vitro. *Cell* **73**: 169-177.

Songyang, Z., Carraway, K.L., III, Eck, M.J., Harrison, S.C., Feldman, R.A., Mohammodi, M., Schlessinger, J., Hubbard, S.R., Smith, D.P., Eng, C., Lorenzo, M.J., Ponder, B.A.J., Mayer, B.J. and Cantley, L.C. (1995) The catalytic specificity of protein tyrosine kinases is critical for selective signaling. *Nature* **373**: 536-539.

Songyang, Z., Shoelson, S.E., Chaudhuri, M., Gish, G., Pawson, T., Haser, W.G., King, F., Roberts, T., Ratnofsky, S., Lechleider, R.J. and et al. (1993) SH2 domains recognize specific phosphopeptide sequences. *Cell* **72**: 767-778.

Spradling, A.C., Stern, D., Beaton, A., Rehm, E.J., Laverty, T., Mozden, N., Misra, S. and Rubin, G. M. (1999) The Berkeley *Drosophila* genome project gene disruption project. Single P-element insertions mutating 25% of vital *Drosophila* genes. *Genetics* **153**: 135-177.

Staveley, B.E., Ruel, L., Jin, J., Stambolic, V., Mastronardi, F.G., Heitzler, P., Woodgett, J.R. and Manoukian, A.S. (1998) Genetic analysis of protein kinase B (AKT) in *Drosophila*. *Curr. Biol.* **8**: 599-602.

Stern, M.J., Marengere, L.E., Daly, R.J., Lowenstein, E.J., Kokel, M., Batzer, A., Olivier, P., Pawson, T. and Schlessinger, J. (1993) The human GRB2 and *Drosophila* Drk genes can functionally replace the *Caenorhabditis elegans* cell signaling gene sem-5. *Mol. Biol. Cell* **4**: 1175-1188.

Stewart, B.A., Mohtashami, M., Zhou, L., Trimble, W. S. and Boulianne, G. L. (2001) SNARE-Dependent signaling at the *Drosophila* wing margin. *Dev. Biol.* **234**: 13-23.

Sturtevant, M.A. and Bier, E. (1995) Analysis of the genetic hierarchy guiding wing vein development in *Drosophila*. *Development* **121**: 785-801.

Sturtevant, M.A., Roark, M. and Bier, E. (1993) The *Drosophila* rhomboid gene mediates the localized formation of wing veins and interacts genetically with components of the EGF-R signaling pathway. *Genes Dev.* **7**: 961-973.

Thackeray, J.R., Gaines, P.C., Ebert, P. and Carlson, J.R. (1998) *small wing* encodes a phospholipase C-(gamma) that acts as a negative regulator of R7 development in *Drosophila*. *Development* **125**: 5033-5042.

Therrien, M., Chang, H.C., Solomon, N.M., Karim, F.D., Wassarman, D.A. and Rubin, G.M. (1995) KSR, a novel protein kinase required for RAS signal transduction. *Cell* **83**: 879-888.

Therrien, M., Michaud, N. R., Rubin, G. M. and Morrison, D. K. (1996) KSR modulates signal propagation within MAPK cascade. *Genes Dev.* **10**: 2684-2695.

Valius, M. and Kazlauskas, A. (1993) Phospholipase C-γ1 and phosphatidylinositol 3 kinase are the downstream mediators of the PDGF receptor's mitogenic signal. *Cell* **73**: 321-334.

van der Geer, P., Wiley, S., Gish, G.D., Lai, V.K., Stephens, R., White, M.F., Kaplan, D. and Pawson, T. (1996) Identification of residues that control specific binding of the Shc phosphotyrosine-binding domain to phosphotyrosine sites. *Proc. Natl. Acad. Sci. USA* **93**: 963-968.

Weiner, D.B., Liu, J., Cohen, J.A., Williams, W.V. and Greene, M.I. (1989) A point mutation in the *neu* oncogene mimics ligand induction of receptor aggregation. *Nature* **339**: 230-231.

White, M.A., Vale, T., Camonis, J.H., Schaefer, E. and Wigler, M.H. (1996) A role for the Ral guanine nucleotide dissociation stimulator in mediating Ras-induced transformation. *J. Biol. Chem.*, **271**: 16439–16442.

White, N.M. and Jarman, A.P. (2000) *Drosophila* atonal controls photoreceptor R8-specific properties and modulates both receptor tyrosine kinase and hedgehog signalling. *Development* **127**: 1681-1689.

Whitfield, C.W., Bernard, C., Barnes, T., Hekimi, S. and Kim, S.K. (1999) Basolateral localization of the *Caenorhabditis elegans* epidermal growth factor receptor in epithelial cells by the PDZ protein LIN-10. *Mol. Biol. Cell* **10**: 2087-2100.

Wides, R.J., Zak, N. and Shilo, B. (1990) Enhancement of tyrosine kinase activity of the *Drosophila* epidermal growth factor receptor homolog by alterations of the transmembrane domain. *Eur. J. Biochem.* **189**: 637-645.

Willis, L. and Perrimon, N. (1997) Specificity of receptor tyrosine kinase signaling pathways: Lessons from *Drosophila*. *Genetic Engineering* **19**: 167-182.

Xiao, H., Hrdlicka, L.A. and Nambu, J.R. (1996) Alternate functions of the *single-minded* and *rhomboid* genes in development of the *Drosophila* ventral neuroectoderm. *Mech. Dev.* **58**: 65-74.

Yarden, Y. and Sliwkowski, M.X. (2000) Untangling the ErbB signaling network. *Mol. Cell Biol.* **2**: 127-137.

Zervas, C. G., Gregory, S. L. and Brown, N. H. (2001). *Drosophila* Integrin-linked kinase is required at sites of integrin adhesion to link the cytoskeleton to the plasma membrane. *J. Cell Bio.* **152**: 1007-1018.

Appendix 1. Range of wing phenotypes and their numerical assignment, as a reference for assigning suppression and enhancement values to genetic interactions noted during wing screening. All genetic interactions herein were assigned numerical values based upon the suppression or severity of the resulting wing phenotypes. The wings used for this figure are all heterozygotes of the neu^{YD} allele and a number of different second and third chromosome deficiencies. A near wild-type wing was given a score of one, indicating almost full suppression of the wing phenotype (A). However, these wings often contained one or several small wing deltas, as seen in the magnified region of the wing margin in panel A (black arrow). A small, individual loss of wing margin was scored as two (B), while multiple regions of wing loss were scored as three (C, black arrows). A mildly rough wing margin, combined with wing deltas was scored as four (D). No interaction was scored as five, and represented the usual wing phenotype found when the neu^{YD} allele was mis-expressed alone (E). This includes loss of wing margin (E, arrowhead), ectopic veins (E, black arrow) and wing deltas (E, white arrow). Further enhancement of the wing phenotype was scored as either six (F) or seven (G), depending on the degree of margin loss. Larger singular regions of margin loss were scored as eight (H, black arrow), while large multiple regions of margin loss were scored as nine (I, black arrows).

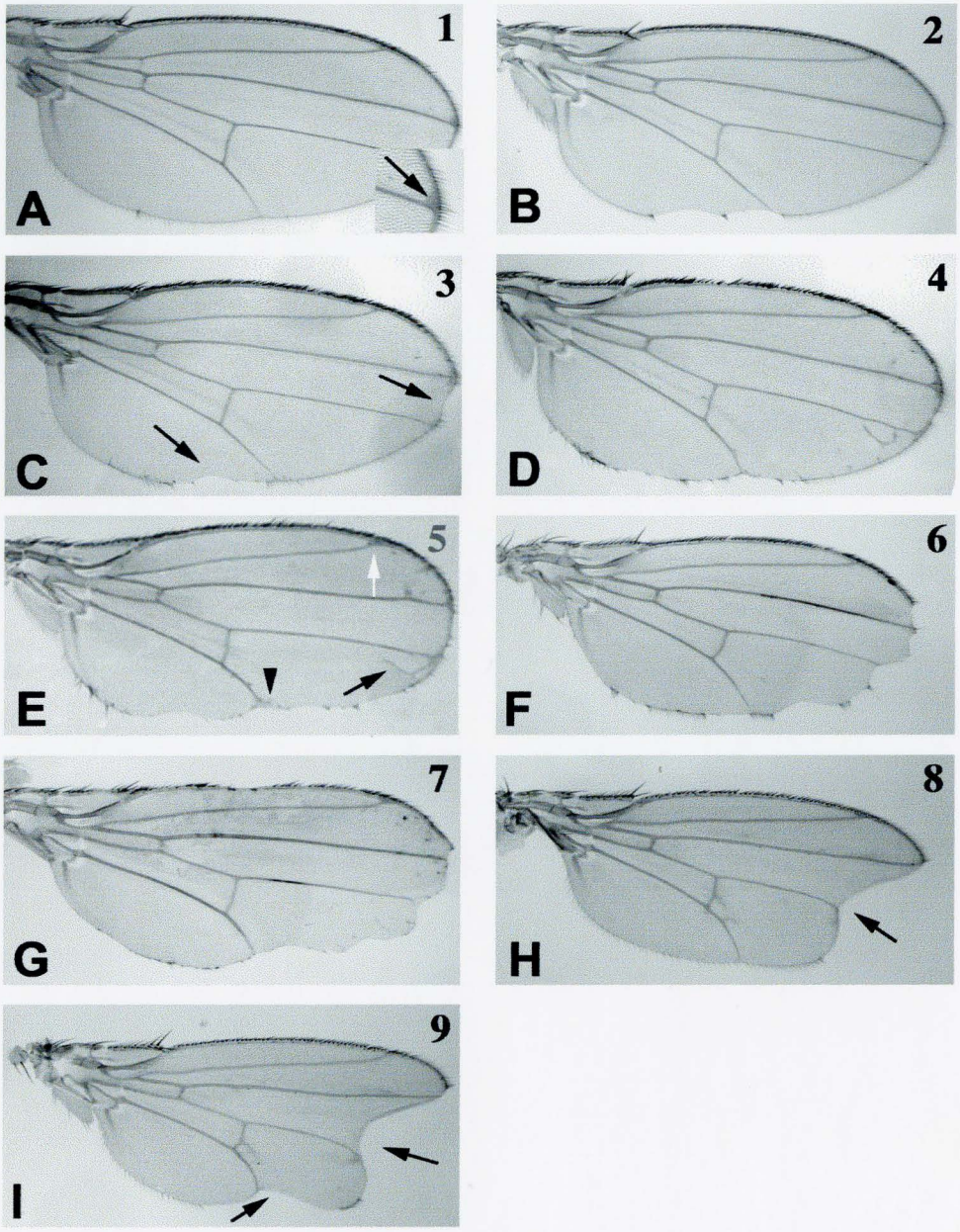
1
A
2
B
3
C
4
D
5
E
6
F
7
G
8
H
9
I

Appendix 2. Neu Phosphotyrosines and candidate adaptors. The surrounding amino acid sequences of the five identified Neu pTyr are indicated, as well as a comparison of each pTyr region to other *Drosophila, C. elegans* and vertebrate orthologues. Analysis of the amino acid sequence of Neu provided the first insight into adaptors and second messengers that may bind to identified pTyr residues. These predictions were based on the conservation of the receptor sequences. The function of each peptide motif is indicated, as it applies to the individual receptors. This chart was kindly adapted from J. Roger Jacobs.

MOTIF	D/ED/E YLXP		PXPEYXNQ		ENPEYL		YYN	
NEU	DAEEYLVPQ	1028 YA	PQPEYVNQS	1144 YB	ENPEYLVPR ENPEYLGLD	1201YC 1253YE	FDNLYYWDQN	1226/7 YD
SEV			KQLYANEG	Y2546			YKSDYYRKEG	Y2380
D-EGFR	DEDDYLMPT	Y1261			DNPEYLLNA	Y1308	SDHEYYNDTQ	Y1356
TORSO	EEELYLEPL	Y918			ENKEYFDLL	Y698		
H-ERB1	ADEYLIPQ	Y1016	PVPEYINQ NPVYHNQP NPEYLNTV	Y1092 Y1110 Y1138	ENAEYLRV	Y1197		
LET-23	DNSYLIPK	Y1242	EAVQYENE	Y1311			NGDYYNQPN SSGYYNEPH	Y1276 Y1289
FUNCTION	Repression of Ras signals, neu, erbB1, LET-23, Torso PLCγ 1 or RasGAP implicated (Obermeier et al., 1996; Cleghon et al., 1998)		YXNX motif, Grb-2 binding in Neu, Sev (Songyang et al., 1993)		NPXY peptides block SHC in *Drosophila* (Lai et al., 1995) low affinitySHC binding in Neu (Kavanaugh et al., 1995)		YYN motif, Grb-2 binding (van der Geer et al., 1996) or SHC in Neu (Dankort et al., 1997) or SHC in Neu (Kavanaugh et al., 1995),(Ricci et al., 1995)	

Appendix 3. Deficiency (2L)cl-h3 suppresses signaling from Neu^{YD} exclusively. Heterozygotes of individual add back *neu* alleles and Df(2L)cl-h3 were found to completely suppress Neu^{YD} signaling (J). In contrast, the remaining *neu* alleles were unaffected by this deficiency and showed no change in the resulting wing phenotypes. For numerical scores and wing assessment refer to Results, Table 3.2 and Appendix, Figure 1.

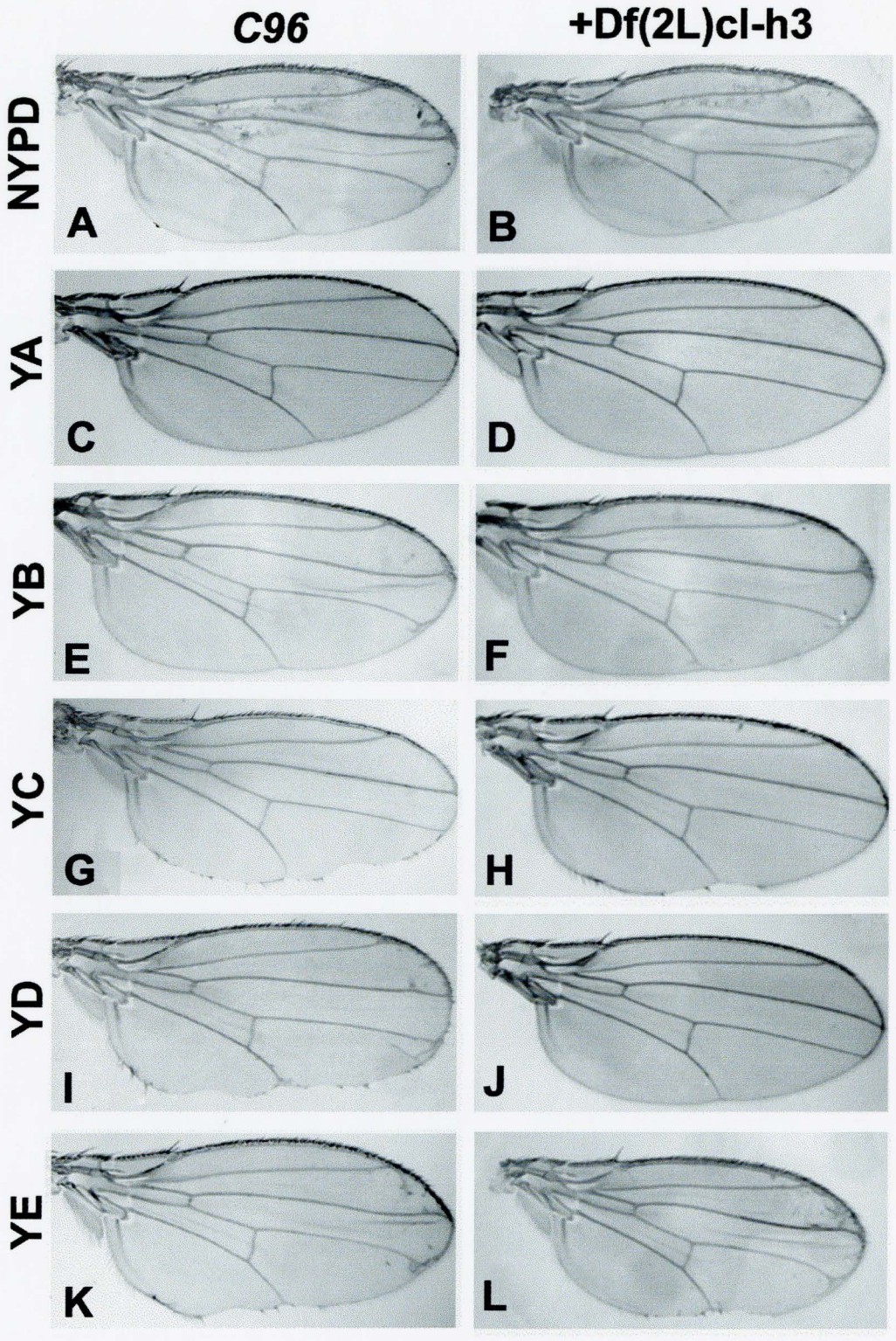
C96
+Df(2L)cl-h3
NYPD
YA
YB
YC
YD
YE
A
B
C
D
E
F
G
H
I
J
K
L

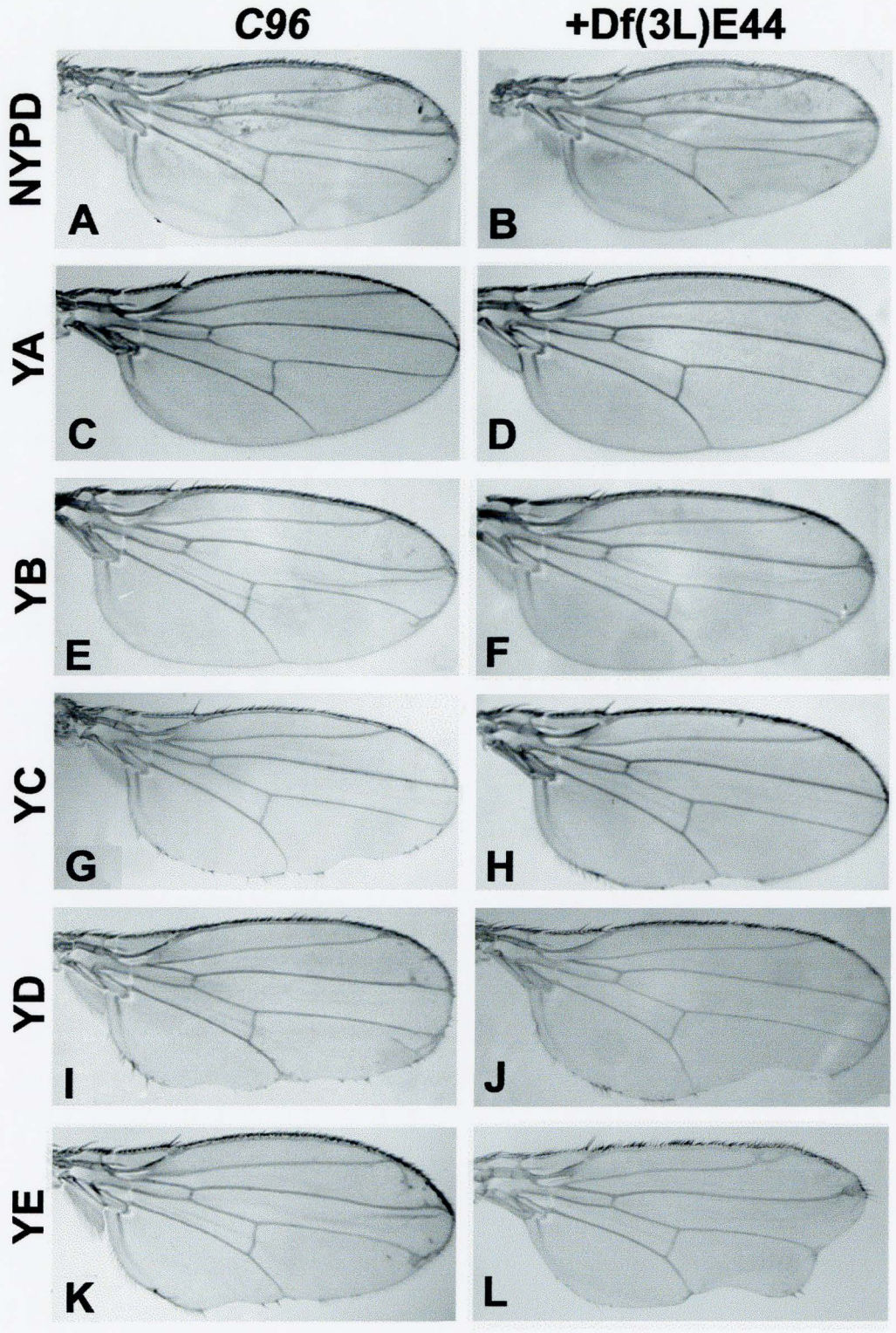
C96
+Df(3L)E44
NYPD
YA
YB
YC
YD
YE
A
B
C
D
E
F
G
H
I
J
K
L

Appendix 5. Deficiency (3R)p-XT103 suppressed signaling from Neu^{YC} exclusively. Heterozygotes of individual add back *neu* alleles and Df(3R)p-XT103 were found to completely suppress Neu^{YC} signaling (H). In contrast, the remaining *neu* alleles were unaffected by this deficiency and showed no change in the resulting wing phenotypes. For numerical scores and wing assessment refer to Results, Table 3.3 and Appendix, Figure 1.

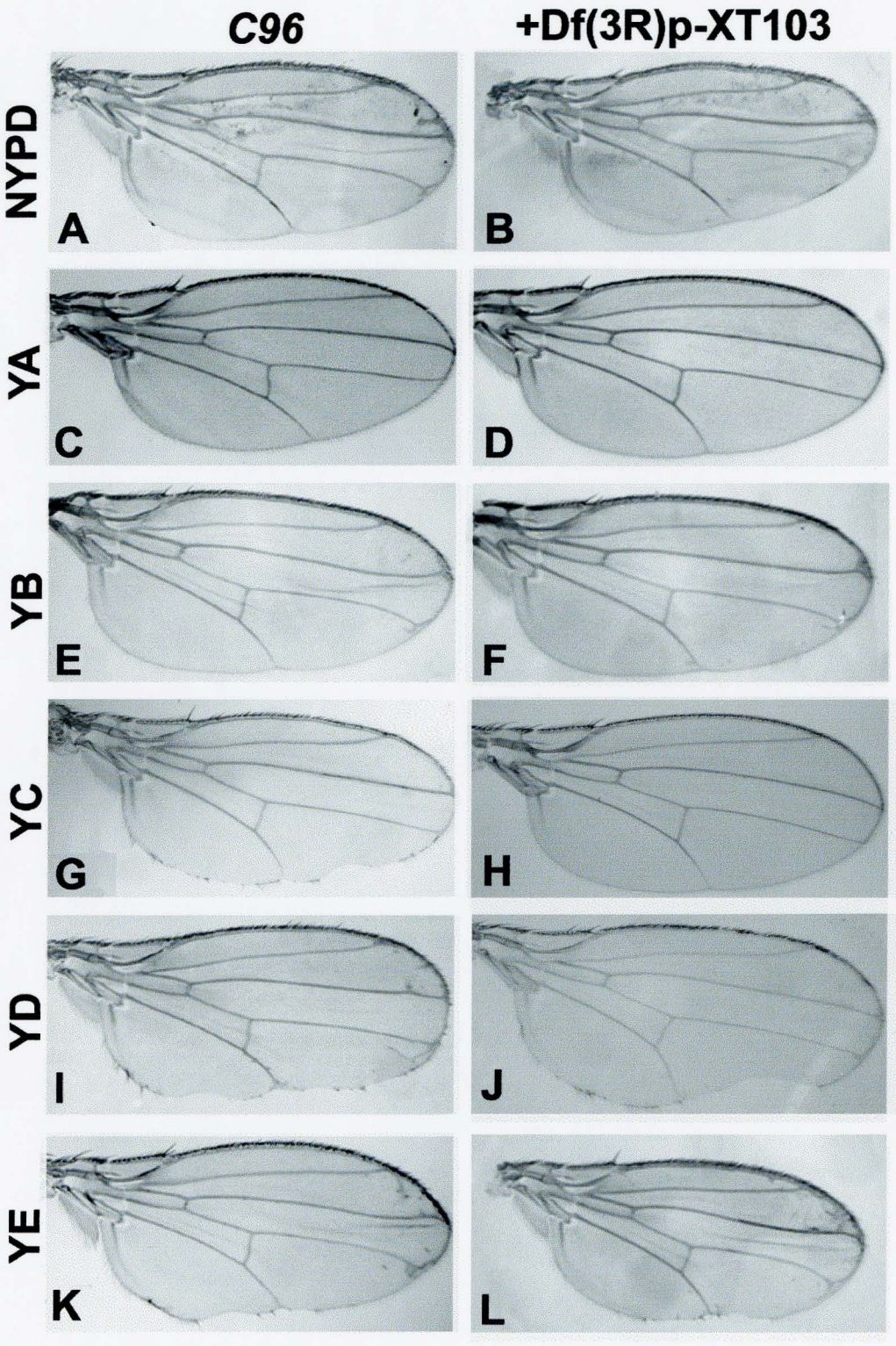
C96
+Df(3R)p-XT103
NYPD
A
B
YA
C
D
YB
E
F
YC
G
H
YD
I
J
YE
K
L

Appendix 6. Deficiency (3R)ea enhanced signaling from multiple Neu outputs. Heterozygotes of individual add back *neu* alleles and Df(3R)ea were found to greatly enhance signaling from $Neu^{NYPD, YB, YC, YD}$ and ^{YE} (B, F, H, J and L, respectively). In contrast, the neu^{YA} allele was unaffected by this deficiency and showed no change in the resulting wing phenotype (D). For numerical scores and wing assessment refer to Results, Table 3.3 and Appendix, Figure 1.

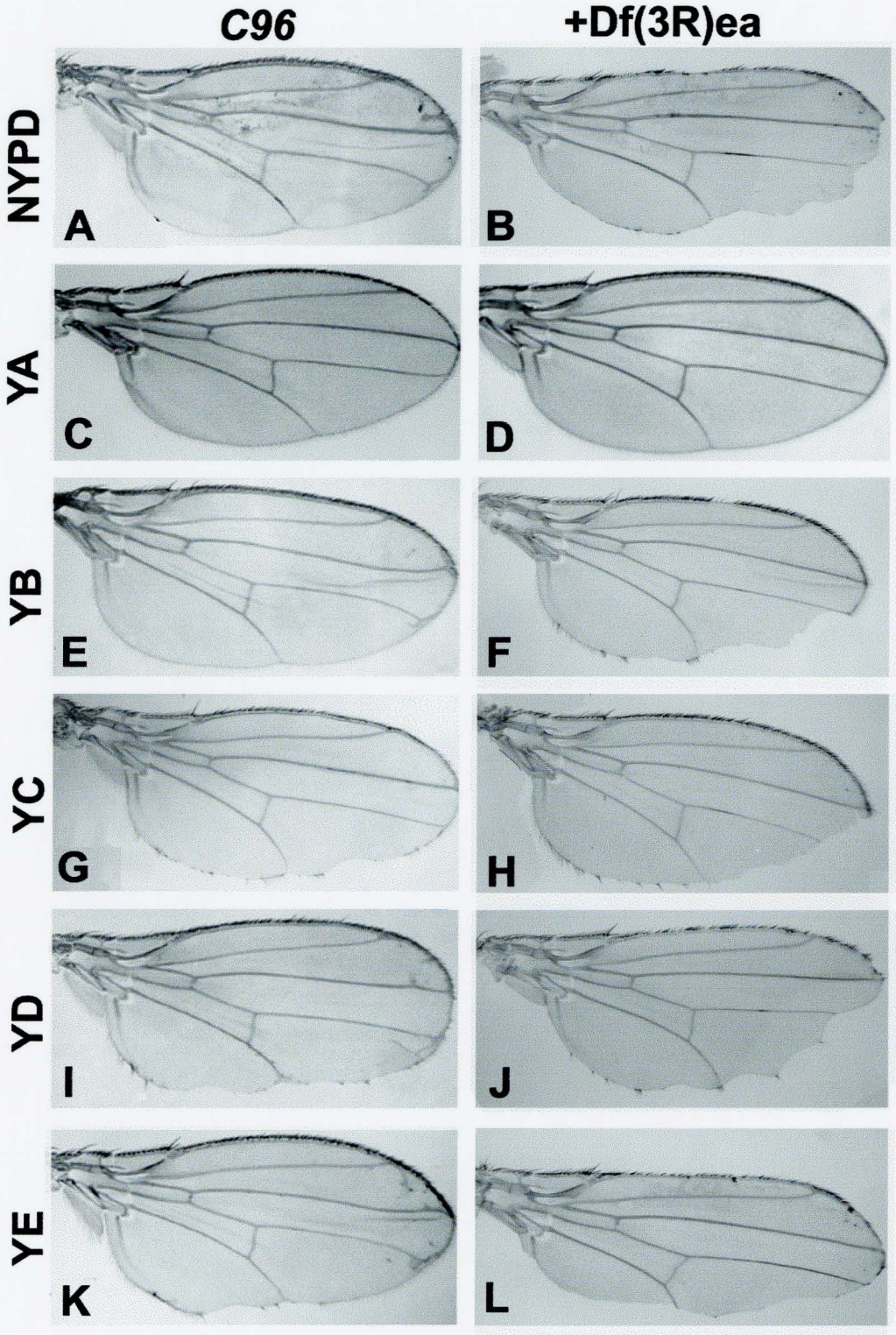
C96
+Df(3R)ea
NYPD
YA
YB
YC
YD
YE
A
B
C
D
E
F
G
H
I
J
K
L

Appendix 7. Deficiency (3L)XS533 suppressed signaling from Neu^{YE} exclusively. Heterozygotes of individual add back *neu* alleles and Df(3L)XS533 were found to dramatically suppress Neu^{YE} signaling (L). In contrast, the remaining *neu* alleles were unaffected by this deficiency and showed no change in the resulting wing phenotypes. For numerical scores and wing assessment refer to Results, Table 3.3 and Appendix, Figure 1.

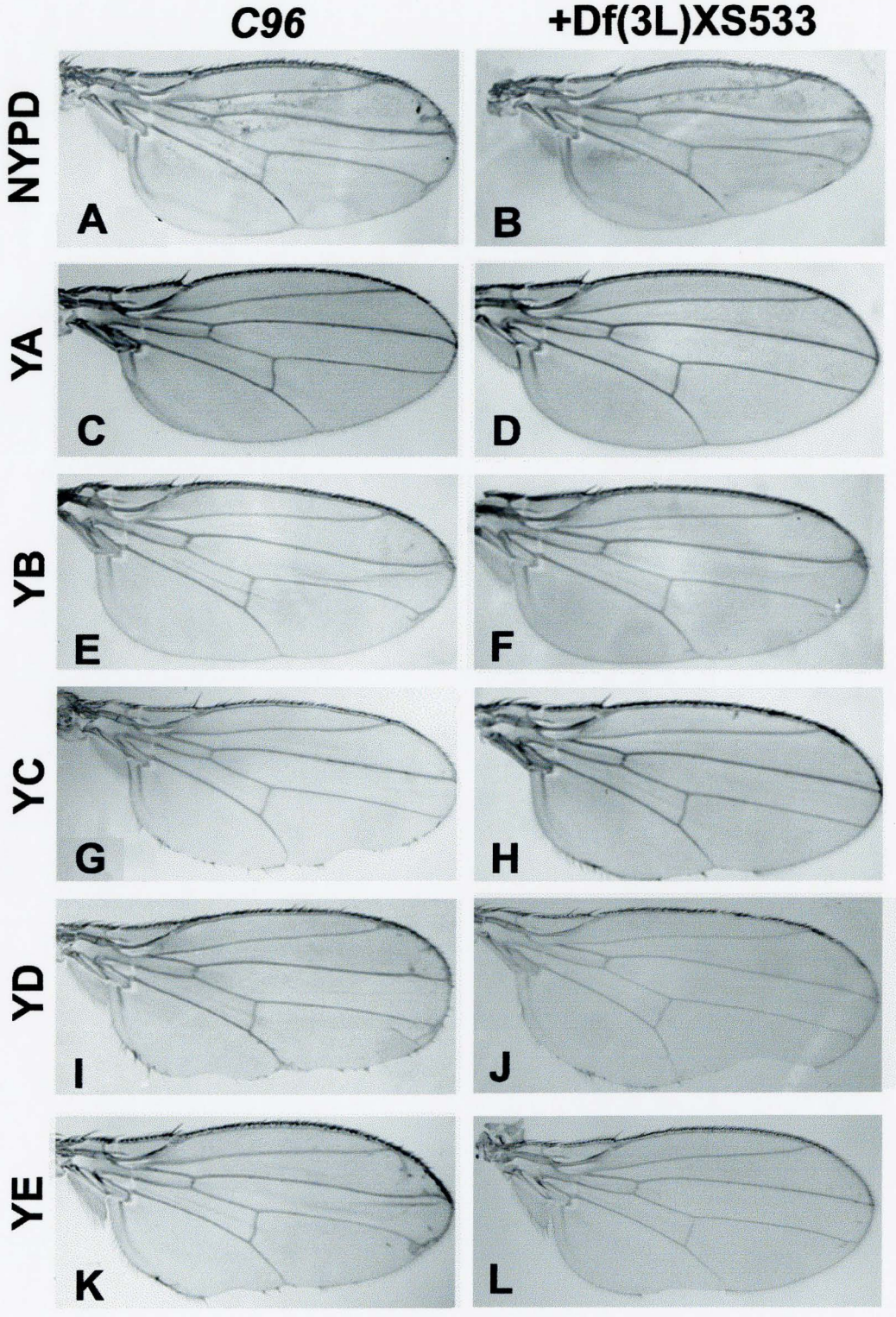
C96
+Df(3L)XS533
NYPD
YA
YB
YC
YD
YE
A
B
C
D
E
F
G
H
I
J
K
L

Appendix 8. Deficiency (2L)Pr1 greatly enhanced signaling from Neu^{YD} exclusively. Heterozygotes of individual add back *neu* alleles and Df(2L)Pr1 were found to greatly enhance Neu^{YD} signaling (J). In contrast, the remaining *neu* alleles were unaffected by this deficiency and showed no change in the resulting wing phenotypes. For numerical scores and wing assessment refer to Results, Table 3.2 and Appendix, Figure 1.

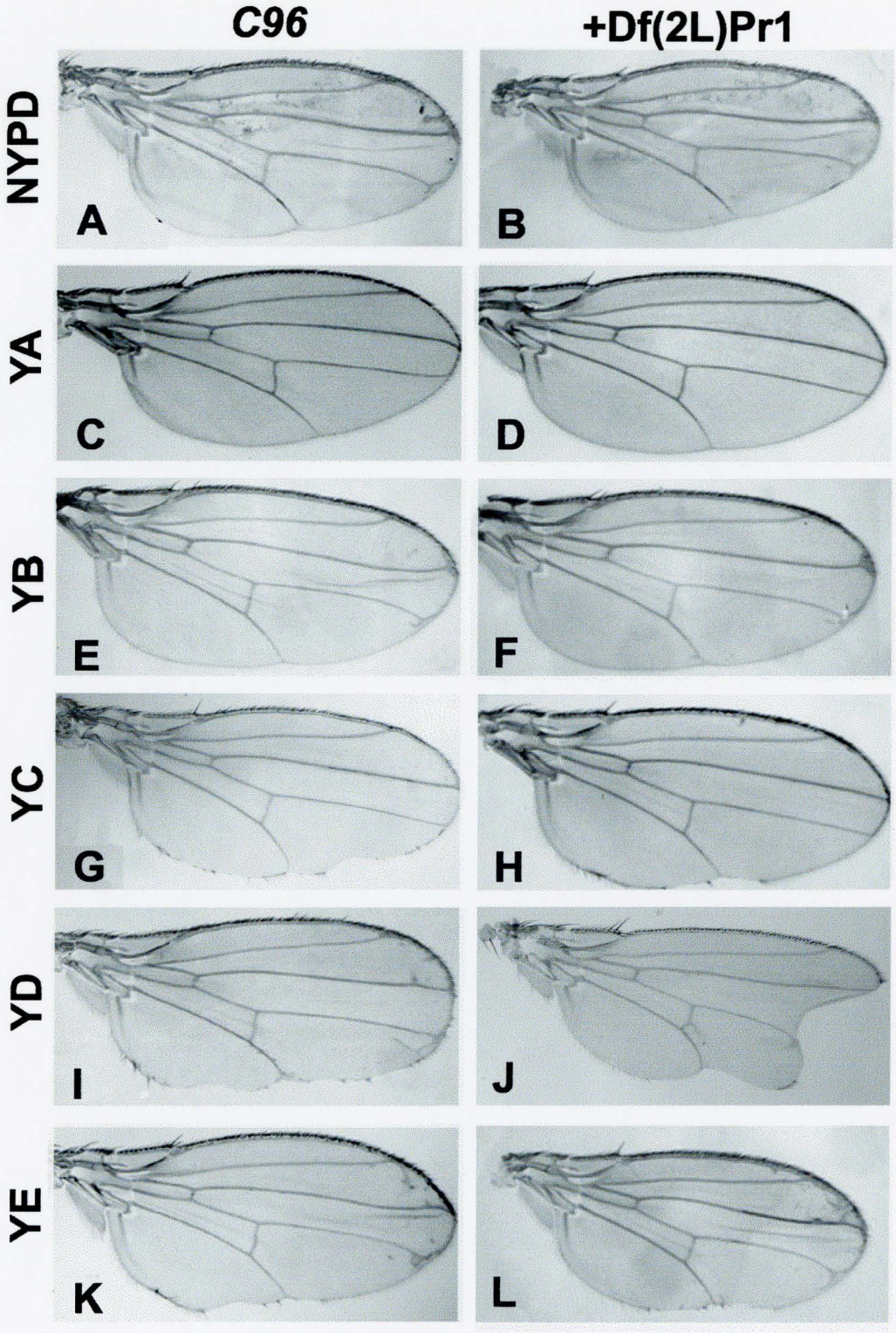
C96
+Df(2L)Pr1
NYPD
YA
YB
YC
YD
YE
A
B
C
D
E
F
G
H
I
J
K
L

Appendix 9. Deficiency (3L)h-122 enhanced signaling from Neu^{YC} and Neu^{YE} exclusively. Heterozygotes of individual add back *neu* alleles and Df(3L)h-122 were found to enhance Neu^{YC} and Neu^{YE} signaling (H and L, respectively). In contrast, the remaining *neu* alleles were unaffected by this deficiency and showed no change in the resulting wing phenotypes. For numerical scores and wing assessment refer to Results, Table 3.3 and Appendix, Figure 1.

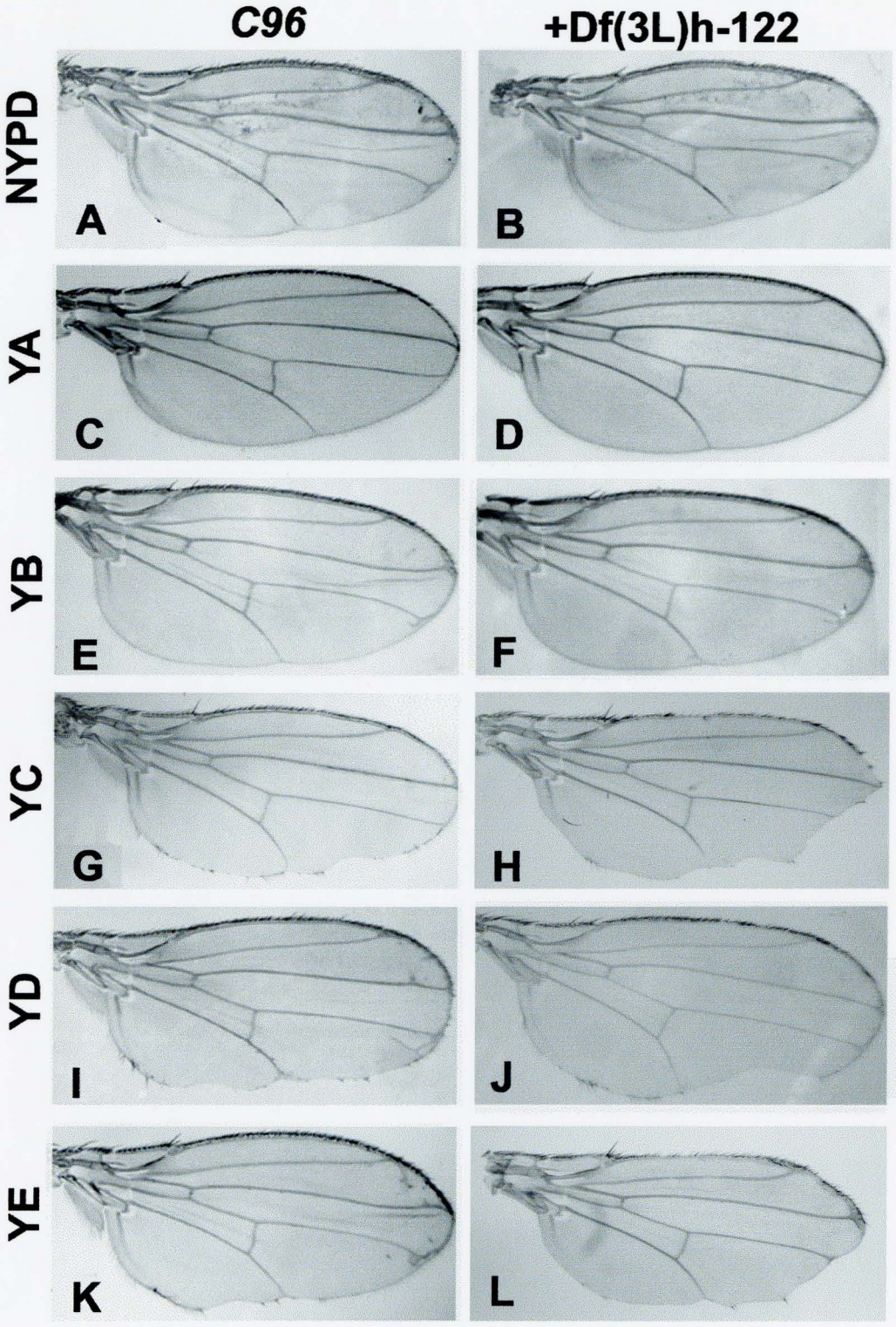
C96
+Df(3L)h-122
NYPD
YA
YB
YC
YD
YE
A
B
C
D
E
F
G
H
I
J
K
L

Appendix 10. DEgfr signaling is suppressed by multiple adaptor mutants. In comparison to a wild-type wing (A), overexpression of activated DEgfr results in a distinct notch phenotype along the ventral margin of the wing (B). We sought to determine if those adaptors which modified Neu signals could similarily suppress signaling from the DEgfr. Interestingly, co-expression of activated $DEgfr^{A887T}$ and $sos^{34Ea\text{-}6}$ (C), $Dshc^{111\text{-}40}$ (D), csw^{LE120} (E), ras^{05703} (F), phl^{C110} (G) or drk^{10626} (H) mutants all suppressed signals from the DEgfr, as demonstrated by a complete loss of the notch phenotype associated with overexpression of the DEgfr alone. We then asked whether those adaptor mutants that demonstrated no genetic interaction with any of the *neu* alleles, would similarly show no interaction with actived DEgfr. Analogous to our findings with Neu signaling, co-expression of activated $DEgfr^{A887T}$ and ilk^{78Ca} (I) or $dock^{P1}$ (J) suggested no genetic interaction, as demonstrated by a lack of suppression of the active $DEgfr^{A887T}$ notch phenotype.

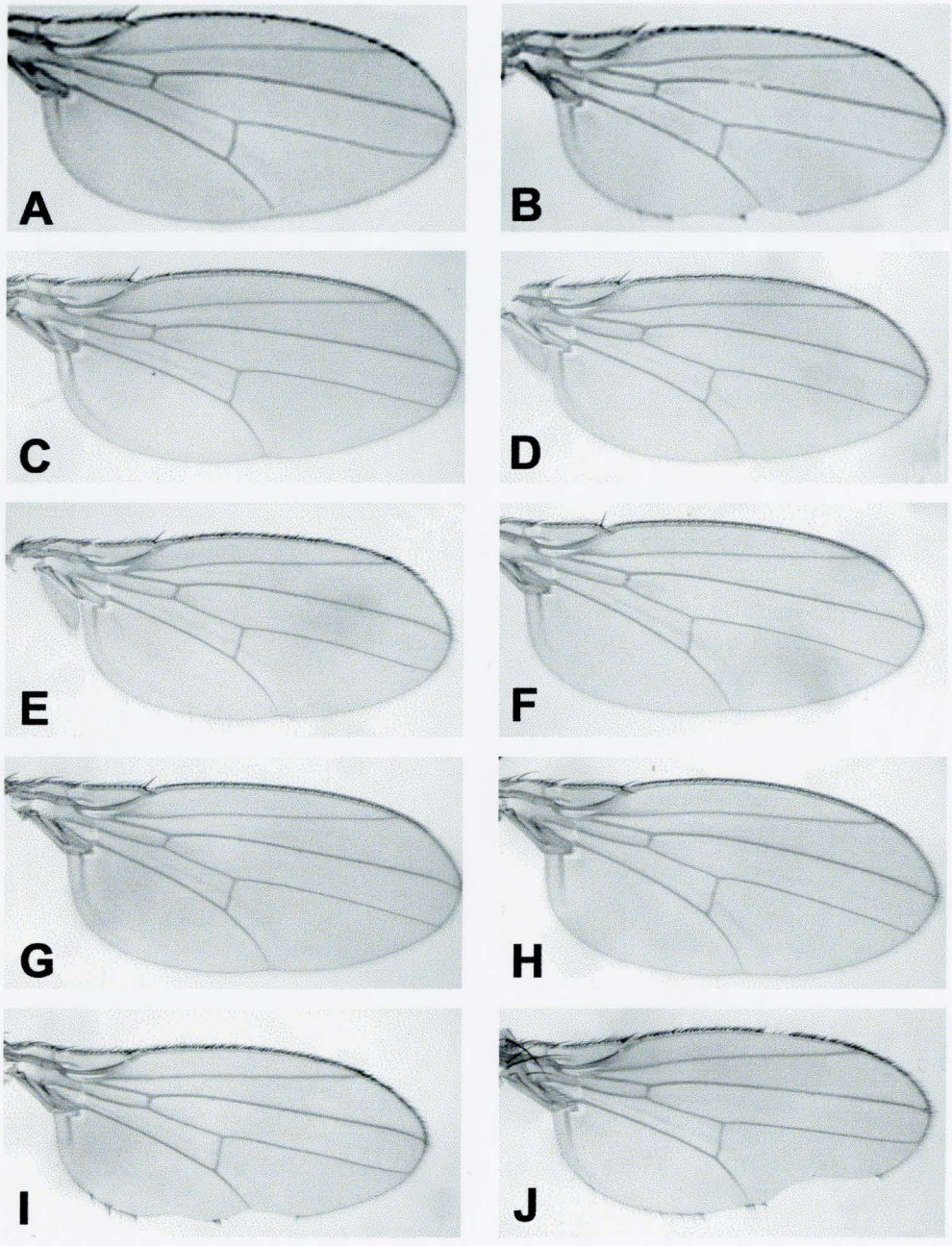
A
B
C
D
E
F
G
H
I
J

Appendix 11. Alignment of the transmembrane domain of the vertebrate EGF receptors, the DEgfr and *C. elegans* Let-23. As many studies have indicated that the transmembrane domain of RTKs play essential roles in proper dimerization and subsequent activation, we examined the conservation of the transmembrane domain of the four vertebrate receptors in relation to the single *Drosophila* and *C. elegans* orthologues. Sequence alignment of these domains revealed that only one residue is conserved between the vertebrate EGF receptors and Let-23 (green), while three regions are semi-conserved among all the receptors (red). The receptors have an overall alignment score of 70% indicating a moderate degree of sequence conservation. While we were able to design a phylogenetic tree, the branch lengths are not indicative of time in this example. This was due to the short sequence lengths, which make it difficult to assign values to these receptors in an evolutionary context. We were able to establish that the DEgfr appears to have evolved first, followed by Let-23 and then the vertebrate receptors. Among these, ErbB-3 appears to have evolved first, which is surprising as this receptor lacks any catalytic activity.

	Transmembrane Sequence	*Residue Numbers*
ErbB1	--SIATGMVGALLLLLVVALGIGLFM	(645-667)
ErbB4	--LIAAGVIGGLFILVIVGLTFAVYV	(652-675)
ErbB2	LTSIVSAVVG-ILLVVVLGVVFGILI	(651-675)
Let23	MVIIGSVLFGFAVMFLFILLVY--W-	(819-841)
ErbB3	LTMALTVIAGLVVIFMMLGGTFLYW-	(642-666)
DEgfr	----NSTMFN-CTSKCPLEMRHVNY-	(823-843)

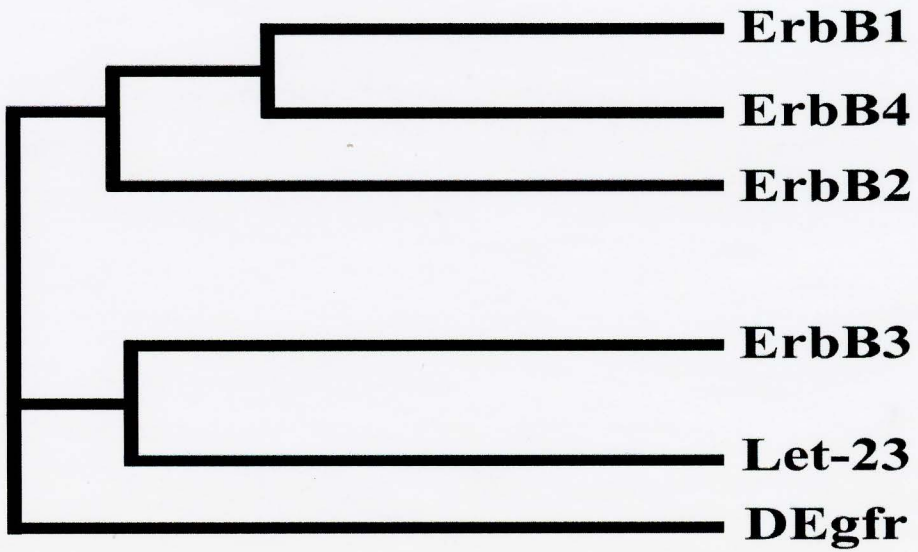

Appendix 12. Homozygous adaptor mutant embryos display abnormal MG cell numbers. Several of the adaptor mutants used in the wing assay were examined for their effects on MG cell numbers. Interestingly, homozygous *scrib*^{1} embryos demonstrated an increase in MG cell numbers, from wild-type three glia per embryonic segment (see Results, Figure 6A), to roughly 4-5 cells per segment (A). This was unexpected as the *scribbled* gene is involved in the basolateral localization of the DEgfr. Mis-localization of this receptor would seemingly involve a loss of the receptor's ability to properly provide anti-apoptotic signals. Our results do not support this view and suggest that additional regulatory mechanisms are involved in the proper localization of the DEgfr and it's subsequent signaling capabilities. Homozygous *sos*$^{34Ea\text{-}6}$ mutant embryos displayed a reduction in MG cell numbers, to two MG per embryonic segment (B). In contrast, homozygous *csw*^{LE120} embryos did not demonstrate a significant change in MG cell numbers (C), relative to wild-type counts, although some segments were seen to have four glia, as opposed to the characteristic three. Analogous to *sos*$^{34Ea\text{-}6}$ mutant embryos, *ras*^{05703} homozygous embryos showed a reduction in glial numbers to two MG per segment (D). All embryos are pictured with the anterior to the left and dorsal to the top.

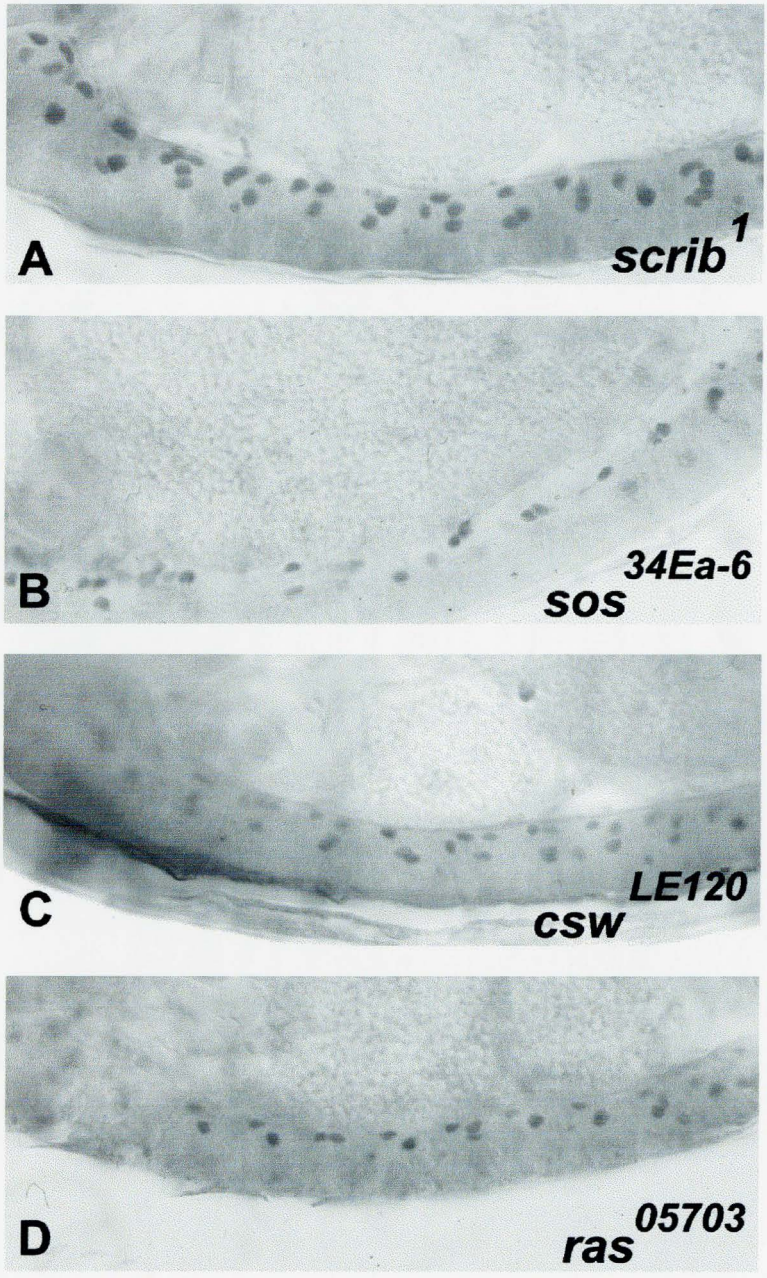
A
scrib 1
B
sos 34Ea-6
C
csw LE120
D
ras 05703

Appendix 13. Generation of uas-neu-sim4 recombinant lines, for use in screening individual Neu pTyr in the midline glial assay. In order to screen individual Neu pTyr against second messenger and adaptor mutants in the midline, second chromosome recombinant lines were generated. The sim Gal4 driver was combined with individual uas-*neu* lines and eventually maintained as homozygous stocks. The third chromosome glial enhancer trap AA142 was also incorporated, so that MG cells could be visualized by staining for β-galactosidase. The actual recombination event occurs in step 2 of the cross, wherein a small fraction (approximately 1/100) of the females carrying *sim* Gal-4 and the uas-*neu* line would demonstrate recombination of these genomic segments. For the remaining steps, all females must be individually maintained so that they can be later tested for potential recombination. In step 3 the glial specific enhancer trap AA142 is incorporated. In step 4 potential homozygous recombinant lines are generated, which can then be tested for both the recombination event and incorporation of the enhancer trap. Those lines that stain positive with Rabbit ∝ Neu must contain both the sim Gal4 driver and the uas-*neu*. Further staining with ∝β-galactosidase will verify incorporation of the enhancer trap as well as incorporation of the uas-*neu* line, which can be detected by increased MG cell numbers. This anti-apoptotic phenotype is typical of mis-expression of most of the *neu* alleles.

Genetic Scheme for Generation of sim4-uas-neu Recombinant Lines

Step 1: yw/Y ; sim4/sim4 ; + X yw/w ; uas-neu/uas-neu ; +

↓

yw/Y or **yw/yw ; sim4/uas-neu ; +**

select red eye females for step 2

Step 2: yw/yw ; uas-neu/sim4 ; + X yw/Y ; Sco/Cyo ; +

↓

yw/yw or yw/Y ; uas-neu/Cyo ; +

yw/yw or yw/Y ; uas-neu/Sco ; +

yw/yw or yw/Y ; sim4/Sco ; +

yw/yw or yw/Y ; sim4/Cyo ; +

yw/yw or yw/Y ; **sim4-uas-neu/Cyo** ; +

select curly wing, red eye females and individually pairwise to later test for possible recombination.

Step 3: yw/yw ;sim4-uas-neu/Cyo; + X yw/Y ; Sco/Cyo ;AA142/AA142

(in individual pairwise tubes) ↓

yw/yw or yw/Y ; sim4-uas-neu/Cyo ; AA142/+

yw/yw or yw/Y ; sim4-uas-neu/Sco ; AA142/+

yw/yw or yw/Y ; Sco/Cyo ; AA142/+

yw/yw or yw/Y ; Cyo/Cyo ; AA142/+ (Embryonic lethal)

select red eyed curly wing males and females, from the same line, and individually pairwise.

Step 4: yw/yw ; sim4·uas-neu/cyo ; AA142/+ X yw/Y; sim4·uas-neu/cyo ; AA142/+

↓

yw/yw or yw/Y ; sim4·uas-neu/Cyo ; AA142/+

yw/yw or yw/Y ; sim4·uas-neu/Cyo ; AA142/AA142

yw/yw or yw/Y ; sim4·uas-neu/sim4·uas-neu ; AA142/+

yw/yw or yw/Y ; sim4·uas-neu/sim4·uas-neu ; AA142/AA142

select straight wing red eye male and females and individually pairwise these flies to maintain a stock and further test for possible recombination.

In order to test for potential recombination, stain individual lines with Rb∝neu to verify cytoplasmic expression of Neu protein in the MG. Also stain potential recombinant lines with ∝β-galactosidase and check for increased MG cell numbers, indicative of Neu expression. Postive β-galactosidase staining indicates stable incorporation of the AA142 enhancer trap. In addition, note what percentage of the embryos stain positive for β-galactosidase, to determine whether AA142 is homozygous (100% staining) or heterozygous (50% staining).

Appendix 14. Second chromosome deficiency stocks used for wing screen.

The following is a complete list of all of the second chromosome deficiency stocks that were screened against individual Neu pTyr. For a summary of those regions that displayed a genetic interaction with individual *neu* alleles, refer to Results, Table 3.2. Stocks are listed in numerical order according to the Bloomington Stock Number. The genotype is also listed as well as the breakpoints for each deficiency. In addition, the date the stock was added, the donor and any additional pertinent comments are provided.

#90 Df(2L)C144, dpp[d-ho] ed[1]/In(2LR)Gla, wg[Gla-1] Bc[1] Egfr[E1]
Ch #: 2 Breakpts: 022F03-04;023C03-05
Date added: 3/30/1995 Donor: Bill Gelbart Donor's source:
Comments: DK2

#97 Df(2L)JS32, dpp[d-ho]/SM6a
Ch #: 2 Breakpts: 023C03-05;023D01-02
Date added: 3/30/1995 Donor: Bill Gelbart Donor's source:
Comments: DK2; no Cy expression, K.M. 2/26/97

#140 y[1] w[67c23]; Df(2L)Trf-C6R31/CyO
Ch #: 2 Breakpts: 028DE (within)
Date added: 10/24/1995 Donor: Tom Crowley Donor's source:
Comments: DK2

#167 Df(2L)TW161, cn[1] bw[1]/CyO
Ch #: 2 Breakpts: 038A06-B01;040A04-B01
Date added: 12/1/1988 Donor: Ted Wright Donor's source:
Comments: DK2; M[-] pr[-]

#179 In(1)w[m4h], y[1]; Df(2L)TE29Aa-11/CyO
Ch #: 1;2 Breakpts: 028E04-07;029B02-C01
Date added: 10/27/1995 Donor: Steve Beckendorf Donor's source: Gunter Reuter
Comments: DK2

#190 Df(2R)en-A/CyO
Ch #: 2 Breakpts: 047D03;048B02
Date added: 11/10/1995 Donor: MaryAnn Martin Donor's source: Umea Stock Center
Comments: DK2; intact copy of this deficiency, fails to complement Df(2R)en28, Df(2R)en-SFX31, Df(2R)en-B, and Df(2R)en30, MA.M.; poor Cy expression, K.M. 2/26/97

#198 w[118]; Df(2R)H3C1/CyO
Ch #: 1;2 Breakpts: 043F;044D03-08
Date added: 2/2/1996 Donor: Ken Howard Donor's source:
Comments: DK2; distal breakpoint should coincide with or overlap proximal breakpoint of Df(2R)H3E1, K.H. 12/15/95; w[118] is not a typo, K.M. 2/2/96

#201 w[118]; Df(2R)H3E1/CyO
Ch #: 1;2 Breakpts: 044D01-04;044F12
Date added: 2/2/1996 Donor: Ken Howard Donor's source:
Comments: DK2; proximal breakpoint should coincide with or overlap distal breakpoint of Df(2R)H3C1, K.H. 12/15/95; w[118] is not a typo, K.M. 2/2/96

#282 Dp(1;Y)y[+]/y[1]; Df(2R)X58-12/SM5
Ch #: 1;Y;2 Breakpts: 058D01-02;059A
Date added: 2/2/1996 Donor: Terry Orr-Weaver Donor's source:
Comments: DK2; deficiency includes M(2)58F, SM5 carries a duplication for this region, adult viability is poor without the duplication, T. O.-W. 5/5/95

#283 Dp(1;Y)y[+]/y[1]; Df(2R)X58-7, pr[1] cn[1]/CyO, bw[1]
Ch #: 1;Y;2 Breakpts: 058A01-02;058E04-10 or 058B01-02;058E01-04
Date added: 2/2/1996 Donor: Terry Orr-Weaver Donor's source:
Comments: DK2

#420 Df(2L)TW137, cn[1] bw[1]/CyO, Dp(2;2)M(2)m[+]
Ch #: 2 Breakpts: 036C02-04;037B09-C01, 036F + ?
Date added: 12/1/1988 Donor: Ted Wright Donor's source:
Comments: DK2

#442 Df(2R)CX1, b[1] pr[1]/SM1
Ch #: 2 Breakpts: 049C01-04;050C23-D02
Date added: 4/1/1993 Donor: Nick Baker Donor's source:
Comments: DK2; Kevin Cook checked polytene squash and says df is intact, K.M. 5/17/96

#490 In(1)w[m4]; Df(2L)E110/CyO
Ch #: 1;2 Breakpts: 003C01-02;020F, 025F03-026A01;026D03-11
Date added: 3/14/1996 Donor: Kenneth Tartof Donor's source:
Comments: DK2; balancer shown as Cy, CyO is a guess, K.M. 3/14/96

#520 Df(2R)E3363/CyO, P{ry[+t7.2]=sevRas1.V12}FK1
Ch #: 2 Breakpts: 047A;047F
Date added: 3/14/1996 Donor: Gerry Rubin Donor's source:
Comments: DK2

#543 Df(2R)017/SM1
Ch #: 2 Breakpts: 056F05;056F015
Date added: 3/14/1996 Donor: Daryl Henderson Donor's source:
Comments: DK2

#556 w[*]; Df(2L)s1402, P{w[+mC]=lacW}s1402/CyO
Ch #: 1;2 Breakpts: 030C01-02;030F, 030B09-10
Date added: 3/14/1996 Donor: Gerry Rubin Donor's source:
Comments: DK2; 30C1-2, rather than 30C, based on location of hoip and Pka-C1, K.M. 4/25/97; P{} at 30B9-10 may or may not cause lethality, per T. Laverty, K.C. 7/29/98

#596 Df(2R)stan2, b[1] pr[1] P{ry[+t7.2]=neoFRT}42D/CyO
Ch #: 2 Breakpts: 046F01-02;047D01-02
Date added: 3/26/1996 Donor: Michael Ashburner Donor's source:
Comments: DK2; renamed from JG68-36 per John Roote, K.M. 4/22/96; Genotype correction per J.R., K.M. 10/4/97

#693 Df(2L)sc19-8/SM6b; Dp(2;1)B19, y[1], ed[1] dp[o2] cl[1]
Ch #: 2 Breakpts: 024C02-08;025C08-09, 024D04;025F02;009B-C
Date added: 12/1/1988 Donor: Janos Szidonya Donor's source:
Comments: DK2

#712 Df(2L)ed1, al[1] b[1]/SM5
Ch #: 2 Breakpts: 024A03-04;024D03-04
Date added: 12/1/1988 Donor: Janos Szidonya Donor's source:
Comments: DK2

#724 In(1)bb[Df], y[1] sl[2]/FM4
Ch #: 1 Breakpts: 004D02-03;020F
Date added: 4/1/1987 Donor: Caltech Stock Center Donor's source:
Comments:

#739 Df(2R)M41A4/SM1
Ch #: 2 Breakpts: 041A
Date added: 4/1/1987 Donor: Caltech Stock Center Donor's source:
Comments: DK2; = M-S4

#749 In(2R)bw[VDe2L]Cy[R]/In(2LR)Gla, wg[Gla-1]
Ch #: 2 Breakpts: Df:041A-B;042A02-03 + Dp:058B01;059D06
Date added: 4/1/1987 Donor: Caltech Stock Center Donor's source:
Comments: DK2

#754 Df(2R)vg-C/SM5
Ch #: 2 Breakpts: 049A04-13;049E07-F01
Date added: 4/1/1987 Donor: Caltech Stock Center Donor's source:
Comments: DK2; proximal breakpoint information from P. Adler, cited as personnal communication in DIS 71:154, K.M. 8/29/95

#757 y[*] w[*]/Dp(1;Y)y[+]; Df(2R)P34/CyO
Ch #: 1;Y;2 Breakpts: 055E02-04;056C01-11
Date added: 8/19/1996 Donor: Winifred Doane Donor's source: Dan Moore
Comments: DK2

#781 Df(2L)cl-h3/SM6b
Ch #: 2 Breakpts: 025D02-04;026B02-05
Date added: 12/1/1988 Donor: Janos Szidonya Donor's source:
Comments: DK2

#1007 Df(2R)nap9/In(2LR)Gla, Dp(2;2)BG, wg[Gla-1]
Ch #: 2 Breakpts: 042A01-02;042E06-F01, 041A-B;042BC
Date added: 8/26/1995 Donor: Barry Ganetzky Donor's source:
Comments: DK2

#1045 Df(2L)Mdh, cn[1]/Dp(2;2)Mdh3, cn[1] ! see comment
Ch #: 2 Breakpts: 030D-30F;031F, 030D01-E01;032D01-032F03
Date added: 4/1/1987 Donor: Caltech Stock Center Donor's source: E.H. Grell
Comments: DK2; dark eye color present, L.C.; assumes MdhA = Mdh, K.M.; deficiency heterozygotes should have a moderate Minute phenotype, K.M.7/28/98

#1104 w[*]; P{w[+mC]=GAL4-ninaE.GMR}12 ! GAL4
Ch #: 2 Breakpts:
Date added: 12/2/1996 Donor: Matthew Freeman Donor's source:
Comments: glass enhancer driving GAL4 in the eye disc, provides strong expression in all cells behind the morphogenetic furrow, M.F.

#1145 Df(2R)en30/SM5; Dp(1;Ybb[-])B[S]
Ch #: 2 Breakpts: 048A03-04;048C06-08
Date added: 4/1/1987 Donor: Caltech Stock Center Donor's source: Sue Eberlein
Comments: DK2

#1150 w[1]/Dp(1;Y)y[+]; Df(2R)knSA3, Tp(1;2)TE21F22A/CyO
Ch #: 1;Y;2 Breakpts: 051B05-11;051F05-13, 003C01-12;003C01-02;021F-022A08
Date added: 10/3/1997 Donor: Jym Mohler Donor's source:
Comments: DK2; y[1] w[1] floating, J.M.

#1357 Df(2L)J-H/SM5
Ch #: 2 Breakpts: 027C02-09;028B03-04
Date added: Donor: Stanley Tiong Donor's source:
Comments: DK2; ade3[-], S.T. says stock breaks down, giving M

#1469 Df(2L)J39/In(2L)Cy; Dp(2;Y)cb50, Dp(1;Y)B[S]Yy[+]/C(1)RM
Ch #: 2 Breakpts: 031C-D;032D-E, 030C;033E;h1-h25
Date added: 4/1/1989 Donor: Peter Bryant Donor's source:
Comments: DK2; deficiency exposes a dominant female sterile Minute, P.B.

#1491 Df(2L)r10, cn[1]/CyO
Ch #: 2 Breakpts: 035E01-02;036A06-07, ?
Date added: 5/1/1991 Donor: Michael Ashburner Donor's source: Seigfreid Roth
Comments: DK2; X-ray excision of ry[+] insert at 36A, J.R.; ry[*] floating?, K.M.

#1547 Df(2R)PC4/CyO
Ch #: 2 Breakpts: 055A;055F
Date added: 11/1/1987 Donor: Jose Bonner Donor's source: Trudi Schupbach or Umea
Comments: DK2

#1587 Df(2R)bw[VDe2L]Px[KR]/SM1
Ch #: 2 Breakpts: 059D06-E01;060C-D
Date added: 4/1/1987 Donor: Thom Kaufman Donor's source:
Comments: DK2; recombinant generated by T. Kaufman; rearrangement more complicated than originally thought, but deficiency is present, K.C. 3/11/99

#1642 Df(2R)vg135, nompA[vg135]/CyO, S[*] bw[1]
Ch #: 2 Breakpts: 049A-B;049D-E, 047F04-048A;049A-B (In associated with Df)
Date added: 5/1/1990 Donor: Lenny Rabinow Donor's source:
Comments: DK2; not simple deficiency, some internal material probably intact, L.R.; sick, rebalanced 7/91, K.M.

#1682 Df(2R)or-BR6, cn[1] bw[1] sp[1]/In(2LR)lt[G16L]bw[V32gR]
Ch #: 2 Breakpts: 059D05-10;060B03-08, 040;060E04[L]40F;059E[R]
Date added: 10/1/1993 Donor: Michael Ashburner Donor's source: Bruce Reed
Comments: DK2; Inversion chromosome carries duplication for 059E;060E04

#1702 Df(2R)X1, Mef2[X1]/CyO, Adh[nB]
Ch #: 2 Breakpts: 046C;047A01
Date added: 7/1/1994 Donor: Martha O'Brien Donor's source:
Comments: DK2; cytology of M. Burg via M. O'Brien, K.M.

#1743 w[1118]; Df(2R)B5, px[1] sp[1]/CyO, Adh[nB]
Ch #: 1;2 Breakpts: 046A;046C
Date added: 7/1/1994 Donor: Martha O'Brien Donor's source:
Comments: DK2; small possibility balancer is SM6, generated as excision of P{A}N21, M.O.

#1888 Df(2R)ST1, Adh[n5] pr[1] cn[*]/CyO
Ch #: 2 Breakpts: 042B03-05;043E15-18
Date added: 11/1/1987 Donor: Jose Bonner Donor's source: Trudi Schupbach
Comments: DK2; M. Ashburner says this is the correct cytology according to both his notes and Genetics 135:105, K.M. 1/25/96

#1896 Df(2R)trix/CyO?
Ch #: 2 Breakpts: 051A01-02;051B06
Date added: 11/1/1987 Donor: Jose Bonner Donor's source: Trudi Schupbach
Comments: DK2

#1930 Df(2R)pk78s/CyO
Ch #: 2 Breakpts: 042C01-07;043F05-08 or 042B;042C max or 42F;43F+
Date added: 11/1/1987 Donor: Jose Bonner Donor's source: Trudi Schupbach
Comments: DK2; J. Mahaffey says 42B;42C, John Roote says their copy removes from about 42F to beyond cn (43F), based on genetic tests, perhaps different stocks (will test ours)?, K.M. 3/14/96

#2471 Df(2R)M60E/In(2LR)bw[V32g], bw[V32g]
Ch #: 2 Breakpts: 060E02-03;060E11-12
Date added: Donor: Donor's source:
Comments: DK2

#2583 Df(2L)cact-255rv64, cact[chif64]/CyO; ry[506]
Ch #: 2;3 Breakpts: 035F-036A;036D
Date added: 12/2/1996 Donor: John Tower Donor's source:
Comments: DK2

#2604 Df(2R)Px2/SM5
Ch #: 2 Breakpts: 060C05-06;060D09-10
Date added: 4/1/1987 Donor: Thom Kaufman Donor's source:
Comments: DK2

#2606 Df(2R)Pu-D17, cn[1] bw[1] sp[1]/SM1
Ch #: 2 Breakpts: 057B04;058B
Date added: Donor: Donor's source:
Comments: DK2

#2892 Df(2L)N22-14/CyO
Ch #: 2 Breakpts: 029C01-02;030C08-09
Date added: 4/25/1997 Donor: Michael Ashburner Donor's source:
Comments: DK2

#3024 Df(3L)h-i22, h[i22] Ki[1] roe[1] p[p]/TM3, Ser[1]
Ch #: 3 Breakpts: 066D10-11;066E01-02
Date added: Donor: Donor's source:
Comments: DK3

#3064 Df(2R)Pcl7B/CyO
Ch #: 2 Breakpts: 054E08-F01;055B09-C01
Date added: Donor: Donor's source:
Comments: DK2

#3077 Df(2L)spd, al[1] dp[ov1]/CyO
Ch #: 2 Breakpts: 027D-E;028C
Date added: Donor: Donor's source:
Comments: DK2

#3079 Df(2L)Prl, Prl[1] nub[Prl]/CyO
Ch #: 2 Breakpts: 032F01-03;033F01-02
Date added: 11/1/1987 Donor: Jose Bonner Donor's source: Trudi Schupback
Comments: DK2

#3084 Df(2L)ast2/SM1
Ch #: 2 Breakpts: 021D01-02;022B02-03
Date added: 11/1/1987 Donor: Jose Bonner Donor's source: Trudi Schupbach
Comments: DK2; rough eye phenotype is not a dominant effect of the deficiency, outcross to CyO stock produces only wild-type (M. McKeown, 12/93); did a squash, deficiency is present, K.M. 2/94

#3133 Df(2L)dp-79b, dp[DA] cn[1]/In(2LR)bw[V1], ds[33k] b[1] bw[V1] ! does not delete dp
Ch #: 2 Breakpts: 022A02-03;022D05-E01, 021C08-D01;060D01-02 + 040F;059D04-E01
Date added: 9/1/1988 Donor: I. Alexandrov Donor's source:
Comments: DK2; neutron-induced, dp[DA] penetrant in 50-60% of the population, I.A.

#3138 Df(2L)b87e25/CyO
Ch #: 2 Breakpts: 034B12-C01;035B10-C01
Date added: 5/19/1998 Donor: Michael Ashburner Donor's source:
Comments: DK2; replaced NS version with CyO version from John Roote, K.M.

#3157 Df(2R)ES1, b[1] pr[1] cn[1] wx[wxt] Kr[If-1]/SM1
Ch #: 2 Breakpts: 060E06-08;060F01-02
Date added: 10/1/1988 Donor: Susan Germeraad Donor's source:
Comments: DK2; gsb[-], S.G.; need to check deficiency, one copy was If[+], and one copy was gsb[+] according to K. Bhat, probably same one, but he discarded his stock before he could check, both our copies reestablished from the If set, K.M.

#3180 Df(2L)H20, b[1] pr[1] cn[1] sca[1]/CyO
Ch #: 2 Breakpts: 036A08-09;036E01-02
Date added: 12/1/1988 Donor: Ted Wright Donor's source:
Comments: DK2

#3189 Df(2L)TW50, cn[1]/CyO, Dp(2;2)M(2)m[+]
Ch #: 2 Breakpts: 036E04-F01;038A06-07, 036F + ?
Date added: 12/1/1988 Donor: Ted Wright Donor's source:
Comments: DK2; very weak M, T.W.

#3344 Df(2L)prd1.7, b[1] Adh[n2] pr[1] cn[1] sca[1]/CyO, P{ry[+t*]=elav-lacZ.H}YH2
Ch #: 2 Breakpts: 033B02-03;034A01-02
Date added: 1/28/1998 Donor: Krishna Bhat Donor's source:
Comments: DK2; original copy (8/1/1990) broken down according to K. Bhat, replaced, K.M. 1/28/98

#3368 Df(2R)cn9/CyO, Roi[1] sp[*] <P>
Ch #: 2 Breakpts: 042E;044C
Date added: 6/1/1989 Donor: C. Nusslein-Volhard Donor's source:
Comments: DK2; Claire Cronmiller says this stock behaves like a P strain, K.M. 10/28/94; breakpoints confirmed by K. Cook, 3/15/96; poor Cy expression in stock, but seen in some outcrosses, K.C. 5/27/99

#3467 Df(2R)AA21, c[1] px[1] sp[1]/SM1
Ch #: 2 Breakpts: 056F09-17;057D11-12, 056D-E;058E-F (In)
Date added: 11/1/1990 Donor: Kim Fetchel Donor's source: Janis O'Donnell
Comments: DK2

#3518 w[a] N[fa-g]; Df(2R)Jp1/CyO
Ch #: 1;2 Breakpts: 051C03;052F05-09
Date added: 6/12/1989 Donor: Bill Saxton Donor's source:
Comments: DK2

#3520 w[a] N[fa-g]; Df(2R)Jp8, w[+]/CyO
Ch #: 1;2 Breakpts: 052F05-09;052F10-53A01
Date added: 6/12/1989 Donor: Bill Saxton Donor's source:
Comments: DK2

#3548 Df(2L)al/In(2L)Cy, Cy[1]
Ch #: 2 Breakpts: 021B08-C01;021C08-D01, 022D01-02;033F05-034A01
Date added: 10/1/1990 Donor: Jim Kennison Donor's source:
Comments: DK2; original #3548 replaced with healthier #1839 version of this deficiency stock; stock does best at 22[o]C, K.M. 6/18/96

#3571 Df(2L)Dwee-delta5/Dp(?;2)bw[D], S[1] wg[Sp-1] Ms(2)M[1] bw[D]/CyO
Ch #: 2 Breakpts: 027A;028A
Date added: 12/2/1996 Donor: Shelagh Campbell Donor's source:
Comments: DK2; very weak stock, deficiency is dominant female sterile, S.C.

Appendix 15. Third chromosome deficiency stocks used for wing screen.

The following is a complete list of all of the third chromosome deficiency stocks that were screened against individual Neu pTyr. For a summary of those regions that displayed a genetic interaction with individual *neu* alleles, refer to Results, Table 3.3. Stocks are listed in numerical order according to the Bloomington Stock Number. The genotype is also listed as well as the breakpoints for each deficiency. In addition, the date the stock was added, the donor and any additional pertinent comments are provided.

Stock Number: 89
Genotype: y[1?]; Df(3L)lxd6/TM3, Sb[1] Ser[1]
Chromosome(s): 1;3
Breakpts/Insertion: 067E01-02;068C01-02
Date added: 11/1/1993 **Donor:** Allen Shearn
Comments: DK3

Stock Number: 383
Genotype: Df(3R)ea, kni[ri-1] p[p]/TM3, Ser[1]
Chromosome(s): 3
Breakpts/Insertion: 088E07-13;089A01
Date added: 1/21/1997 **Donor:** Kathryn Anderson
Comments: DK3; cause of variable bristle defect unknown, but may be a function of the deficiency, K.A.; E. Rushton says df appears to carry a Me allele, K.M. 12/21/99

Stock Number: 430
Genotype: w[1118]; Df(3R)3450/TM6B, Tb[1]
Chromosome(s): 1;3
Breakpts/Insertion: 098E03;099A06-08
Date added: 6/1/1992 **Donor:** Shigeo Hayashi
Comments: DK3; gamma excision of P at 98F, S.H.

Stock Number: 439
Genotype: Df(3L)Ar14-8, red[1]/TM2, p[p]
Chromosome(s): 3
Breakpts/Insertion: 061C05-08;062A08
Date added: 2/11/1993 **Donor:** Hilary Ellis
Comments: DK3; new distal breakpoint information from Janice Vize, based on exclusion of marb from the deficiency, K.M. 6/6/95

Stock Number: 669
Genotype: w[*]; Df(3R)Dr-rv1, ry[506]/TM3, ry[RK] Sb[1] Ser[1]
Chromosome(s): 1;3
Breakpts/Insertion: 099A01-02;099B06-11
Date added: 6/7/1996 **Donor:** Adelaide Carpenter
Comments: DK3; Progenitor carried P{w[+mC] sox[hs]}, w[+mC] still there, but don't know about the rest, A.T.C.C.

Stock Number: 823
Genotype: Df(3R)D605/TM3, Sb[1] Ser[1]
Chromosome(s): 3
Breakpts/Insertion: 097E03;098A05
Date added: 1/21/1997 **Donor:** Kathryn Anderson
Comments: DK3

Stock Number: 977
Genotype: Df(1)DCB1-35b/FM6/Dp(1;Y)y[+]mal[106], mal[106]
Chromosome(s): 1
Breakpts/Insertion: 019F01-02;020E-F, 001A01;001B02 + 018F;020h;Y
Date added: 4/1/1987 **Donor:** Caltech Stock Center
Comments: DK1

Stock Number: 983
Genotype: v[71P]; red[1] su(Hw)[2] Sb[sbd-2]/TM1
Chromosome(s): 1;2
Date added: 4/1/1987 **Donor:** Caltech Stock Center

Stock Number: 997
Genotype: Df(3L)AC1, roe[1] p[p]/TM3, Sb[1]
Chromosome(s): 3
Breakpts/Insertion: 067A02;067D07-13 or 067A05;067D09-13
Date added: 4/1/1987 **Donor:** Thom Kaufman **Donor's source:** Adelaide Carpenter
Comments: DK3; X-ray induced, first set of cytology from B. Leicht, second from A.T.C.C., TM3, Ser version replaced with TM3, Sb 1/92, K.M.

Stock Number: 1420
Genotype: Df(3L)pbl-X1/TM6B, Tb[1]
Chromosome(s): 3
Breakpts/Insertion: 065F03;066B10
Date added: 12/1/1991 **Donor:** Rob Saint
Comments: DK3; w[*] floating, K.M.; may contain Dp(1;Y)y[+] or similar, K.C. 10/27/99

Stock Number: 1467
Genotype: Df(3R)P115, e[11]/TM1; Dp(3;1)P115/+
Chromosome(s): 3
Breakpts/Insertion: 089B07-08;089E07;020
Date added: **Donor:**
Comments: DK3

Stock Number: 1518
Genotype: Df(YS)bb[-]; Df(3R)ME15, mwh[1] red[1] e[4]/MKRS
Chromosome(s): Y;3
Breakpts/Insertion: 081F03-06;082F05-07
Date added: 6/14/1995 **Donor:** Adelaide Carpenter
Comments: presence of Ybb[-] per M. Green, K.C. 1/5/00; on outcross, 20-30% of males have rotated genitalia, per M. Green, K.M. 2/1/00

Stock Number: 1534
Genotype: Tp(3;Y)ry506-85C/MKRS
Chromosome(s): 3
Breakpts/Insertion: 087D01-02;088E05-06;Y
Date added: 8/1/1987 **Donor:** Karen Palter
Comments: DK3

Stock Number: 1541
Genotype: y[1] w[1] N[spl-1]; Df(3L)66C-G28/TM3, Sb[1]
Chromosome(s): 1;3
Breakpts/Insertion: 066B08-09;066C09-10
Date added: 6/8/1992 **Donor:** Jeanette Natzle
Comments: DK3; mobilization of P at 66C (#P881), fails to complement #1420, J.N.

Stock Number: 1688
Genotype: Df(3L)Rdl-2, e[1]/TM3, Sb[1]
Chromosome(s): 3
Breakpts/Insertion: 066F05;066F05
Date added: 6/14/1995 **Donor:** Richard Roush
Comments: DK3

Stock Number: 1842
Genotype: Df(3R)Antp17/TM3, Sb[1] Ser[1]
Chromosome(s): 3
Breakpts/Insertion: 084B01-02;084D11-12 or A06,D14
Date added: 4/1/1987 **Donor:** Thom Kaufman **Donor's source:** Tulle Hazelrigg
Comments: DK3

Stock Number: 1884
Genotype: Df(3R)Scr, p[p] e[s]/TM3, Sb[1]
Chromosome(s): 3
Breakpts/Insertion: 084A01-02;084B01-02
Date added: 4/1/1987 **Donor:** Thom Kaufman
Comments: DK3

Stock Number: 1893
Genotype: Df(3R)by62, red[1]/TM1, p[p]
Chromosome(s): 3
Breakpts/Insertion: 085D11-14;085F06 041h;085F06 (T)
Date added: 4/1/1987 **Donor:** Thom Kaufman
Comments: DK3; deficiency plus 2;3 translocation, K.M.; J. Belote says translocation no longer present, appears to be a simple df, K.M. 1/25/00

Stock Number: **1910**
Genotype: Df(3R)TI-P, e[1] ca[1]/TM3, Ser[1]
Chromosome(s): 3
Breakpts/Insertion: 097A;098A01-02
Date added: 4/1/1987 **Donor:** Thom Kaufman **Donor's source:** Kathryn Anderson
Comments: DK3

Stock Number: **1931**
Genotype: Df(3R)by10, red[1] e[1]/TM3, Sb[1] Ser[1]
Chromosome(s): 3
Breakpts/Insertion: 085D08-12;085E07-F01
Date added: 4/1/1987 **Donor:** Thom Kaufman
Comments: DK3

Stock Number: **1962**
Genotype: Df(3R)p-XT103, ru[1] st[1] e[1] ca[1]/TM3, Sb[1]
Chromosome(s): 3
Breakpts/Insertion: 085A02;085C01-02
Date added: 4/1/1987 **Donor:** Thom Kaufman **Donor's source:** Mel Green
Comments: DK3

Stock Number: **1968**
Genotype: Df(3R)p712, red[1] e[1]/TM3, Sb[1] Ser[1]
Chromosome(s): 3
Breakpts/Insertion: 084D04-06;085B06, 025D;085B06 (T)
Date added: 4/1/1987 **Donor:** Thom Kaufman
Comments: DK3; deficiency associated with a 2;3 translocation, K.M.

Stock Number: **1990**
Genotype: Df(3R)Tpl10, Dp(3;3)Dfd[rv1], kni[ri-1] Dfd[rv1] p[p] Doa[10]/TM3, Sb[1]
Chromosome(s): 3
Breakpts/Insertion: 083C01-02;084B01-02, 083D04-05;084A04-05;098F01-02
Date added: 4/1/1987 **Donor:** Thom Kaufman **Donor's source:** Rob Denell
Comments: DK3

Stock Number: **2052**
Genotype: Df(3L)rdgC-co2, th[1] st[1] in[1] kni[ri-1] p[p]/TM6C, cu[1] Sb[1] ca[1]
Chromosome(s): 3
Breakpts/Insertion: 077A01;077D01
Date added: 6/1/1990 **Donor:** Fintan Steele
Comments: DK3

Stock Number: **2363**
Genotype: Df(3R)crb87-5, st[1] e[1]/TM3, Ser[1]
Chromosome(s): 3
Breakpts/Insertion: 095F07;096A17-18
Date added: 5/1/1991 **Donor:** Ulrich Tepass
Comments: DK3

Stock Number: **2400**
Genotype: Df(3L)R-G7, rho[ve-1]/TM6B, Tb[+]
Chromosome(s): 3
Breakpts/Insertion: 062B08-09;062F02-05
Date added: 10/1/1992 **Donor:** Jim Mason **Donor's source:** Tim Sliter
Comments: DK3

Stock Number: **2425**
Genotype: Df(3R)e-N19/TM2
Chromosome(s): 3
Breakpts/Insertion: 093B;094
Date added: **Donor:**
Comments: DK3; B. Savakis found Wolbachia dnaA sequences in this stock suggesting it is infected (1/94)

Stock Number: 2479
Genotype: Df(3L)29A6, kni[ri-1] p[p]/TM3, Sb[1]
Chromosome(s): 3
Breakpts/Insertion: 066F05;067B01
Date added: 4/1/1987 **Donor:** Thom Kaufman **Donor's source:** Brenda Leicht
Comments: DK3

Stock Number: 2577
Genotype: Df(3L)emc-E12/TM6B, Tb[1] ca[1]
Chromosome(s): 3
Breakpts/Insertion: 061A;061D03
Date added: 8/26/1995 **Donor:** Janice Fischer Vize **Donor's source:** Francesca Pignoni
Comments: DK3

Stock Number: 2585
Genotype: cn[1]; Df(3R)mbc-R1, ry[506]/TM3, ry[*] Sb[1] Ser[1]
Chromosome(s): 2;3
Breakpts/Insertion: 095A05-07;095D06-11
Date added: 12/2/1996 **Donor:** Emma Rushton **Donor's source:** Rachel Drysdale
Comments: DK3

Stock Number: 2608
Genotype: Df(3L)W10, ru[1] h[1] Sb[sbd-2]/TM6B, Tb[1] ! = see comment
Chromosome(s): 3
Breakpts/Insertion: 075A06-07;075C01-02
Date added: 11/1/1987 **Donor:** Jose Bonner **Donor's source:** Bill Seagraves
Comments: DK3; Adelaide Carpenter says many deficiency chromosomes in stock carry Tb; revised cytology from FlyBase, 4/12/95 K.M.

Stock Number: 2611
Genotype: Df(3L)vin5, ru[1] h[1] gl[2] e[4] ca[1]/TM3, Sb[1] Ser[1]
Chromosome(s): 3
Breakpts/Insertion: 068A02-03;069A01-03
Date added: 4/1/1987 **Donor:** Thom Kaufman **Donor's source:** Rollin Richmond
Comments: DK3

Stock Number: 2612
Genotype: Df(3L)vin7, h[1] gl[2] e[4] ca[1]/TM3, Sb[1] Ser[1]
Chromosome(s): 3
Breakpts/Insertion: 068C08-11;069B04-05
Date added: 4/1/1987 **Donor:** Thom Kaufman **Donor's source:** Rollin Richmond
Comments: DK3

Stock Number: 2990
Genotype: Df(3L)Cat, kni[ri-1] Sb[sbd-1] e[*]/TM3, Ser[1]
Chromosome(s): 3
Breakpts/Insertion: 075B08;075F01
Date added: 3/2/1992 **Donor:** Mid-America Stock Center
Comments: DK3; no Ser expression, K.M. 3/92

Stock Number: 2992
Genotype: Df(3L)BK10, ru[1] Ly[1] red[1] cv-c[1] Sb[sbd-1] sr[1] e[1]/TM3, Sb[1]
Chromosome(s): 3
Breakpts/Insertion: 071C;071F
Date added: 4/1/1987 **Donor:** Thom Kaufman **Donor's source:** Brenda Leicht
Comments: DK3

Stock Number: 2993
Genotype: Df(3L)st-f13, Ki[1] roe[1] p[p]/TM6B, Tb[1]
Chromosome(s): 3
Breakpts/Insertion: 072C01-D01;073A03-04
Date added: 11/1/1987 **Donor:** Jose Bonner **Donor's source:** Adelaide Carpenter
Comments: DK3

Stock Number: 2998
Genotype: Df(3L)81k19/TM6B, Tb[1]
Chromosome(s): 3
Breakpts/Insertion: 073A03;074F
Date added: **Donor:**
Comments: DK3

Stock Number: 3000
Genotype: Df(3L)VW3/TM3, Sb[1] Ser[1]
Chromosome(s): 3
Breakpts/Insertion: 076A03;076B02
Date added: 11/1/1987 **Donor:** Jose Bonner **Donor's source:** Umea Stock Center
Comments: DK3

Stock Number: 3003
Genotype: Df(3R)T-32, (kni[ri-1]) cu[1] sr[1] e[s]/MRS
Chromosome(s): 3
Breakpts/Insertion: 086E02-04;087C06-07
Date added: 11/1/1987 **Donor:** Jose Bonner **Donor's source:** Umea Stock Center
Comments: DK3

Stock Number: 3007
Genotype: Df(3R)ry615/TM3, Sb[1] Ser[1]
Chromosome(s): 3
Breakpts/Insertion: 087B11-13;087E08-11
Date added: 11/1/1987 **Donor:** Jose Bonner **Donor's source:** Umea Stock Center
Comments: DK3

Stock Number: 3011
Genotype: Df(3R)Cha7/TM6B, Tb[1]
Chromosome(s): 3
Breakpts/Insertion: 090F01-F04;091F05
Date added: 11/1/1987 **Donor:** Jose Bonner **Donor's source:** Marc Muskavitch
Comments: DK3; no balancer information, but stock is Tb so TM6B, Tb[1] is the most likely, K.M.

Stock Number: 3012
Genotype: Df(3R)DI-BX12, ss[1] e[4] ro[1]/TM6B, Tb[1]
Chromosome(s): 3
Breakpts/Insertion: 091F01-02;092D03-06
Date added: 11/1/1987 **Donor:** Jose Bonner **Donor's source:** Marc Muskavitch
Comments: DK3

Stock Number: 3024
Genotype: Df(3L)h-i22, h[i22] Ki[1] roe[1] p[p]/TM3, Ser[1]
Chromosome(s): 3
Breakpts/Insertion: 066D10-11;066E01-02
Date added: **Donor:**
Comments: DK3

Stock Number: 3048
Genotype: T(1;Y)106, y[1]: B[S]/FM4, w[1] f[1] B[+]
Chromosome(s): 1;Y
Breakpts/Insertion: 016A;YL
Date added: 6/13/1997 **Donor:** Mid-America Stock Center **Donor's source:** Dan Lindsley

Stock Number: 3071
Genotype: Df(3R)C4, p[*]/Dp(3;3)P5, Sb[1]
Chromosome(s): 3
Breakpts/Insertion: 089E03-04;090A01-07, 089E01-02;090A
Date added: 8/1/1988 **Donor:** Rob Denell
Comments: DK3; other markers?

Stock Number: 3096
Genotype: Df(3L)ZN47, ry[506]/TM3, Sb[1]
Chromosome(s): 3
Breakpts/Insertion: 064C;065C
Date added: 10/1/1992 **Donor:** Rob Rawson
Comments: DK3; gamma-ray excision of #P466, P{ry[+]} at 64F, vein- & Vein-like wing defect, lethal over Me jv se by, R.R.

Stock Number: 3124
Genotype: Df(3L)fz-GF3b, P{w[+tAR] ry[+t7.2AR]=wA[R]}66E/TM6B, Tb[1] ca[1]
Chromosome(s): 3
Breakpts/Insertion: 070C01-02;070D04-05, 066E
Date added: 8/1/1988 **Donor:** Charles Girdham **Donor's source:** Charles Vinson
Comments: DK3; new breakpoint information from John Belote, 3/93; Adelaide Carpenter says 70C02;70D05, 11/94

Stock Number: 3126
Genotype: Df(3L)fz-M21, st[1]/TM6
Chromosome(s): 3
Breakpts/Insertion: 070D02-03;071E04-05
Date added: 8/1/1988 **Donor:** Charles Girdham **Donor's source:** Charles Vinson
Comments: DK3; Holly Irick says 70D3;71E5, Mark Seeger says 71E3-5 is removed based on deletion of comm, K.M. 7/7/95

Stock Number: 3127
Genotype: Df(3L)ri-79c/TM3, Sb[1]
Chromosome(s): 3
Breakpts/Insertion: 077B-C;077F-78A
Date added: 8/1/1988 **Donor:** Charles Girdham **Donor's source:** G. Jurgens
Comments: DK3

Stock Number: 3128
Genotype: Df(3R)M-Kx1/TM3, Sb[1] Ser[1]
Chromosome(s): 3
Breakpts/Insertion: 086C01;087B01-05
Date added: 8/1/1988 **Donor:** Charles Girdham **Donor's source:** J. Gausz
Comments: DK3

Stock Number: 3340
Genotype: Df(3R)e-R1, Ki[1]/TM3, Sb[1] Ser[1]
Chromosome(s): 3
Breakpts/Insertion: 093B06-07;093D02
Date added: 6/1/1989 **Donor:** C. Nusslein-Volhard
Comments: DK3; no markers indicated, but carries Ki, maybe others, K.M. 3/28/95

Stock Number: 3468
Genotype: Df(3R)slo8/Dp(3;3)Su[8]
Chromosome(s): 3
Breakpts/Insertion: 096A02-07;096D02-04 (Df), 096A;096F11-14 (Dp)
Date added: 5/31/1999 **Donor:** Emma Rushton **Donor's source:** Barry Ganetsky
Comments: DK3; df heterozygotes without the duplication will be Pc[-], K.M. 2/18/00

Stock Number: 3546
Genotype: Df(3R)B81, P{ry[+t7.2]=RP49}F2-80A e[1]/TM3, Sb[1]; Dp(3;1)67A
Chromosome(s): 3
Breakpts/Insertion: 099C08;100F05, 099D;100F
Date added: 8/1/1989 **Donor:** John Merriam
Comments: DK3

Stock Number: 3547
Genotype: Df(3R)L127/TM6; Dp(3;1)B152
Chromosome(s): 3
Breakpts/Insertion: 099B05-06;099E04-F01, 098F;100F
Date added: 8/1/1989 **Donor:** John Merriam
Comments: DK3

Stock Number: **3617**
Genotype: Df(3L)kto2/TM6B, Tb[1]
Chromosome(s): 3
Breakpts/Insertion: 076B01-02;076D05
Date added: 8/1/1990 **Donor:** Angela Pattatucci **Donor's source:** Jim Kennison
Comments: DK3; no cytological information, K.M.

Stock Number: **3627**
Genotype: Df(3L)31A/Dp(3;3)C126, cp[1] in[1] kni[ri-1] p[p]
Chromosome(s): 3
Breakpts/Insertion: 078A;078E, 078D;079B
Date added: 8/1/1990 **Donor:** Angela Pattatucci **Donor's source:** Jim Kennison
Comments: DK3; df heterozygotes without the duplication will be M[-], K.M. 2/18/00

Stock Number: **3640**
Genotype: Df(3L)brm11/TM6C, cu[1] Sb[1] ca[1]
Chromosome(s): 3
Breakpts/Insertion: 071F01-04;072D01-10
Date added: 9/1/1990 **Donor:** Jim Kennison
Comments: DK3; breakpoints originally given as 71F;72D1-10, but Kennison finds distal breakpoint is proximal to th102, K.M. 10/93

Stock Number: **3649**
Genotype: Df(3L)HR119/TM6B, Tb[1] ca[1]
Chromosome(s): 3
Breakpts/Insertion: 063C02;063F07
Date added: 3/1/1991 **Donor:** Arthur Wohlwill
Comments: DK3; distal breakpoint 63E6-9 based on location of l(3)63Eb (thus overlaps with #3687), K.M. 4/25/97

Stock Number: **3650**
Genotype: Df(3L)M21, kni[ri-1] p[p]/In(3LR)T33[L]f19[R] ! see comment
Chromosome(s): 3
Breakpts/Insertion: 062F;063D, 062A;064C (Dp on In)
Date added: 3/1/1991 **Donor:** Arthur Wohlwill
Comments: DK3; inversion chromosome carries a duplication for 62A-64C, recessive lethal, some with ri p[p], deficiency is Minute, eye color floating, A.W.; adult viability in the absence of the duplication is very poor, K.M. 3/21/96

Stock Number: **3686**
Genotype: Df(3L)GN24/TM8, l(3)DTS4[1]
Chromosome(s): 3
Breakpts/Insertion: 063F06-07;064C13-15
Date added: 4/1/1991 **Donor:** Steven Wasserman
Comments: DK3; no temperature-sensitive effect at 25[o], S.W.

Stock Number: **4247**
Genotype: y[1] ac[Hw-1] dm[1] lz[1]; su(Hw)[2] Sb[sbd-2]/TM6, su(Hw)[5]
Chromosome(s): 1;3
Date added: 12/12/1997 **Donor:** Mid-America Stock Center

Stock Number: **4366**
Genotype: In(3LR)C190[L]Ubx[42TR], Ubx[-]/sti[1]
Chromosome(s): 3
Breakpts/Insertion: Df: 069F03-04;070C03-04 + 089;089 (small df somewhere in 89)
Date added: 12/12/1997 **Donor:** Adelaide Carpenter
Comments: DK3; sti is just distal to the 3L deficiency so the stock is balanced, sti[1] chromosome may carry a tandem duplication for 69A-70C (based on cytology), mwh[1], red[1] and e[1] are segregating in the stock, A.T.C.C.

Stock Number: **4370**
Genotype: Df(3L)Delta1AK, ru[1] h[1] ry[506] sr[1] e[s] ca[1]/TM3, ry[RK] Sb[1] Ser[1]
Chromosome(s): 3
Breakpts/Insertion: 079F;080A
Date added: 12/15/1997 **Donor:** Hugo Bellen
Comments: DK3

Stock Number: 4393
Genotype: w[*]; Df(3L)XDI98, e[1]/TM6B, Tb[1]
Chromosome(s): 3
Breakpts/Insertion: 065A02;065E01
Date added: 12/15/1997 **Donor:** Hugo Bellen **Donor's source:** Wayne Johnson
Comments: DK3

Stock Number: 4429
Genotype: Df(3L)ME107, mwh[1] red[1] e[1]/TM1, red[*]
Chromosome(s): 3
Breakpts/Insertion: 077F03;078C08-09
Date added: 3/2/1998 **Donor:** Peter Deak
Comments: DK3

Stock Number: 4430
Genotype: Df(3L)Pc-2q, ry[506]/TM2
Chromosome(s): 3
Breakpts/Insertion: 078C05-06;078E03-079A01
Date added: 3/2/1998 **Donor:** Peter Deak
Comments: DK3

Stock Number: 4431
Genotype: Df(3R)DG2/TM2
Chromosome(s): 3
Breakpts/Insertion: 089E01-F04;091B01-B02
Date added: 3/2/1998 **Donor:** Peter Deak
Comments: DK3

Stock Number: 4432
Genotype: Df(3R)crb-F89-4, st[1] e[1]/TM3, Ser[1]
Chromosome(s): 3
Breakpts/Insertion: 095D07-D11;095F15
Date added: 3/2/1998 **Donor:** Peter Deak
Comments: DK3

Stock Number: 4500
Genotype: Df(3L)Scf-R6, th[1] st[1] cu[1] sr[1] e[s] ca[1]/TM3, Sb[1]
Chromosome(s): 3
Breakpts/Insertion: 066E01-06;066F01-06
Date added: 5/19/1998 **Donor:** Ian Duncan
Comments: DK3

Stock Number: 4506
Genotype: Df(3L)Ten-m-AL29/TM3, ry[RK] Sb[1] Ser[1]
Chromosome(s): 3
Breakpts/Insertion: 079C01-03;079E03-08
Date added: 5/19/1998 **Donor:** Ron Wides
Comments: DK3

Stock Number: 4507
Genotype: Df(3L)iro-2, Sb[sbd-2]/TM3, Sb[1]
Chromosome(s): 3
Breakpts/Insertion: 069B01-05;069D01-06
Date added: 5/19/1998 **Donor:** Juan Modolell
Comments: DK3

Stock Number: 4787
Genotype: Df(3R)3-4, ru[1] th[1] st[1]/TM3, Sb[1] Ser[1]
Chromosome(s): 3
Breakpts/Insertion: 082F03-04;082F10-11
Date added: 10/14/1998 **Donor:** Thom Kaufman **Donor's source:** Adelaide Carpenter
Comments: DK3

Stock Number: **4940**
Genotype: cn[1]; Df(3R)mbc-30/TM3, Sb[1]
Chromosome(s): 2;3
Breakpts/Insertion: 095A05-07;095C10-11
Date added: 11/25/1998 **Donor:** Susan Abmayr
Comments: DK3

Stock Number: **4962**
Genotype: Df(3R)H-B79, e[*]/TM2
Chromosome(s): 3
Breakpts/Insertion: 092B03;092F13
Date added: 12/10/1998 **Donor:** Peter Deak
Comments: DK3

Stock Number: **5126**
Genotype: Df(3L)XS533/TM6B, Sb[1] Tb[1] ca[1]
Chromosome(s): 3
Breakpts/Insertion: 076B04;077B
Date added: 3/11/1999 **Donor:** Jim Kennison **Donor's source:** Jurg Muller
Comments: DK3

Stock Number: **5411**
Genotype: Df(3L)Aprt-32/TM6
Chromosome(s): 3
Breakpts/Insertion: 062B01;062E03
Date added: 9/23/1999 **Donor:** Berkeley Drosophila Genome Proj.
Comments: DK3

Stock Number: **5601**
Genotype: Df(3R)Espl3/TM6C, Sb[1] Tb[1]
Chromosome(s): 3
Breakpts/Insertion: 096F01;097B01
Date added: 2/24/2000 **Donor:** Marc Muskavitch
Comments: DK3

Stock Number: **5694**
Genotype: w[*]; Df(3R)e1025-14/TM6B, Tb[1]
Chromosome(s): 1;3
Breakpts/Insertion: 082F08-10;083A01-03
Date added: 4/19/2000 **Donor:** Gerry Rubin
Comments: DK3

Stock Number: **5915**
Genotype: Df(3L)E44/TM3, Ser[1]
Chromosome(s): 3
Breakpts/Insertion: 069D02;069E03-05
Date added: 1/2/2001 **Donor:** Adelaide Carpenter **Donor's source:** Y. Henry Sun
Comments: DK3. May be segregating w[*], A.C. 12/00

Stock Number: **11679** **Old Stock Number:** P1679
Genotype: P{ry[+t7.2]=PZ}l(3)06240[06240] ry[506]/TM3, ry[RK] Sb[1] Ser[1]
Chromosome(s): 3
Breakpts/Insertion: 061B01-02
Date added: 6/19/2000 **Donor:** Berkeley Drosophila Genome Proj. **Donor's source:** Allan Spradling
Comments: semilethal, B.D.G.P.; died, new copy from A.S. added 8/16/96; died, new copy from BDGP, 6/00 K.C.